CHILDHOOD & ADOLESCENT FRACTURES IN THE POST-MEDIEVAL NETHERLANDS

LIVES OF BROKEN BONES: CHILDHOOD AND ADOLESCENT FRACTURES IN POST-MEDIEVAL DUTCH COMMUNITIES (1650–1850 CE)

BY: MEGHAN LANGLOIS, B.A. HON.

A Thesis Submitted to the School of Graduate Studies in Partial Fulfillment of the Requirements for the Degree Master of Arts

McMaster University MASTER OF ARTS (2024) Hamilton, Ontario (Anthropology)

TITLE:	Lives of Broken Bones: Childhood and Adolescent Fractures in Post-Medieval Dutch Communities (1650–1850 CE)
AUTHOR:	Meghan Langlois, B.A. Hon. (University of Alberta)
SUPERVISOR:	Dr. Megan Brickley
NUMBER OF PAGES:	xiii, 176

Lay Abstract

Patterns of trauma and broken bones in the past can be used to investigate the activities people engaged in and their role in society. This research examines fractures in children and adolescents from four early modern sites in the Netherlands to understand their lives and experiences. Analysis involved careful inspection of the bones, combined with microscopy, micro-CT imaging, and historical records. Young people of all ages, both males and females, experienced fractures, but the most notable pattern was trauma to the spine in teenagers. The results indicate that adolescents from the lower classes likely engaged in strenuous labour as a survival strategy and for educational training in the form of apprenticeships. Poor diet and living conditions may also have led to impaired bone health, contributing to the fractures. In this case, lower class people experienced worse health outcomes related to hazardous working conditions and limited access to nutritious foods.

Abstract

Trauma analysis in bioarchaeology provides an understanding of lived experiences by contributing information on how aspects of individual identity, including socioeconomic status and occupation, influence the presence and consequences of fractures. Yet, few systematic studies have undertaken the analysis of fractures in children and adolescents. This thesis examines ante-mortem fractures in children and adolescents (1–20 years) from the urban centers of Arnhem, Eindhoven, Alkmaar, and Zwolle from 1650–1850 CE in the Netherlands. Assessment was carried out using macroscopic, microscopic, and micro-computed tomography (micro-CT) analyses. In total, 16/55 individuals displayed evidence of fracture. Children of all ages experienced fractures in the examined collections, but there was a peak in the occurrence of fractures in those who died in the middle adolescence age category (15-17 years) followed by early adolescence (10-14 years). The increase in fractures during adolescence follows the expected pattern for modern and archaeological populations, likely resulting from engagement with new activities. Males and females experienced fractures equally, indicating both undertook activities with risk of fracture. The only clear relationship in the analysed data was the presence of vertebral compression fractures and Schmorl's nodes in adolescents of mid- to low-socioeconomic status ($p<0.05$). There is a significant correlation between the occurrence of compression fractures and Schmorl's nodes (<0.0001), suggesting they are the result of shared or similar activities. Explanations include strenuous labour, impaired bone health, or a combination of both as those in the lower classes engaged in labour for pay and apprenticeships. Findings from this investigation indicate that detailed bioarchaeological assessments of fractures in children and adolescents are likely to contribute details about their social identities and lived experiences.

Acknowledgements

First and foremost, a huge thank you to my supervisor Dr. Megan Brickley. Your support and input have been greatly appreciated throughout this process and the opportunities you have provided me are unparalleled. Thank you to my committee member, Dr. Tina Moffat, and my third reader, Dr. Amanda Wissler. Your support and suggestions have greatly improved my thesis. And thank you to Drs. Rachel Schats and Allie Van der Merwe for access to the collections and without whom this research would not have been possible. The generous funding provided by the Social Sciences and Humanities Research Council (SSHRC) is also greatly appreciated.

Appreciation and thanks to the anthropology department faculty and staff for creating such a wonderful and supportive environment. To my graduate cohort, office buddies, roommates, and all the people I have met in Hamilton, thank you for letting me rant and talk through the various issues I had during the writing process, and for keeping me sane with fun outings, jokes, and silly distractions. I don't think I would have survived this program and the move across Canada without you.

To my partner Dan, I couldn't ask for a more supportive and loving person to stand beside me while I went through this program. Thank you for sticking out the long-distance relationship and thank you for taking care of our kitties in my absence. I can't wait to be reunited. Titan, Tuna, and Bo, for taking all my stress away with your fuzzy bellies, you deserve all the treats in the world. A final huge thank you to my family and friends back home, especially my mum, Mary, for reading through drafts of papers and providing helpful advice. You can talk scurvy with the best of them now.

Table of Contents

List of Figures

Chapter 2

Chapter 3

Chapter 4

List of Tables

Chapter 2

Chapter 3

Chapter 4

Chapter 5

Declaration of Academic Achievement

The research contained in this thesis was completed by Meghan Langlois under the supervision of Dr. Megan Brickley and Dr. Tina Moffat. Research questions and methodology were developed in consultation with Dr. Brickley and Dr. Moffat. Permission to access the skeletal collections of ARJB, EHV-CK, and ZW-87 at the University of Leiden were granted by Dr. Rachel Schats. Permission to access the GRK skeletal collection at Amsterdam UMC was granted by Dr. A. E. van der Merwe. Data collection and analysis was undertaken by Meghan Langlois. Funding for this project was received from the Social Sciences and Humanities Research Council (SSHRC). Ethics approval was granted by the Human Tissue Committee of the Hamilton Integrated Research Ethics Board (HiREB) as part of the project "Health across the Life Course: An Investigation of the Impact of the Maternal-Child Nexus and Lifeways on Non-Adult and Adult Health" (ID# 16436).

Chapter 1 Introduction

1.1 Introduction

Health is innately biocultural, influenced by social environment, cultural norms, and individual biology (Grauer, 2019; Halcrow & Tayles, 2011); the analysis of fracture patterns in archaeological contexts may bridge the gap between skeletal lesions, environment, and individual lives (Glencross, 2011). However, the study of childhood and adolescent fractures are under-studied in the archaeological record as compared to adults (Lewis, 2014; Lewis, 2018). In this thesis I examine ante-mortem fractures in children and adolescents (1–20 years) from skeletal collections derived from the urban centers of Arnhem, Eindhoven, Alkmaar, and Zwolle from 1650–1850 CE in the Netherlands. Fractures resulting from direct and in-direct force, pathology, and stress are included. Assessment was carried out using macroscopic, microscopic, and micro-computed tomography (Micro-CT) analyses. Of the 55 individuals included in this study, 16 display evidence of fracture.

The under-representation of childhood and adolescent trauma in archaeology results from a number of compounding methodological issues. The archaeology of children is a relatively new field of inquiry, having emerged from feminist archaeology in the late 1980s and early 1990s (Baxter, 2008; Lillehammer, 1989; Perry, 2005). Lewis (2022) states that interest in adolescence, the transitory period between childhood and adulthood, has likewise only recently come to the attention of bioarchaeologists. The study of fractures in children and adolescents is further problematized by the nature of developing bone, which differs in morphology, anatomy, and physiology from adult bone (Glencross & Stuart-Macadam, 2000; Lewis, 2018; Ogden, 2000, p. 47; Scannell & Frick, 2020; Verlinden & Lewis, 2015). Extensive vascularization and lower mineralization result in distinct fracture types and rates of healing as compared to adults

(Calmar & Vinci, 2002; Glencross & Stuart-Macadam, 2000; Lewis, 2014; Lewis, 2018; Verlinden & Lewis, 2015; Wenger et al., 2018), complicating the identification of fractures in developing bone in archaeological contexts. Outside of studies of intentional violence, few archaeological studies have systematically undertaken the examination of fractures in children and adolescents and scholarly descriptions and visual representations are limited, impacting our ability to identify fractures in archaeological collections. As a result, the current reported prevalence of childhood and adolescent fractures in the past is likely an underestimate (Lewis, 2014; Lewis, 2018). The current thesis explores the crude and true prevalence of fracture within and between four post-medieval Dutch sites. In so doing, it provides detailed descriptions and imaging of the appearance of fractures in developing bone for use in other archaeological contexts.

In modern populations, age and biological sex are associated with the frequency, location, and type of fractures young people experience (Glencross & Stuart-Macadam, 2000; Ogden, 2000, p. 47; Scannell & Frick, 2020). Typically, males experience more fractures than females across age categories (Cooper et al., 2004; Hedström et al., 2010; Naranje et al., 2016; Valerio et al., 2010), and adolescents are at an increased risk for fracture compared to younger children due to engagement with new activities and delays in bone mineralization related to the adolescent growth spurt and the beginning of puberty (Hedström et al., 2010; Mathison & Agrawal, 2010; Valerio et al., 2010). Socioeconomic status and living conditions likewise dictate the type of activities young people engage in and the trauma they are exposed to (Dittmar et al., 2021; Glencross & Stuart-Macadam, 2000; Hedström et al., 2021; Lewis, 2014; Lewis, 2018; Trinidad & Kotagal, 2023). However, Lewis (2014) states that the primary causes of fracture in modern contexts (sports injury, vehicular accident) are unlikely to have existed in the past, meaning the

types and prevalence of fractures across age, biological sex categories, and socioeconomic status in the past would be expected to differ. This thesis aims to examine the patterning of fractures across and between socioeconomic classes, biological sex, and age categories.

The archaeological study of trauma is frequently used to investigate activities and risk-factors for adults (Dittmar et al., 2021; Judd & Roberts, 1999; Pedersen et al., 2019; Scott et al., 2019), yet few studies have undertaken similar research on children (Glencross & Stuart-Macadam, 2000; Lewis, 2010, 2016; Penny-Mason & Gowland, 2014; Verlinden & Lewis, 2015). Mant et al. (2021) explains how trauma analysis serves as an important tool for understanding lived experiences by contributing information on how aspects of individual identity, such as gender, socioeconomic status, and occupation, influence the presence and consequences of fractures. Biological factors (age, biological sex, pathological conditions) combined with social factors (socioeconomic status, income, employment) play an important role in determining activities, risk-factors, and health outcomes (Cooper et al., 2004; Hedström et al., 2021; Ogden, 2000; Scannell & Frick, 2020; Trinidad & Kotagal, 2023; Valerio et al., 2010; World Health Organization, 2024). The patterning of fractures in young people may be used to recreate past lifeways, behaviours, and risk-factors. But our failure to recognize fractures in developing bone affects our ability to interpret the sociocultural role of children and adolescents in past societies and undermines our knowledge of risk-factors for trauma tied to social identity and social age. This thesis explores how the analysis of fractures in young people can provide information on their social identities, lifeways, and lived experiences.

The three key aims of this study are: 1) to investigate childhood and adolescent fracture prevalence from post-medieval urban centers in the Netherlands; 2) to explore how fracture patterns relate to socioeconomic status, biological sex, and age; and 3) to determine what the

patterning of fractures can tell us about the activities, social roles, and risk-factors for children and adolescents, and how this information can contribute to the understanding of their lived experiences and social identities.

1.2 Thesis Organization

This thesis is organized into six chapters, with the recording forms, raw data, additional images, and statistical equations available in Appendices A-E. Chapter two contains relevant background information on the sites and the historical context in the post-medieval Netherlands. Additionally, information on fracture mechanisms and types, as well as fracture repair for adults and individuals undergoing growth and development are presented. The theoretical framework of social determinants of health is also introduced. Chapter three presents the materials and methodology used for data collection including age and biological sex estimates, fracture recording, post-traumatic time interval estimations, and imaging technologies. These methods form an important part of the combined approach to fracture analysis employed in this research and may be applicable in other archaeological contexts. The fourth chapter presents the results of the analysis including the crude and true prevalence of fracture, and fracture prevalence according to age, biological sex, and socioeconomic categories. In chapter five, the results are interpreted utilising what is known about the historical and cultural context of the post-medieval Netherlands, and the application of social determinants of health to examine the relationship between lifeways and health inequities. Chapter six provides a summary of the findings and presents the final conclusions.

Chapter 2 Background

In their analysis of economic development in the Netherlands, de Vries and van der Woude (1997) state that 17th to 19th century was marked by increasing urbanization, industrialization, and colonial expansion, resulting in rising class divisions, and shifting cultural norms. The urban cemeteries at Arnhem (1650–1829 CE), Eindhoven (1650–1850 CE), Alkmaar (1716–1830 CE), and Zwolle (1675–1828 CE) (Fig. 2.1) present a prime opportunity to examine the social roles and activities of children and adolescents during this tumultuous period. This chapter begins with contextual information for each site to provide the sociocultural context in which the individuals lived (sections 2.1-2.4). Information on fracture types and mechanics (section 2.5) are presented for adults and individuals undergoing growth and development to provide context on how patterns of fractures may differ in children and adolescents and how they can be used to reconstruct activities. The process of fracture repair and complications (section 2.5.3) are presented to provide context for the estimation of post-traumatic time intervals. Additionally, social determinants of health (section 2.6) are introduced as a framework through which health inequities in the past may be studied.

Figure 2.1 *A map of the Netherlands showing the locations of the sites included in this study (Source: Creative Commons Attribution-Share Alike 3.0 Unported).*

2.1 Arnhem (ARJB)

Arnhem is the capital of the Gelderland province located in the eastern Netherlands on the banks of the Nederrijn and Sint-Jansbeek rivers. In 1233, Arnhem gained city rights and in 1541 joined the Hanseatic League, an alliance of trading guilds that held a monopoly over large

areas of Northern Europe, leading to increased economic development between 1650 and 1795 CE (van Bath, 1968). Beginning in 1795, systematic immigration led to the population growing to around 20,000 people by the early 19th century, making Arnhem one of the largest urban centers in the Netherlands. Many immigrants from within the Netherlands and beyond came in search of employment in the small-scale production of tobacco, shoemaking, and papermaking (Casna & Schrader, 2022; Nijkamp & Goede, 2002). However, according to van Zanden (1995), the growing population led to increasing wealth inequality in Arnhem and in cities across the Netherlands.

The graveyard around Eusebius Church served the general populace of Arnhem. The earliest mention of the northern cemetery dates to 1361, and records indicate extensive use until 1636 when fear of spreading the plague temporarily closed the graveyard. However, due to the dissatisfaction of the public, the cemetery was reopened with new plots to the west of Eusebiuskerk; burials continued until 1829 and the permanent closure of the cemetery. When the cemetery was full, older graves were removed and the bones piled in the charnel house where they were displayed and served as a memento mori (Zielman & Baetsen, 2020).

2.2 Eindhoven (EHV-CK)

The urban center of Eindhoven is located in the North Brabant province in the southern Netherlands. The town was founded in the 13th century by Hendrik I of Brabant and remained a small municipality until an economic boom in the 19th century. Arts (2019) states that between 1567 and 1687 the population nearly doubled from around 900 inhabitants to 1,726, remaining relatively stable thereafter with a population of 1,792 people in 1837 CE. The Eighty Years' War (1568-1648 CE) between Habsburg Netherlands and Spain negatively impacted the economy in the Brabant province. However, with the Peace of Münster in 1648, Eindhoven came under

control of the United Provinces of the northern Netherlands, allowing for the development of the textile, brewing, and pottery industries between the 17th and 18th centuries. However, industrialisation remained limited until the 19th century, after which the textile, tobacco, and match making industries dominated (Alumni Meeting Eindhoven, 2023). As the 19th century progressed, Eindhoven became a major industrial center.

The Church of Saint Catherine's (Caterinakerk) is the only medieval church in Eindhoven, with the oldest mention dating to 1340 CE (Arts, 2019). Originally a Catholic church, the building was seized by the Dutch Reformed movement in 1648, but Catholic burials in the surrounding cemetery continued alongside Reformed burials until 1793. Following renovations in 1810, a new cemetery to the North of the church was added in 1858 and became the cheapest location to bury the dead. Much of the original building was demolished in 1860 and a new, larger church was constructed between 1860 and 1867. It is estimated that between 1200-1850 approximately 55,000 individuals were buried in the church and graveyard. Wealthy citizens were able to purchase plots inside the church but middle to low class citizens were buried in the graveyard outside (Arts, 2019).

2.3 Alkmaar (GRK)

Alkmaar is a small city located 40km north of Amsterdam, in the province of Holland. From 1500–1650 CE, the population boomed from approximately 4,000 to over 13,000 people as a result of agricultural and economic prosperity (van Zanden, 1992). This "Golden Age" was followed by a period of economic decline between 1650 and 1850 CE during which the population decreased to around 8,000 people (Bitter, 2018, p. 87). According to de Vries and Van der Woude (1997), the province of Holland had a high urbanization rate during the early modern period, with over 60% of the population residing in cities. The high urbanization rate was related

to economic activity centered on shipping, regional trade, and small-scale non-agrarian activities. As with the rest of the Northern Netherlands, individuals in Alkmaar experienced a generally high standard of living compared to the rest of Europe, with high nominal wage, though inequality did exist. Alkmaar's economy was dominated by cheese and textile production and shipbuilding (de Vries & Van der Woude, 1997; van Zanden & van der Berg, 1993).

Originally built between 1470 and 1520 CE, the present-day Church of Saint Lawrence (Grote Kerk) functioned as the main parish church for the city. Burials occurred both below the church floors and in the cemetery outside. Bitter (2018) explains that while it is unknown when burials inside the church began, the oldest tombstones inside the church date to the 16th century and the high number of burials each year led to the removal of most graves from before the mid-18th century. Burials inside the church ceased in 1830, following the 1827 prohibition of burials inside the town limits. Church records indicate graves dating to the late 18th and early 19th centuries contain high status individuals, but prior to 1780 CE burial plots inside the church were owned by both the middle- and upper-classes. Burial in the cemetery outside the church was reserved for individuals of the lowest socio-economic status and children (Bitter, 2018).

2.4 Zwolle (ZW-87)

Zwolle is a small urban center in the province of Overijssel in the northeastern Netherlands. Granted town rights in 1230 CE by the Bishop of Utrecht, Zwolle experienced significant economic growth through the medieval period and was crowned the capital of the Overijssel province in 1798. Throughout the post-medieval period, the construction and textile industries accounted for the most important economic sectors in Zwolle. In 1795, construction accounted for 18% of the city's industrial labour and tailors dominated occupational frequency at 6.9/1000 people (de Vries & van der Woude, 1997). Van Zanden (1995) states that citizens in

Zwolle during this period had the highest average income in the region, and the city experienced less income inequality compared to larger centers.

Broerenkerk ("Brother Church") was established by Dominican monks and construction was completed in 1560 CE (Aten, 1992). The church served both the monks and the general people of Zwolle. In 1639, the Dutch Reformed movement took control of the Church and renovated the building but, between 1795 and 1803, the building was used to house soldiers and horses following the establishment of the Batavian Republic. The Dutch Reformed regained access in 1803. The final inhumations occurred in 1828 following the implementation of a national law prohibiting burials inside churches (Aten & Clevis, 2019). Burial records for the identified individuals indicate occupations included lower military personnel, merchants, and domestic workers, among others.

2.5 Fractures

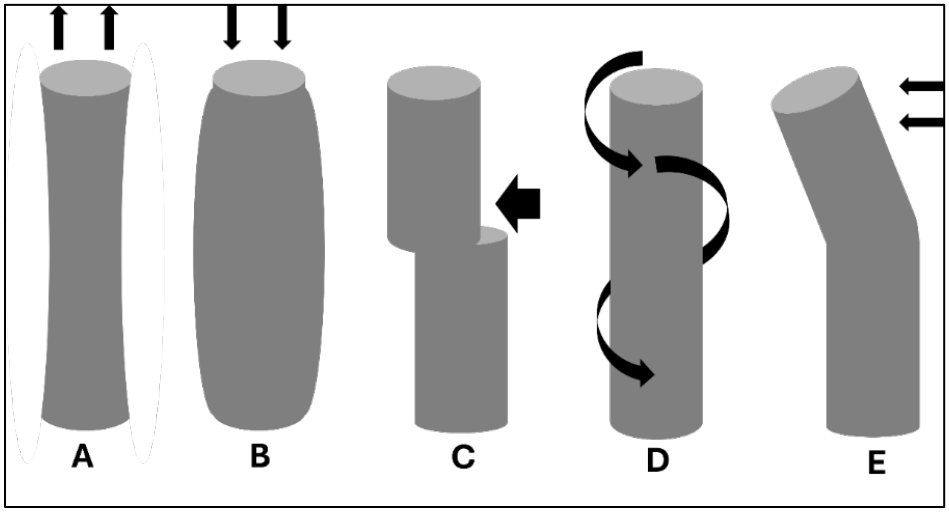

Figure 2.2 *Types of force that can result in fractures: tension (A), compression (B), shearing (C), twisting (D), and bending (E) (Source: after Redfern & Roberts, 2019, Figure 9.1, p. 213).*

A fracture is defined as a complete or incomplete break in the continuity of a bone resulting from the application of abnormal stress (Lovell, 1997; Ogden, 2000, p. 48; Redfern &

Roberts, 2019). All fractures can be classified as intra-articular (involving a joint) or extra-articular (not involving a joint) and open (piercing the skin) or closed (simple). The types of force that result in fractures can be broken down into five categories: tension, compression, shearing, twisting, and bending (Fig. 2.2). Fracture mechanisms are varied, including direct or indirect force, pathological conditions, or stress and repetitive motions, and often result in distinct fracture patterns (Lovell, 1997). The types of fracture associated with the four fracture mechanisms can be found in Table 2.1.

Table 2.1 *Injury mechanism and resulting fracture types (Source: after Lovell, 1997, Table 2, p. 141).*

Injury Mechanism	**Fracture Type**
Direct	Transverse: perpendicular to longitudinal axis
	Penetrating: penetration of the cortex
	Comminuted: break in more than 2 pieces, typically forming a 'T' or 'Y' pattern
	Crush: when bone collapses on itself, typically seen in cancellous bone
Indirect	Oblique: fracture line angles across the longitudinal axis
	Spiral: fracture line winds around the shaft
	Greenstick: incomplete break involving the convex side of bone subjected to bending
	Impaction: bone ends driven into each other
	Avulsion: occurs due to tension from a soft tissue attachment removing a piece of the underlying bone
	Burst: complete collapse of the vertebral body
Stress	Fracture resulting from repetitive stress or fatigue, usually perpendicular to the longitudinal axis.
Pathological	Fracture occurring secondary to disease, especially metabolic conditions, nutritional deficiencies, and neoplasms

When direct force is applied to bone, it typically results in distinct fracture types, including transverse, penetrating, comminuted, and crush (Lovell, 1997; Redfern & Roberts, 2019; Lewis, 2018). A transverse fracture typically occurs when a small amount of force is applied to a small area, whereas a penetration of the cortex, either complete or incomplete, results from a large force applied to a small area. Penetrating fractures are often associated with intentional violence (e.g. arrowheads or blades) and medical interventions (e.g. trephination). Crush fractures can be subdivided into three types: depression, compression, and pressure. A depression fracture occurs on one side of the bone and compressions affects both sides of the

bone. Pressure fractures typically occur on developing bone through the intentional application of force (Lovell, 1997). Indirect fractures occur at a place not directly impacted by the force and include oblique, spiral, greenstick, impaction, burst, and avulsion fractures. An oblique fracture is caused by the application of angled or rotated force, in comparison, a spiral fracture is the result of downward, rotational force. A burst fracture is a severe form of disc herniation caused by vertical compression of the spine wherein the entire vertebral body collapses. Greenstick fractures typically occur in developing bone and will be reviewed in section 2.5.1. Many fractures result from more than one type of force, and once healing has begun, specific mechanisms of fracture may be difficult to distinguish in dry bone. However, understanding the mechanism of a fracture may provide useful information on the types of activities or accidents that produced a fracture in archaeological contexts.

Prolonged, intermittent periods of stress caused by repetitive activities or overuse tend to result in stress or fatigue fractures (Redfern & Roberts, 2019). Stress fractures are generally incomplete or result in stable fractures (e.g. hairline fractures) and can affect both weight-bearing and non-weight bearing bones (Anderson & Greenspan, 1996). Reeder et al. (2012) states that stress fractures may result through three separate mechanical events: 1) the mechanical load may increase, 2) the number of applied stress (repeat activities) increases, and 3) the surface area to which the stress is applied decreases. In paleopathology, stress fractures are most often found in the spine in the form of anterior depressions or anterior wedging and spondylolysis (Lewis, 2018; Redfern & Roberts, 2019). The internal architecture of bone may also be affected by repeat stress and compression fractures, particularly in the vertebrae. Ataizi et al. (2018) explains that regional thinning of the trabecular structure is often seen in cases of vertebral fracture. Other common features include disarrangement of the trabeculae below the fracture zone, loss of

continuity in the longitudinal trabeculae, and decreased trabeculae in the anterior portion of the body (Brinckmann et al., 1988; Wáng et al., 2017). Variation in these trabecular features may result from differences in the stage of healing, nutritional status, and mechanical loading (Ma et al., 2023; Weinkamer et al., 2019).

Pathological fractures occur when a disease affects the quantity, quality, or architecture of bone, resulting in the inability of the bone to withstand normal biomechanical stress (Redfern & Roberts, 2019). The most common types of pathological fractures are those occurring secondary to osteoporosis (fragility fractures), a condition Marcus et al. (2013) characterize by low bone strength. Osteoporosis-related fractures occur in the absence of or following minimal trauma. Other causes of pathological fractures include metabolic conditions, nutritional deficiencies, infectious diseases, congenital anomalies, and neoplasms (Adler, 1989; Redfern & Roberts, 2019). Additionally, there is a relationship between underlying pathology and stress fractures (Anderson & Greenspans, 1996; Ogden, 2000, p. 23), as bone is more likely to fracture from minor stresses if the bone quantity or quality is compromised. Stress and pathological fractures may provide additional information of lifeways for individuals in the past.

2.5.1 Developing Bone and Fractures

Developing bone differs from adult bone in morphology, anatomy, and physiology, resulting in distinct fracture types, which vary according to the stage of skeletal development and maturity (Ogden, 2000, pp. 38–47). One of the primary differences between immature and mature bone is the presence of a thick periosteum which impacts fracture mechanics and repair and affects our ability to identify fractures in developing bone from archaeological contexts. The periosteum surrounding developing bone is less likely to be torn during fracture but more easily stripped off the bone as compared to adults (Scannell & Frick, 2020), meaning fractures are less

likely to be displaced which explains why stable fractures are more common in young individuals. The periosteum is also very active, with extensive vascularization and the presence of active osteoblastic cells that promote callus formation, leading to the rapid rate of fracture repair. Developing bone also has a lower mineral content than mature bone (Ogden, 2000, p. 23), meaning a greater amount of force is required for a fracture to occur. Instead, children are more likely to experience plastic deformation or bowing of the bone without fracture, which is unique to immature bone (Lewis, 2018, p. 93; Scannell & Frick, 2020). In dry bone, plastic deformation may be difficult to detect due to post-mortem alteration.

The most common type of fractures to affect children are torus or buckle, greenstick, and physeal (Lewis, 2018, p. 9; Ogden, 2000, p. 125; Scannell & Frick, 2020). Torus fractures are caused by compressive force that results in the cortex collapsing and creating a slight bulge in the cortical surface of the affected bone. Scannell & Frick (2020) explain how torus fractures primarily affect the junction between the metaphysis and diaphysis where the more porous bone of the metaphysis is compressed by the denser bone of the diaphysis. A greenstick fracture is the most common type of fracture in developing bone and is characterized by an incomplete fracture penetrating the cortex but halting at the medullary cavity. Greenstick fractures result when the bone bends under tension forces, leading to cortical failure on the compressed side (Lewis, 2018, p. 92; Scannell & Frick, 2020). The presence of growth plates means physeal fractures are unique to developing bone and may result from shearing, avulsion, or compressive force. Lewis (2018, p. 94) explains that physeal fractures may involve only the cartilage of the growth plate or bone and cartilage and can affect only the metaphysis or, more rarely, both the metaphysis and epiphysis. In clinical settings, the Salter-Harris scale is used to evaluate the severity of fracture. In Type I the epiphysis separates completely from the metaphysis. Type II, the most common

fracture pattern, the fracture line passes through the metaphysis on an angle, resulting in a corner separating (bucket-handle or corner fracture). Type III fracture only affects the epiphysis, with the fracture line running vertically through the bone with separation from the metaphysis. In Type IV, an oblique fracture lines traverses the epiphysis, metaphysis, and diaphysis. Type V is rare but involves compression of the epiphysis resulting in a crush fracture (Lewis, 2018, p. 95; Scannell & Frick, 2020). When complete fractures occur in developing bone, they tend to be transverse, oblique or spiral (Scannell & Frick, 2020). Comminuted fractures are rare in young children, but when they do occur, the periosteum tends to minimize displacement of the fragments (Ogden, 2000, p. 431).

According to Ogden (2000, p. 43), the level of skeletal development plays an important role in the location, frequency, and type of fractures young individuals experience. In young children, plastic deformation and greenstick fractures are more common, whereas in adolescents, greenstick fractures are rare. Older adolescents tend to follow fracture patterns more akin to those seen in adults. Age and biological sex are also important factors, dictating the level of fracture risk. The lowest incidence of fracture is found in individuals below one year of age, and highest between 1-2 years as children are learning to walk, and in adolescents aged 13-18 years. Fracture incidences differ little according to biological sex for young children (up to approximately 1 year of age) but males begin to outpace females during childhood, with the difference peaking in adolescence (1.9:1.0) (Ogden, 2000, p. 43). These factors must be kept in mind when evaluating fractures in developing bone.

2.5.2 Spinal Fractures

In modern populations, spinal injuries are rare in children and adolescents (Martus & Mencio, 2020; Saul & Dresing, 2018). In a healthy developing spine, the vertebral endplate is

covered by a thick, cartilaginous intervertebral disc, which protects the vertebrae from sheering and compressive forces (Saul & Dresing, 2019). In pediatric populations, the majority of spinal fractures affecting the thoracolumbar region occur in older individuals (~12> years), and the most common causes include falls from a height, sports injury, and motor vehicle accidents (Clark & Letts, 2001; Donnally et al., 2023). When fractures do occur in the developing spine, the most common fracture types are compression and Schmorl's nodes (Martus & Mencio, 2020; Saul & Dresing, 2019). The following two sections review current clinical understandings in the aetiology of compression fractures and Schmorl's nodes.

2.5.2.1 Compression Fractures

In clinical work, vertebral compression fractures are defined as the collapse of the anterior vertebral body, affecting the anterior longitudinal ligament and anterior half of the vertebral body (Alexandru & So, 2012; Donnally et al., 2023). In a study by Madassery (2020), compression fractures primarily occurred secondary to osteoporosis, affecting 25% of women and 5.6% of men over the age of 65 years, although infections, neoplasms, and trauma may also result in compression fractures. Vertebral compression fractures result from compression and flexion of the spine, typically affecting the thoracolumbar junction (Alexandru & So, 2012; Brinckmann et al., 1988; Donnally et al., 2023), but in younger individuals are often related to traumatic episodes such as falls from a height, motor vehicle accidents, and sports (Clark & Letts, 2001; Saul & Dresing, 2018; Sayama et al., 2014).

In the developing spine, the growth plate is at greatest risk for injury (Baranto et al., 2005; Clark & Letts, 2001; Karlsson et al., 1998). The immature endplate is composed of a layer of hyaline cartilage adjacent to the nucleus and bony endplate. The apophyseal ring epiphysis appears radiographically between 8 and 12 years of age. Union may commence around 16-19

years but is not fully completed until 25 years of age (Clark & Letts, 2001; Scheuer & Black, 2004). Spinal flexion may result in fractures traversing the growth zone resulting in a physeal fracture (Clark & Letts, 2012). Karlsson et al. (1998) conducted cadaveric experiments with spines of adolescents (14-18 years) and found that compression caused three injury types: rupture of the cartilaginous endplate, separation of the endplate from the vertebral body, and compression fracture. A similar study by Baranto et al. (2005) conducted on adolescent porcine spines examined fracture patterns resulting from flexion-compression and extension-compression. Fracture/separation occurred in all 16 cases. The extension-compression injuries all affected the anterior vertebral column and extended through the calcified cartilage, the growth plate, and the vertebral body. Flexion-compression injuries occurred posteriorly 6 times and anteriorly 5 times, primarily affecting the growth zone (Baranto et al., 2005).

Impaired bone health may increase the risk for vertebral compression fracture in children and adolescents. Mäyränpää et al. (2012) examined the prevalence of vertebral fracture in young people (4-16 years) in relation to bone health and found that 44% (n=8) of people with compression fractures had vitamin D deficiency (<37 nmol/L S-25OHD), and 39% (n=7) had insufficient vitamin D serum levels (38-49 nmol/L S-25OHD). Only 13% (n=4) of analyzed individuals had normal vitamin D serum levels. Additionally, the individuals with vertebral compression fractures were found to have significantly lower bone mineral density Z-scores at the lumbar spine than those without, indicating possible osteoporosis (Mäyränpää et al., 2012). Karlsson et al. (1998) likewise found a relationship between vertebral fractures from compression and bone mineral content. Degenerative disc disease (DDD) may also predispose individuals to compression fractures. Adams et al. (2006) found that disc degeneration transferred load bearing to the posterior vertebral column, reducing bone mineral density in the

anterior vertebral body. Flexed postures resulted in increased load bearing on the weakened anterior portion and compressive failure and fracture (Adams et al., 2016). Although vertebral compression fractures are generally associated with advanced age, impaired bone health, excessive loading and hyperflexion/extension of the spine, DDD, and trauma may result in fractures in younger people (Baranto et al., 2005; Imai, 2015; Karlsson et al., 1998; Kim et al., 2023; Lau et al., 2008; Mäyränpää et al., 2012).

2.5.2.2 Schmorl's Nodes

Schmorl's nodes result from herniation of the nucleus pulposus through the adjacent vertebral endplate, causing displacement and fracturing of the subchondral trabeculae (Azzouzi & Ichchou, 2022; Dar et al., 2010; Kyere et al., 2012). First described by Christian Georg Schmorl in 1927, the prevalence of Schmorl's nodes in modern populations has been estimated to be between 3.8%-76%, varying according to what type of imaging technology was used (x-ray, MRI, macroscopic examination) and the definition employed (see Azzouzi & Ichchou, 2022). While reasons for their development are debated, the aetiology of Schmorl's nodes likely involves a combination of factors, including compression and torsion of the spine, degenerative disc disease, and developmental processes resulting in a weak spot in the affected vertebral endplate, factors that may be aggravated by underlying pathological conditions (Azzouzi & Ichchou, 2022; Dar et al., 2010; Hamanishi et al., 1994; Hilton et al., 1976; Kyere et al., 2012; Junghanns, 1971; Wang et al., 2012).

Clinical findings vary in who is affected, what ages, and where Schmorl's nodes are most likely to occur. Schmorl's nodes are typically reported to be more common in males than females (Hilton et al., 1976; Mok et al., 2010; Plomp et al., 2012; Yin et al., 2015), but the age of onset is debated. Dar et al. (2010) posits that cortical thickness between vertebrae and across the endplate

is not uniform, resulting in a centralized region of weakened endplate during spinal maturation. Hamanishi et al (1994) found that children <10 years did not present with Schmorl's nodes, but otherwise there was no relationship with age. Hilton et al. (1976) likewise reported no relationship between age (those above and below 50 years) and the presence of Schmorl's nodes, but did find an association between age, degenerative disc disease, and Schmorl's nodes.

Degenerative disc disease (DDD) has been found to be associated with the development of Schmorl's nodes in a number of studies (Hamanishi et al., 1994; Hilton et al., 1976; Mok et al., 2010; Samartzis et al., 2016; Wang et al., 2012; Yin et al., 2015). Maturation of the intervertebral disc occurs as young as 11 years of age, and diminished blood supply to the vertebral endplates, leading to disc degeneration, occurs during the second decade of life with increasing prevalence with advancing age (Benneker et al., 2005; Boos et al., 2002). DDD is a pathological condition associated with intervertebral disc degeneration involving structural failure of the disc and is closely associated with advancing age (Dowdell et al., 2017). Modic and Ross (2017) state that traumatic, genetic, nutritional, and especially mechanical factors all play a role in the development of DDD.

Despite finding an association between DDD and Schmorl's nodes, Hilton et al. (1976) suggest a developmental pathogenesis for Schmorl's nodes in conjunction with the distribution of stress in the thoracolumbar region. The developmental model posits that disruptions during notochord regression, ossification gaps, vascular channels, and Scheuermann's disease may result in indentations in the surface of the vertebrae that the disc may then herniate into (Kyere et al., 2012; Mattei & Rehman, 2014).

Most researchers suggest a multifactorial cause for Schmorl's nodes. Azzouzi and Ichchou (2022) posit a combination of compression and axial rotation (torsion) of the spine, disc

degeneration, bone mineral density, and developmental factors in the formation of Schmorl's nnodes. Wang et al., (2012) found an association between heavy occupation and Schmorl's nodes. Their findings are consistent with Junghanns (1971) theory that Schmorl's nodes result from the protrusion of the nucleus through the developmental weak spot of the endplate due to axial loading. Dar et al. (2010) likewise believe a combination of vertebral endplate weakness combined with axial rotation and stress ultimately result in the development of Schmorl's nodes during adolescence. Wáng and Xiáng (2023) suggest two types of Schmorl's nodes, one of developmental origin and the other acquired. However, the authors themselves do not provide an explanation for the ultimate cause of the two types. Callaghan and McGill (2001) examined the effects of repeat low magnitude loading on healthy, porcine spines and found herniation of the disc through the annulus occurred with relatively modest joint compression but with highly repetitive flexion/extension moments.

2.5.3 Fracture Repair

Fracture repair is a regenerative process aimed at restoring damaged bone to its pre-injury cellular composition, structure, and biomechanical function (Einhorn & Gerstenfeld, 2015; Sheen et al., 2023). There are two types of fracture repair: primary and secondary healing (Baker et al., 2018; Pountos & Giannoudis, 2018; Sheen et al, 2023). Primary fracture repair, also known as direct healing, occurs when there is a small fracture gap and the fracture is mechanically stable with little to no movement (Baker et al., 2018; Pountos & Giannoudis, 2018). Healing occurs via intramembranous ossification, with normal bone production and apposition originating at the periosteal surface and progressing towards the medullary cavity (Baker et al., 2018; Pountos & Giannoudis, 2018). This type of fracture repair displays reduced bone remodeling and fracture healing beneath the periosteal surface. There is no intermittent

cartilaginous phase and healing does not result in callus formation (Baker et al., 2018; McKinley, 2003). Primary fracture repair is less common than secondary fracture repair (Pountos & Giannoudis, 2018), but is the typical repair method for stress fractures (Baker et al., 2018).

McKinley (2003) states that secondary fracture repair, affecting the medullary cavity, cortical bone, and surrounding soft tissues, occurs in the absence of rigid fixation and involves an intermittent cartilaginous phase preceding bone formation. Secondary fracture repair can be generalized into five stages: 1) haematoma formation, 2) granulation, 3) primary or soft callus formation, 4) secondary or hard callus formation, and 5) remodeling (Baker et al., 2018; Pountos & Giannoudis, 2018; Redfern & Roberts, 2019; Schindeler et al., 2008; Sheen et al. 2023). Formation of a haematoma occurs immediately following fracture. Fracture causes disruption to the blood vessels supplying the periosteum, resulting in bleeding and the formation of a haematoma at the site of the fracture (Schindeler et al., 2008; Sheen et al., 2023). The haematoma clots, forming the temporary frame for subsequent healing. During haematoma formation, pro-inflammatory cytokines are released, which are crucial for the healing process as they promote osteogenic growth factors (Pountos & Giannoudis, 2018; Sheen et al, 2023). Blood vessels penetrate the clot, which is subsequently reorganized into granulation tissue (Schindeler et al., 2008). Granulation tissue formation, or the fibrocartilaginous callus, occurs within two weeks of the initial injury, providing additional provisional stability and acting as a template for the later bony callus (Schindeler et al., 2008; Sheen et al., 2023). Chondrocytes excrete cartilaginous matrix which replaces the granulation tissue with cartilage through endochondral ossification (Schindeler et al., 2008). The chondrocytes then undergo hypertrophy, mineralizing the cartilaginous matrix and leading to formation of the soft callus. In clinical literature (Pountos & Giannoudis, 2008; Schindeler et al., 2008), the appearance of woven bone is associated with

both the soft callus stage of fracture repair and the hard callus stage. Because granulation tissue and the cartilage callus are not available in dry bone, for the purposes of this thesis, the soft callus stage is defined by the appearance of woven bone. The gradual replacement of the fibrocartilaginous tissues with woven bone proceeds via endochondral ossification. There are three types of soft callus associated with different areas of the fracture site: the intermediate callus that joins the ends of the broken bone, the endosteal callus that unites the marrow spaces forming a plug, and the bridging callus that arches over the fracture margins and provides visible evidence of fracture repair in archaeological bone (Redfern & Roberts, 2019). Following the conversion of the cartilage tissue into woven bone, the hard callus stage proceeds as woven bone is remodeled into lamellar bone (Redfern & Roberts, 2019; Schindeler et al., 2008). The process involves the apposition of lamellar bone on existing woven bone, the removal of woven bone via osteoclasts, and internal osteon remodeling (Redfern & Roberts, 2019). The final stage of fracture repair involves removal of the hard callus to return the morphological structure, osteon structure, and haversian system to a pre-injury state (Einhorn & Gerstenfeld, 2015; Pountos & Giannoudis, 2008). During this stage, the medullary cavity is reestablished (Einhorn & Gerstenfeld, 2015; Marsell & Einhorn, 2011). Remodeling may last several months to several years. For the purposes of this thesis, remodeling in the context of fracture repair is defined as the transformation of primary woven bone into secondary lamellar bone and the removal of the hard callus (Wei & Cooper, 2023).

Clinicians Ogden (2000) and Scannell and Frick (2020) state that age plays an important factor in fracture repair. Rates of healing in infants are extremely rapid but the pace progressively slows throughout childhood and into adolescence as skeletal maturity is achieved. In developing bone, the periosteum is extremely osteogenic with abundant blood flow. Extensive

vascularization allows for a greater inflammatory response immediately following fracture. Vasodilation conveys inflammatory cells, growth factors, and cytokines to the fracture site, kickstarting the initial stage of fractur repair. In mature bone, the vascular response is slower, leading to delayed fracture repair. The presence of osteogenic cells beneath the periosteum in developing bone likewise results in faster fracture repair by promoting new bone formation. The degree to which the periosteum lifts away from the underlying cortical bone determines the size of the hematoma at the fracture site. Because the presence of a hematoma initiates agents active in fracture repair, a larger hematoma (more displaced periosteum) leads to faster repair. Minimally displaced or greenstick fractures may not result in a fracture callus, and therefore heal more slowly. Estimating post-traumatic time intervals based on the stage of fracture repair by age category is discussed in section 3.2.2.

2.5.3.1 Factors Affecting Fracture Repair and Fracture Complications

In adults, the typical timeline for formation of the soft callus is six weeks (Redfern & Roberts, 2019). But fracture repair may be impacted by a variety of factors including: the location and extent of fracture, biomechanical forces, infection or disease, and nutritional status, among others (Redfern & Roberts, 2019; Schindeler et al., 2008; Sheen et al., 2023). While many complications involve soft tissues, the focus here is on complications affecting osseus tissues that may be visible in dry bone. Complications during fracture repair may result in delayed union, malunion, or non-union. Delayed union is the absence of bony union within the expected timeline. In dry bone, delayed healing may be difficult to detect as it resembles the typical stages of fracture repair (Djurić et al., 2006; Lovell, 1997). Malunion occurs when the bone heals out of anatomical alignment. Types of deformities include angulation, rotation, overlap/shortening, and lengthening potentially resulting in functional impairment, pain, and

osteoarthritis (Lovell, 1997). Non-union is defined as the "cessation of all reparative processes of healing without bone union" (Panagiotis, 2015, p. S30), or when the fracture ends fail to unite and the marrow cavity is sealed (Lovell, 1997). Brickley & Buckberry (2015) show how non-union may result in the formation of a pseudoarthrosis or false articular surface which is recognizable in dry bone as sclerotic margins and eburnation.

Different bones have been shown to heal at different rates depending on the ratio of cancellous to cortical bone and malunion is more likely for specific bones. Additionally, the orientation of the fracture ends, and the width of the fracture gap, have been shown to affect callus formation and the rapidity of healing (Pountos & Giannoudis, 2018). Mechanical loading is vital for bone regeneration and plays a crucial role in fracture healing. Ma et al. (2023) explain that mechanical forces play a role in fracture remodeling throughout the stages of healing by initially stimulating the development of osteogenic cells, then promoting callus tissue formation, and finally by improving tissue reconstruction during the remodelling phase. However, the benefits of mechanical loading are dependent on the magnitude, direction, and timing of force application (Frost, 1989), and loading at the fracture site may delay healing and result in inferior outcomes. Infection may occur as a result of open fractures or soft tissue injury at the time of trauma. Bacterial infection at the injury site and osteomyelitis (infection of the bone marrow) may result in chronic inflammation and delayed or absent callus formation (Einhorn & Gerstenfeld, 2015). Nutritional deficiencies and metabolic conditions are important risk-factors in delayed or unsuccessful fracture healing. Systemic metabolic conditions may impact bone formation by reducing cartilage formation or via reduced bone mineralization, resulting in reduced or nonexistent callus formation during fracture repair and non-union or delayed union (Frost, 1989). Vitamins C and D, calcium, and iron deficiencies have been shown to have the

greatest impact on fracture repair (Pountos & Giannoudis, 2018). Causes of non-union or malunion may be difficult to detect in dry bone, but these fracture complications provide visibility for healed fractures in paleopathology.

Clinical literature (Ogden, 2000; Scannell & Frick, 2020) explains that because of the rapid fracture repair and the likelihood of an intact periosteum, developing bone is less prone to complications than mature bone. Additionally, children have greater remodeling capacity than adults, and some degree of angulation and deformity can remodel with growth. Still, there are a couple of complications that may arise in young individuals in addition to the above-mentioned factors. Physeal fractures or fractures affecting the growth plate may result in long-term complications including premature physis closure and growth arrest resulting from vascular damage or bony bridging across the growth plate (Lewis, 2018, p. 96; Ogden, 2000, p. 150; Scannell & Frick, 2020). Lewis (2018, pp. 96-98) explains that growth interruptions and the degree of shortening is dependent on the location of fracture and the age of the individual at the time of fracture and may be difficult to detect. Partial fusion of the epiphysis may also result in angulation or disruption of the joint surface leading to functional deformities. Overgrowth of a fractured limb, resulting in limb lengthening, may also be a consequence of fractures in those still undergoing growth and development. Overgrowth results from significant separation of the periosteum from the cortex, leading to increased vascular supply and overgrowth of the bone. Overgrowth most commonly affects the femur and may result from complete, greenstick, or torus fractures. Shortening and overgrowth as a result of physeal injuries may be detectable in dry bone through comparison of paired skeletal elements.

2.5.4 Identification of Fractures in Paleopathology

The study of trauma, including fractures, in adult skeletal remains has a long history (Lovell, 1997), as the anatomical importance and sociocultural implications are well understood. Traumatic injuries are one of the most commonly encountered skeletal lesions, and may be easily identifiable, such as through the presence of a fracture callus (Redfern & Roberts, 2019; Roberts, 2000). However, as Redfern and Roberts (2019) explain, taphonomic factors and individual variables in break patterns and healing may complicate the identification of fractures in dry bone; therefore, detailed recording systems have been established to aid in the recognition and interpretation of fractures in archaeological contexts.

The analysis of fractures in dry bone must begin with a proper and detailed description (Lovell, 1997). Description should include accurate identification of the bone(s) present, the location of the trauma, its appearance, and state of healing (Redfern & Roberts, 2019, p. 234; Roberts, 2000). Complications resulting in deformity, including apposition, overlap, linear or rotational deformity, and infection or joint degradation are useful clues for identifying fractures and their later interpretation (Roberts, 2000). An understanding of taphonomy is also critical for determining ante- peri- and post-mortem fractures. Following the description of the lesion(s), the ultimate cause of the injury can be considered (Lovell, 1997; Redfern & Roberts, 2019) drawing on clinical data. Interpretations of trauma should consider the characteristics of the fracture itself, the pattern of trauma in the individual and the population, and the social/historical and environmental context (Lovell, 1997).

Paleopathological methods for the recognition of fractures in developing bone are hampered by the nature of immature bone and rapid healing in young individuals (see section 2.5.3). Extensive vascularization resulting in porous bones and lower mineralization mean that

taphonomic processes are more likely to adversely affect younger individuals, resulting in poor preservation (Lewis, 2006, 2018). Pathological conditions that impact the integrity of bone, including fractures, likewise have the potential to result in skeletal remains that are less well preserved (Kemp, 2016; Redfern & Roberts, 2019). Few archaeological studies have systematically undertaken the examination of fractures in children and young adolescents within a given population and scholarly descriptions and visual representations are limited, impacting our ability to identify fractures in developing bone in archaeological populations. As a result, the study of childhood and adolescent trauma is under-represented in the archaeological record compared to adult trauma (Lewis, 2014; Lewis, 2018).

2.6 Social Determinants of Health

Based on the work of population health researchers (Marmot, 2005; Marmot & Wilkinson, 2000; Raphael, 1990, 2006), the World Health Organization (2024) defines social determinants of health (SDH) as non-biological factors that influence health outcomes and have an important influence on health inequities. Health is deeply impacted by the conditions in which people are born, grow, work, and live and lower socioeconomic status often results in worse health outcomes. Factors that may result in differential health outcomes include income and social protections, education, employment status and working conditions, food security, housing, and structural conflict amongst others (World Health Organization, 2024). SDH are particularly important for understanding who is likely to become sick or injured, and socioeconomic factors, including income, wealth, and education, are among the most important factors in determining health outcomes (Braveman & Gottlieb, 2014). According to Raphael (2006), factors that affect health operate at the structural and individual level. State or national systems can influence health through the unequal distribution of wealth, social stratification, and availability of welfare

services (structural violence), while identity may expose individuals to different factors and vulnerabilities that influence health at the community and individual level (Hahn, 2021; Viner et al., 2012). Hahn (2021) argues that SDH not only influence health over the life course, but also impact health at the population level, demographic distributions, and mortality patterns.

Socioeconomic status has clear connections to health in modern populations, and plays a role in determining access to resources, nutrition, and medical care (Miszkiewicz & Cooke, 2019), but SDH can also be applied to examine health trends in the past. In a series of articles examining health and mortality trends in England, Thomas McKeown and colleagues (McKeown & Brown, 1955; McKeown & Record, 1962; McKeown et al., 1975) traced the increase in population and decline in mortality between 1770 and 1960 to increased standards of living, including nutrition, sanitation, housing, and the availability of clean water. The use of SDH sheds light on patterns in health between and within contemporary populations (Marmot, 2005), and by reversing this equation, the patterning of disease and trauma in human skeletal remains can potentially be used to understand social inequalities and living standards in the past. For this reason, I use the SDH framework as the lens through which to examine patterns of fracture in young individuals, in an effort to understand their lifeways, and reconstruct the activities in which they engaged. By framing our understanding of mortality and health through the framework of SDH, we can better understand social processes influencing health outcomes in the past, and recenter our attention on the lived experiences of past peoples (Perry & Gowland, 2022).

2.7 Summary

De Vries & Van der Woude (1997) explain how economic expansion in the Netherlands during the early modern period (1500–1815 CE) led to a dense urban population, a relatively

high standard of living, and a flourishing labour market in the industrial sector. However, increased urbanization, rising skill premiums, and a shift in the distribution of incomes led to rising class divisions and social inequalities in the 17th and 18th centuries (van Zanden, 1995; van Zanden & van der Berg, 1993). This chapter presented the sociocultural context for 17th to 19th century urban Dutch sites of Arnhem, Eindhoven, Alkmaar, and Zwolle. Additionally, fracture mechanics and types, followed by fracture repair and complications, have been reviewed in-depth to provide background on fractures, their consequences, and their identification in developing bone. Moving forward, this thesis will examine fractures through the framework of social determinants of health in order to examine lifeways of children and adolescents in the past.

Chapter 3 Materials & Methods

3.1 Materials

The skeletal collections included in this study originate from four Dutch urban centers dating between the 17th and 19th centuries: Arnhem, Eindhoven, Alkmaar, and Zwolle (Table 3.1). The collections from Arnhem, Eindhoven, and Zwolle are held by the Department of Archaeology, Leiden University and the Alkmaar collection is held by Amsterdam UMC (AMC). Data collection took place in the Netherlands in May and June of 2022. A total of 61 individuals between 1–20 years of age were assessed. However, individuals for whom the level of preservation was below ~25% complete and/or for whom a precise age estimation was not possible, were excluded from study, resulting in a final sample size of 55 individuals. The focus of this research is on the activities and social roles of children and adolescents; therefore, a minimum age of one was selected as infants are largely dependent on their caregivers and have limited agency. The social age of adulthood in the post-medieval Netherlands varied between 21 and 25 years of age (Blom et al., 2021; van Nederveen Meerkerk & Schmidt 2008), a maximum age of 20 years was chosen for this research to guarantee that the examined individuals were considered social minors. Archaeological and contextual data for each site is provided in sections 3.1.1 to 3.1.4. Socioeconomic status for each site was ascertained based on provenience detailed in the following sections.

Table 3.1 *A list of the four sites under study with site codes, cemetery dates, and socioeconomic status.*

SITE	SITE CODE	DATES	SOCIOECONOMIC STATUS
ARNHEM	ARJB	1650–1829 CE	Low
EINDHOVEN	EHV-CK	1650–1850 CE	Low to Middle
ALKMAAR	GRK	1716–1830 CE	Middle to High
ZWOLLE	ZW87	1675–1828 CE	Middle to High

3.1.1 Arnhem

According to church records dating to 1821 CE, the cemetery at Eusebiuskerk covered an area of 0.36 ha. Excavations conducted in 2017 by Zielman and Baetsen (2020) uncovered primary graves in three locations north of the church containing five, 24, and 630 burials respectively, with the addition of several charnel pits. Excavation trenches focused on a 172 m^2 area in the uppermost layer, labeled WP10, where a total 495 primary burials were found, with an average of 3.9 graves per m^2. However, successive burials and continued use of the cemetery resulted in disturbed graves and a homogenous composition of burial deposits within the layer.

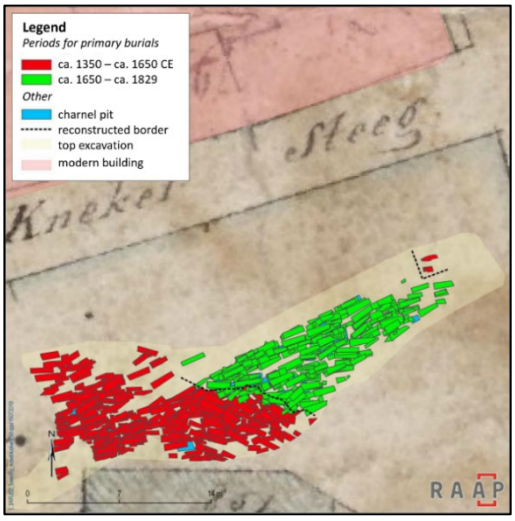

Figure 3.1 *Periodization of burials at Arnhem Eusebiuskerk (Source: after Zielman & Baetsen, 2020).*

Dating of the charnel pits and inhumations were based on artifact deposition, stratigraphy, and radiocarbon dating of bone collagen. Graves were periodized in the horizontal plane, with graves in the western section dating to pre-1650 and in the eastern portion dating to post-1650 CE (Fig. 3.1) (Zielman & Baetsen, 2020). All individuals included in this study were excavated from the eastern section of the cemetery, and therefore date to the period between 1650 and closure of the cemetery in 1829 CE (Casna & Schrader, 2022).

The Arnhem collection contributed the largest number of individuals to this study consisting of 26 individuals. The excavation area focused on the northern cemetery, which was the cheapest burial location available during the early modern period, indicating a lower socioeconomic status (Casna & Schrader, 2022; Casna et al. 2021). As such, the individuals from Arnhem represent the lowest socioeconomic status included in the present study.

3.1.2 Eindhoven

In 2002, a test pit measuring 3.2m by 8.5m was dug on the grounds of Eindhoven's Caterinakerk to find the foundations of the original medieval church and to determine the presence of skeletal remains. According to Arts (2019), who participated in the excavation, the original excavation included one burial with visible contours located in front of the altar foundation. The recovery of the remains of a child from this grave, with viable DNA, resulted in an extensive excavation of the cemetery in 2005 and 2006. Excavations were restricted to the eastern area of the former church, including the graveyard, and covered 376m^2. This area only accounts for about 5.5% of the original site as much of the graveyard and medieval church now lay beneath the modern church that was constructed in 1860-1867 CE. The location of the graves is associated with socioeconomic status due to the costs associated with burials. The northern cemetery represents the lower socioeconomic class as the cheapest burial option while the southern cemetery likely holds middle to lower socioeconomic status individuals. Burial inside the church choir was reserved for the elite or wealthy (Casna & Schrader, 2022). Five phases of construction of the church choir were discovered over the course of excavations, dating between the 14th and 17th/18th centuries (Arts, 2019).

A total of 754 primary burials and remains from a minimum of 303 secondary burials were recovered from within and outside the medieval church (Arts, 2019). Primary burials are defined as articulated whole or partial remains while secondary burials are isolated bones from previous burials which were disarticulated through human activity. Occasionally, these isolated remains were reburied in charnel pits, all of which date to the post-medieval period. All burials were found in a 1.8m layer and were often disturbed through the process of successive burials. But, using radiocarbon dating from five skeletal remains, stimulated luminescence dating of

brick foundations, coins, pottery, and a Harris-matrix, burials were grouped into four time periods: 1200-1350 (N=82), 1350-1500 (N=134), 1500-1650 (N=141), and 1650-1850 (N=260) (Arts, 2019). The remaining 162 individuals were undated.

A sample of individuals from Eindhoven underwent DNA analysis for a previous study by Baetsen and Weterings-Korthorst (2013). The results of the DNA analysis were available, but no DNA analysis was undertaken in the present study. All individuals included in this study date to the period between 1650 and 1850 CE which contained a total of 260 sets of remains. Unfortunately, the limited number of younger individuals and poor preservation resulted in only 11 individuals from Eindhoven being included in the analysis.

3.1.3 Alkmaar

Renovations to Alkmaar's Grote Kerk in 1994-1995 led to the excavation of 901 coffins and 62 bone boxes from beneath the church floors (Baetsen & Bitter, 2001). The floor of the church consists of 1755 gravestones, with between one and six coffins below each tombstone (Bitter, 2018). Each gravestone was lifted, and the burials excavated; therefore, the excavation map follows the same pattern as the gravestones (Fig. 3.2). Using burial records dating between 1716 and 1830 CE (Bitter, 2018), Steffan Baetsen and Bitter (2001) identified 298 individuals. Of these, researchers analyzed a random sample of 250 individuals. While the burial dates of the undocumented individuals are unknown, the high number of burials each year led to the removal of most graves from before the mid-18th century (Bitter, 2018). As such, the undocumented individuals likely fall within the 1716 to 1830

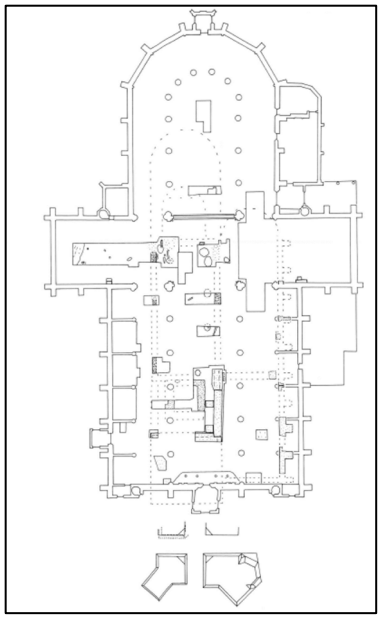

Figure 3.2 *Excavation trenches at Grote Kerk, Alkmaar (Source: Bitter, 2002).*

CE period. Many children were located in graves lining the edges of the floor, where space restrictions prevented late adolescent and adult burials (Bitter, 2018). Graves located inside the church represent the middle to upper social class, as burial inside the church was more expensive than burial in the cemetery outside. In total, 12 individuals from the Grote Kerk collection were analyzed, among these, there are burial records for four individuals with information pertaining to age and sex.

3.1.4 Zwolle

Large-scale renovations to Broerenkerk led to the excavation of 529 individuals from beneath the church floors between 1987 and 1988. Burial registers covering the final period of use, between 1819 and 1828 CE, were available, however, few gravestones remained in their original positions. As a result, researchers were only able to identify a total of 141 individuals (Aten & Clevis, 2019; Casna & Schrader, 2022). According to Aten and Clevis (2019), excavations began by reordering the gravestones to reconstruct the original pattern of graves, followed by manual exhumation carried out by volunteers. Trenches measured two meters wide with a maximum depth of two and a half meters. A single grave pit contained up to six superimposed burials. Excavation trenches were positioned to maximize exhumations of children and individuals dating to the 1819-1828 period, resulting in the over-representation of children in the sample (Aten & Clevis, 2019). Individuals buried inside Broerenkerk represent the middle to upper socioeconomic classes, with the wealthiest individuals from Zwolle being primarily buried at the main church, Grote of St. Michaelskerk, and lower-class citizens only being able to afford burial outside the church (Casna & Schrader, 2022). Only a portion of the collection from Zwolle was housed at the University of Leiden and available for analysis. A total of six individuals from

Zwolle were included in this study. Among these, burial records indicating biological sex and age were available for three individuals.

3.2 Methods

3.2.1 Fracture Identification

All available skeletal elements were examined macroscopically for evidence of fracture, and all ante-mortem fracture types were considered, including fractures caused by direct or indirect trauma, stress, and underlying pathological conditions. Fracture assessment relied on identifying features consistent with fresh bone fractures as described by Lovell (1997) (see section 2.5). Fracture recording methods were adapted from "Trauma Analysis in Paleopathology*"* (Lovell, 1997) and "Trauma*"* (Redfern & Roberts, 2019). The bone, side, and segment for each suspected fracture was recorded and characteristics of the fracture profile, including taphonomic changes and evidence of healing were considered during the assessment of fracture presence. A summary of characteristics used to determine ante- and post-mortem fractures are available in Table 3.2. A detailed description of the appearance, and the characteristics of the fracture, were recorded and a list of potential fracture complications were considered. Fractures with clear evidence of healing were marked as present, suspected peri-mortem fractures were further analyzed with microscopic and micro-computed tomography (micro-CT) imaging (see section 3.2.2) to distinguish ante-mortem from post-mortem fractures.

Table 3.2 *List of characteristics considered in the designation of antemortem and postmortem fractures.*

FRACTURE PROFILE	HEALING PROFILE
Smooth / Even Fracture Margins	Rounded Fracture Margins
Hinging	New Bone Formation
Hairline Fracture	Cortical Striations
Depressed Cortical Surface	Sclerosis of Margins
Defined Fracture Line	Lamellar Conversion
Discoloration	Pitting
Sharp Fracture Margin	Woven / Lamellar Callus Formation

If less than 25% of a skeletal element was preserved, the element was excluded from analysis, with the exception of the cranial vault and the vertebrae. Following Dittmar et al. (2021), bones that make up the cranial vault (combined occipital, frontal, and parietals) required over 75% to be preserved to be considered for analysis. Due to the inconsistent preservation of vertebrae, each spinal level (cervical (C), thoracic (T), lumbar (L)) has been considered separately. Following Maat and Mastwijk (2000), only individuals with an adequate number of vertebrae (>50% per level) (Maat, personal communication, 2023) have been included in the analysis. Each fractured vertebra is counted as a single fracture, even if the vertebra shows evidence for two types of fractures (e.g. a compression fracture and Schmorl's node). In this thesis, 'endplate defects' are considered when either the superior or inferior vertebral endplate does not meet the anterior edge of the vertebral body. The edges of the endplate in these cases are smooth and rounded, often with uneven projections of bone reaching towards the anterior edge of the vertebra. The bone appears to be well-remodeled, with no or little reactive or porous bone present. They have been counted as fractures in the prevalence results and statistical testing. The data collection form, containing methods for age and biological sex estimations and fracture recording can be found in Appendix A. All methods of analysis were non-destructive, and ethics permission was granted from the Hamilton Integrated Research Ethics Board (project 16436).

3.2.2 Post-Traumatic Time Interval

An analysis of the post-traumatic time interval has been undertaken for all fractures. An analysis of the post-traumatic time interval provides additional descriptive clarity for ante-mortem fractures from archaeological contexts and may provide insight into health status and care at the time of death and information on injury recidivism (de Boer et al., 2013; Spencer, 2012). Because the rate of fracture healing is dependent on age, different fracture healing

estimates have been applied for different age categories. While descriptions of fracture repair and stages of healing vary between researchers, Prosser et al. (2012), Islam et al. (2000), and Viero et al. (2020) have been chosen because they offer comparable stages of fracture healing combined with characteristics that are visible in dry bone. Stages of fracture healing can overlap (Islam et al., 2000; Prosser et al., 2012; Viero et al., 2020), and nutritional status, fracture severity, and health status can affect rates of fracture repair (see section 2.5.5.1). All post-traumatic time interval reference studies were conducted on otherwise healthy children, and the health status of that archaeological sample prior to death is unknown. Consequently, the post-traumatic time intervals discussed in this thesis are an estimate based on the available evidence. Stages of fracture repair for ages 1-5, 6-13, and 14+ with estimated post-traumatic time intervals are available in Table 3.3.

Table 3.3 *Table showing stages of fracture repair with post-traumatic time interval estimate by age category. Range describes the first appearance to final appearance of features in all study participants, while peak is the strongest appearance of the features (Source: adapted from Islam et al. (2000), Prosser et al. (2012), and Viero et al. (2021)).*

Fracture Repair Stage	Features repair stage	Age Category	Post-traumatic Time Interval Range (Days)	Post-traumatic Time Interval Peak (Days)
Stage 1	Periosteal reaction and sclerosis of fracture margin	1-5 years	5-96	15-35
		6-13 years	21-84[1]	28-42[1]
		14+ years	9-142	23-51
Stage 2	Soft callus formation defined by appearance of reactive new bone	1-5 years	12-66	22-35
		6-13 years	14-98	28-49
		14+ years	22-179[3]	68.6[3]
Stage 3	Hard callus with well demarcated and dense new bone	1-5 years	19-96	>22
		6-13 years	35-98	91
		14+ years	22-179[2]	68.6[2]
Stage 4	Loss of a defined fracture line with complete bridging by soft- or hard-callus	1-5 years	19-300	>36
		6-13 years	35-98	91
		14+ years	30-160	76.3
Stage 5	Complete healing with gradual loss of focal callus	1-5 years	45-421	>36
		6-13 years	28-730	>49
		14+ years	29-385	147.7

[1]*Limited radiographs were available between 7- and 14-days post-trauma and visibility was impacted by the presence of casts.*

[2]*Viero et al. (2021) did not differentiate between soft- and hard-callus, therefore the estimate encompasses both stages.*

For individuals five years and younger, fracture repair stages and associated time estimates by Prosser et al. (2012) have been applied. The authors used radiographic images of fractures in children <5 years to create six stages of fracture repair based on evidence of healing. For each stage, the day at which features were first recorded, the peak period in days for recorded features, and the last day at which features were recorded were noted, providing a time range in days for each fracture repair stage. For individuals aged six to 13 years, fracture repair stages and time estimates have been drawn from Islam et al. (2000). The researchers established stages of fracture repair and post-traumatic time intervals based on radiographs of children and adolescents aged 1 to 17 years with a mean age of 8.4 years for males and 7.1 years for females. The time intervals are provided in weeks but have been converted to days to conform to the Prosser et al. (2012) and Viero et al. (2020) studies. For individuals aged 14+ years, a post-traumatic time interval estimation based on adults (20≥ years) was applied (Viero et al., 2020). Viero et al. (2020) divided fracture repair into six categories based on radiographic features; however, the authors did not differentiate between soft and hard callus formation, therefore the estimated time interval encompasses both stages.

Micro-CT imaging provides increased resolution and clarity compared to X-ray imaging, resulting in a higher level of detail available to researchers. For example, subtle signs of healing, such a sclerosis of the fracture margins, are likely more visible in micro-CT reconstructions than x-rays. As a result, there are limitations in comparing micro-CT reconstructions to radiographs and the post-traumatic time intervals established in the clinical studies may overestimate the time at which features first appear. The use of reference studies employing x-ray imaging as a comparison for the micro-CT reconstructions employed in this study may have resulted in a margin of error in the post-traumatic time-interval estimates.

3.2.3 Imaging

A sample of skeletal elements with evidence for fracture were further analyzed using microscopic and micro-computed tomography (micro-CT) imaging to examine the cortical and trabecular structures. A portable Keyence VHX- 2000 digital microscope was used to examine the margins of suspected ante-mortem fractures to identify bone spicules, woven bone, margin discoloration, and smoothing. A total of 13 skeletal elements were also scanned using a Nikon XT H 225 ST micro-CT scanner at the Museum of Ontario Archaeology, Western University, London, Ontario, Canada. Micro-CT scan parameters were as follows: Tungsten target; 115 kV; 75 µA; 3141 projections with 1 second exposure and a voxel size between 15 µm and 30.9 µm depending on the size of the element. Different voxel sizes were selected to maximize the resolution for each reconstruction. Micro-CT scans were reconstructed using CT Pro and analysed with Dragonfly (v. 2021.3) software. A list of individuals and their associated elements, as well as the voxel size for each scan, can be found in Table 3.4.

Table 3.4 *Individuals and associated skeletal elements with voxel sizes for micro-CT scans.*

INDIVIDUAL	ELEMENTS SCANNED	VOXEL SIZE (UM)
ARJB V556	Fifth Lumbar Vertebra	29.2
ARJB V1437	Fourth Lumbar Vertebra	29.2
ARJB V1463	Fourth Thoracic Vertebra	22.5
ARJB V1556	Fifth Lumbar Vertebra	29.2
ARJB V1827	Eleventh Thoracic Vertebra	29.2
ARJB V1890	Right Femur	28.75
ARJB V1912	Fourth Lumbar Vertebra	29.2
EHV-CK S979	Left Zygomatic	19
EHV-CK S2567	Left Humerus	24.7
EHV-CK S3507	Fourth Lumbar Vertebra	30.9
GRK V59	Left Fibula	15
ZW87 235	Fifth Cervical Vertebra	22.5

3.2.4 Statistical Analysis

Fischer's Exact tests were used to investigate statistically significant associations (α=0.05) between fractures, biological sex, and socioeconomic status. A Fischer's exact test uses contingency tables, which examine the interactions between two variables, and are often employed when sample sizes are small. Fischer's exact tests have been chosen over a chi-squared test because with chi-square the approximated sampling distribution is poor when the sample size is small. The null hypothesis for all statistical tests assumed there was no association between variables.

3.2.5 Age Estimation

Age estimation used a combination of dental development and eruption and epiphyseal fusion. Multiple methods were employed because not all skeletal and dental elements are consistently represented across individuals. For individuals aged ~<16 years, preference was given to dental development and eruption when estimated ranges based on dentition and epiphyseal fusion disagreed. For individuals aged ~>16 years, epiphyseal fusion was favoured due to the variability in the timing of the development and eruption of the third molar (AlQahtani et al., 2010). Past the age of puberty, the ability to estimate age via epiphyseal fusion also becomes more accurate due to the ability to differentiate between sex-based rates of development (Scheuer & Black, 2004).

Age categories have been adapted from *The Juvenile Skeleton* (Scheuer & Black, 2004, p. 6) and "Exploring adolescence as a key life history stage in bioarchaeology" (Lewis, 2022). Individuals were divided into five categories based on estimated age ranges: early childhood (1-5 years), late childhood (6-9 years), early adolescence (10-14 years), middle adolescence (15-17 years), and late adolescence (18+ years) (Lewis, 2022; Scheuer & Black, 2004). A median age

for each individual was estimated from the available data, which was then used to assign the individual to an age category. Burial records provided a known age for seven individuals.

3.2.5.1 Dental Development and Eruption

Humans have two sets of dentition: deciduous and permanent. The period of development for all dentition begins around six weeks in utero and eruption continues into early adulthood, providing the means for accurate age-at-death estimates (AlQahtani et al., 2008). The development, eruption, and shedding of dentition occur at relatively predictable rates based on genetics, and while sex and individual variation may impact the timing and sequence of events, dental development and eruption is less impacted by environment and therefore provides a more reliable age-at-death estimate than other methods (AlQahtani et al., 2008; Lewis, 2006; White & Folkens, 2005). Age estimations were based on an analysis of each tooth, and then a range was created considering all available detention.

The London Atlas of human tooth development and eruption (2008) provides age estimations between 28 weeks in utero and 23 years. The atlas was developed using human remains of known individuals for ages 28 weeks in utero to two years from the Spitalfields Collection and the Maurice Stack Collection. For ages two through 24 years, archived panoramic radiographs from the Institute of Dentistry, Barts and the London School of Medicine and Dentistry were assessed. The materials included males and females, and while approximately half the radiographs were from white individuals and half from Bangladeshi individuals, the mean timing for tooth development and eruption was not significantly different between groups (AlQahtani et al., 2008). The varied sex, ancestry, and lifeways of the individuals allows for precise age estimations and is applicable to a European sample. The London Atlas was chosen over Gustafson and Koch (1974) and Ubelaker (1989) because Gustafson and Koch only provide

age estimations up to 16 years, which does not cover the middle and late adolescent individuals included in this study, and Ubelaker's atlas was created using the remains of Indigenous Native Americans, which are not applicable to a European setting.

3.2.5.2 Epiphyseal Fusion

Ossification centers appear and fuse through the entire period of skeletal development, therefore, age may be estimated for individuals still undergoing growth and development using the timing in the appearance and fusion of ossification centers (Scheuer and Black, 2004). Age estimates for epiphyseal fusion are drawn from Scheuer and Black's *The Juvenile Skeleton* (2004) and Cardoso (2008a, 2008b, 2011). Scheuer and Black (2004) provide detailed information on the timing of epiphyseal fusion for both males and females, from in utero development to final fusion of the medial clavicle at approximately 30 years of age. Scheuer and Black account for differences in sex-based rates of development by providing separate age ranges for fusion timing for males and females.

In his study of epiphyseal fusion in adolescents, Cardoso (2008a, 2008b, 2011) created age ranges for epiphyseal fusion based on individuals of known identity from the Lisbon documented skeletal collection. This collection is more temporally and geographically contemporaneous to the sites included in this study, and individuals are of a lower socio-economic status, which may more accurately reflect conditions in the past. Cardoso primarily focuses on fusion during adolescence and provides separate age ranges for males and females. Only features with a combined sample size of greater than ten individuals were considered, which includes: the proximal humerus, the distal radius, the iliac crest, the femoral head, the proximal tibia, and the vertebral annular rings.

Final age estimates considered each available ossification center, and a range was created based on the available data. Epiphyseal fusion was chosen over long bone length because stature varies considerably between the sexes, between populations, and between individuals (Scheuer & Black 2004).

3.2.6 Sex Estimation

Sex estimation is based on sexually dimorphic features of the skeleton; however, the expression of dimorphism varies between populations and individuals and generally only appear following the release of reproductive hormones during puberty (Rogers, 2009). Sex estimations of children are generally considered unreliable (Buckberry, 2018; Rogers, 2009; Scheuer & Black, 2004; Wilson & Humphrey, 2017). For this reason, sex estimations were only done for individuals aged 15 years and older (middle and late adolescents) or if puberty had already commenced as evidenced by fusion centers in the sacrum and ossa coxae (Scheuer & Black, 2004). Sex estimates involved standard methods used for adults based on the cranium and pelvis (Buikstra and Ubelaker, 1994). Because of the young age of many individuals, sex estimation methods with a high accuracy rate for adolescent populations, including sexually dimorphic features in the distal humerus (Rogers, 2009), were also considered. In cases of disagreement, sex estimates based on pubic morphology were given preference because it is the most reliable indicator of sex (Buikstra & Ubelaker, 1994).

Sex estimations conformed to standard categories of Undetermined, Male, Probable Male, Ambiguous, Probable Female, and Female (Buikstra and Ubelaker, 1994). The designation of Undetermined was used when poor preservation precluded the ability to assess sex and when a sex estimation was not undertaken due to age. Of the 55 individuals included in this study, 12

individuals were evaluated for sex. Sex was known for an additional ten individuals through burial records or previous DNA analysis (Baetsen & Weterings-Korthorst, 2013).

3.2.6.1 Pelvic Morphology

The pelvis is the most sexually dimorphic skeletal element and provides the most reliable indicator of sex in skeletal remains (Buikstra & Ubelaker, 1994). Four characteristics, as outlined in *Standards for Data Collection of Human Remain*s (Buikstra & Ubelaker, 1994), were used to assess sex. Females typically represent positive expressions of the ventral arc, subpubic concavity, and ischiopubic ramus ridge. These traits were scored as either more male or more female and the greater sciatic notch was scored on a five-point scale with females typically exhibiting a lower score.

Ventral arc: in females the ventral arc is more squared and in males slopes inferiorly.

Subpubic concavity: in females the ischiopubic ramus is concave, in males it is more convex.

Ischiopubic ridge: in females the ischiopubic ramus directly inferior to the pubic symphysis forms a crest-like ridge, in males it is broad and flat.

Angle of the greater sciatic notch: the notch tends to be broad in females and narrow in males.

3.2.6.2 Cranial Traits

Sexual dimorphism in the adult cranium is marked by variations in size, shape, and robusticity, with males generally having larger and more robust crania (Buikstra & Ubelaker, 1994). Five cranial features, as described in *Standards for Data Collection of Human Remain*s (Buikstra & Ubelaker, 1994), were scored on a five-point scale. Gracile, more feminine features score lower and more robust, masculine characteristics score higher. All features were scored

independently, and sex was estimated considering all available data. The cranial features assessed include:

Nuchal Crest: in males the nuchal crest is more rugose and projecting, in females it is less developed and smooth.

Mastoid Process: in males the mastoid process is more voluminous in proportion to the surrounding structures, in females it is less developed and smaller.

Supraorbital Margin: in males the supraorbital margin is thicker and more rounded, in females the margin is thinner and sharper.

Supraorbital Ridge: in males the supraorbital ridge is more prominent with a rounded projection, in females it is less developed and smooth with little or no projection.

Mental Eminence: males typically exhibit a larger mental eminence that occupies most of the anterior portion of the mandible, females typically exhibit minimal expression with little or no projection beyond the surrounding bone.

3.2.6.3 Distal Humerus

Sexual dimorphism in the posterior distal humerus is related to the carrying angle of the arm, or the lateral deviation of the forearm from the humeral axis (Rogers, 1999). Males exhibit a carrying angle of approximately ten to 15 degrees whereas in females the approximate deviation is 20 to 25 degrees (Rogers, 1999). Differences in the carrying angle result in variations in the morphology of the posterior distal humerus. While originally developed for adults, Rogers (2009) found the accuracy of sex estimation using the distal humerus in adolescent individuals, aged 11 to 20 years, to be 81%. Sexually dimorphic features include:

Olecranon fossa depth/shape: females exhibit a deep oval fossa while males show a shallow triangular shape.

Angle of the medial epicondyle: in males the epicondyle is flat and in females it is angled posteriorly.

Trochlear constriction: in females the trochlea is more constricted and spindle-shaped and less constricted in males.

Trochlear symmetry: in males the trochlea is asymmetric and in females symmetric.

3.3 Summary

The materials used in this study are drawn from the four post-medieval, urban sites of Arnhem, Eindhoven, Alkmaar, and Zwolle from the Netherlands. A total of 51 individuals between 1–20 years of age were assessed. Methods for estimating age and sex conformed to standard protocols while the identification and recording of fractures was adapted from recommended methodologies. The use of established bioarchaeological methods allows for the duplication and comparison of data across sites in future studies. All methods of analysis were non-destructive, and ethics permission was granted from the Hamilton Integrated Research Ethics Board (project 16436).

Chapter 4 Results

The following chapter presents the results of the age and sex estimations for all individuals and information pertaining to the observed fractures. Results of the age and sex estimates, along with socioeconomic status are available in Appendix B. Each fracture will be reviewed in depth, with descriptions of the macroscopic appearance and, when available, additional information provided by microscopy and micro-CT imaging. In addition, characteristics evincing healing are used to approximate the timing of fractures prior to death (see section 3.2.2). A total of 47 fractures were observed across 16 individuals. The raw data for all individuals analyzed is available in Appendix C. Additional photos of the macroscopic appearance of fractures, and micro-CT and microscopy images, when available, can be found in Appendix D. Statistical equations for the analyses are available in Appendix E.

4.1 Age and Biological Sex Estimations

Distributions for age and sex by collection are plotted in Table 4.1. Across all collections, deaths during early childhood (1-5 years) accounted for the largest number of individuals assessed. Of the individuals assessed from Arnhem and Eindhoven there is an increase in the number of individuals represented from the early and middle adolescent periods, and these increases are reflected in the overall age-at-death distribution. There is a total of 18 individuals with sex estimations, with relatively equal representation of males and females. Males and probable males and females and probable females have been grouped together to allow for analysis.

Table 4.1 *Number of analyzed individuals from each collection by age and sex*.*

Arnhem (ARJB)								
Age Category	Male	Probable Male	Ambiguous	Probable Female	Female	Undetermined	Total	% of Sample (n=26)
Early Child (1-5)	0	0	0	0	0	10	10	38.5 (10/26)
Late Child (6-9)	0	0	0	0	0	3	3	11.5 (3/26)
Early Adolescent (10-14)	0	1	1	0	0	4	6	23.1 (6/26)
Middle Adolescent (15-17)	0	2	0	3	1	1	7	26.9 (7/26)
Late Adolescent (18+)	0	0	0	0	0	0	0	0 (0/26)
Eindhoven (EHV-CK)								
Age Category	Male	Probable Male	Ambiguous	Probable Female	Female	Undetermined	Total	% of Sample (n=11)
Early Child (1-5)	1	0	0	1	0	1	3	27.3 (3/11)
Late Child (6-9)	1	0	0	0	1	0	2	18.2 (2/11)
Early Adolescent (10-14)	0	0	0	0	0	4	4	36.3 (4/11)
Middle Adolescent (15-17)	1	0	0	0	1	0	2	18.2 (2/11)
Late Adolescent (18+)	0	0	0	0	0	0	0	0 (0/11)
Alkmaar (GRK)								
Age Category	Male	Probable Male	Ambiguous	Probable Female	Female	Undetermined	Total	% of Sample (n=12)
Early Child (1-5)	0	0	0	0	0	6	6	50.0 (6/12)
Late Child (6-9)	1	0	0	0	0	2	3	25.0 (3/12)
Early Adolescent (10-14)	0	0	0	0	0	2	2	16.7 (2/12)
Middle Adolescent (15-17)	1	0	0	0	0	0	1	8.3 (1/12)
Late Adolescent (18+)	0	0	0	0	0	0	0	0 (0/12)
Zwolle (ZW-87)								
Age Category	Male	Probable Male	Ambiguous	Probable Female	Female	Undetermined	Total	% of Sample (n=6)
Early Child (1-5)	0	0	0	0	0	2	2	33.2 (2/6)
Late Child (6-9)	0	0	0	0	0	1	1	16.7 (1/6)
Early Adolescent (10-14)	0	0	0	0	0	1	1	16.7 (1/6)
Middle Adolescent (15-17)	0	0	0	1	0	0	1	16.7 (1.6)
Late Adolescent (18+)	0	0	0	0	1	0	1	16.7 (1/6)
Total								
Age Category	Male	Probable Male	Ambiguous	Probable Female	Female	Undetermined	Total	% of Sample (n=55)
Early Child (1-5)	1	0	0	1	0	19	21	38.2 (21/55)
Late Child (6-9)	2	0	0	0	1	6	9	16.4 (9/55)
Early Adolescent (10-14)	0	1	1	0	0	11	13	23.6 (13/55)
Middle Adolescent (15-17)	2	2	0	4	2	1	11	20.0 (11/55)
Late Adolescent (18+)	0	0	0	0	1	0	1	1.8 (1/55)

** The ambiguous category contains individuals with observable sex features but who could not be classified with certainty. The undetermined category contains individuals that were too young to undergo a sex estimation (<15) and individuals with insufficient sex features.*

4.2 Fracture Prevalence

Of the 55 individuals analyzed, 16 (29.1%) showed evidence for ante-mortem fractures. The distribution of the overall crude fracture prevalence (per individual) (CP) by site is illustrated in Figure 4.1. When accounting for the number of individuals in each collection, crude prevalence is as follows: Arnhem 26.9% (7/26), Eindhoven 36.4% (4/11), Alkmaar 16.7% (2/12), and Zwolle 50% (3/6). The high crude prevalence in Zwolle may be biased by which remains were kept onsite at Leiden University, with preference given to those with pathological conditions. The lower socioeconomic sites of Arnhem and Eindhoven have a combined crude

prevalence of fracture of 30.6% (11/36) and the higher socioeconomic sites of Alkmaar and Zwolle have a combined crude prevalence of 27.8% (5/18). A Fischer's Exact test for significance found no correlation between the presence of at least one fracture and socioeconomic status ($p>0.05$). The distribution of fractures by age and sex categories are available in Table 4.2. The overall pattern shows a rise in fracture prevalence in those that died during the middle adolescent period (63.6%, 7/11) followed by the early adolescent period (30.8%, 4/13). The prevalence of fractures for the late adolescence category is 100% but is skewed by small sample size (n=1), as a result, they have been excluded from further analysis. The crude prevalence of fracture among females is 66.7% (6/9) and 50% (4/8) for males. A Fischer's Exact test for significance found no correlation between biological sex and fractures ($p>0.05$). Crude and true prevalence by site and age is available in Table 4.3.

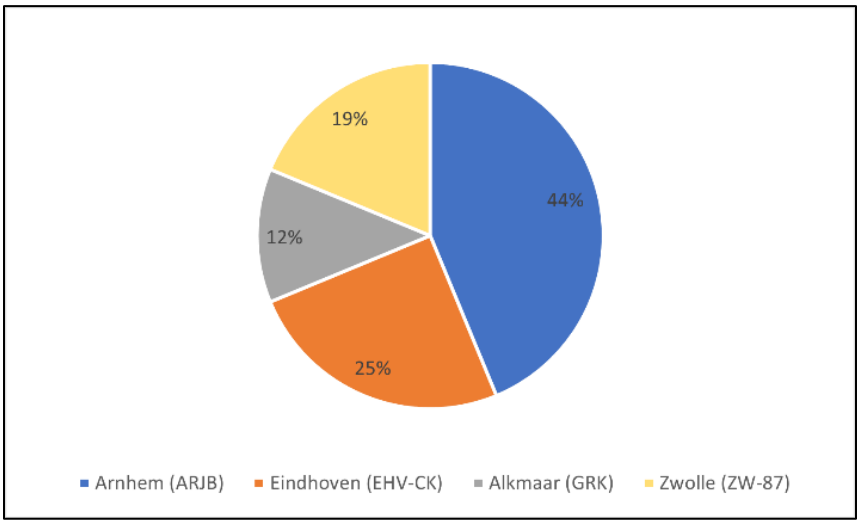

Figure 4.1 *Pie chart displaying the distribution of crude fracture prevalence by site.*

Table 4.2 *Individuals with evidence of fracture by age and biological sex* for each collection.*

Arnhem (ARJB)								
Age Category	Male	Probable Male	Ambiguous	Probable Female	Female	Undetermined	Total	% of Sample (n=26)
Early Child (1-5)	0	0	0	0	0	0	0	0 (0/26)
Late Child (6-9)	0	0	0	0	0	0	0	0 (0/26)
Early Adolescent (10-14)	0	1	1	0	0	0	2	7.7 (2/26)
Middle Adolescent (15-17)	0	1	0	2	1	1	5	19.2 (5/26)
Late Adolescent (18+)	0	0	0	0	0	0	0	0 (0/26)
Eindhoven (EHV-CK)								
Age Category	Male	Probable Male	Ambiguous	Probable Female	Female	Undetermined	Total	% of Sample (n=11)
Early Child (1-5)	1	0	0	0	0	0	1	9.1 (1/11)
Late Child (6-9)	0	0	0	0	1	0	1	9.1 (1/11)
Early Adolescent (10-14)	0	0	0	0	0	1	1	9.1 (1/11)
Middle Adolescent (15-17)	0	0	0	0	1	0	1	9.1 (1/11)
Late Adolescent (18+)	0	0	0	0	0	0	0	0 (0/11)
Alkmaar (GRK)								
Age Category	Male	Probable Male	Ambiguous	Probable Female	Female	Undetermined	Total	% of Sample (n=12)
Early Child (1-5)	0	0	0	0	0	0	0	0 (0/12)
Late Child (6-9)	0	0	0	0	0	0	0	0 (0/12)
Early Adolescent (10-14)	0	0	0	0	0	1	1	8.3 (1/12)
Middle Adolescent (15-17)	1	0	0	0	0	0	1	8.3 (1/12)
Late Adolescent (18+)	0	0	0	0	0	0	0	0 (0/12)
Zwolle (ZW-87)								
Age Category	Male	Probable Male	Ambiguous	Probable Female	Female	Undetermined	Total	% of Sample (n=6)
Early Child (1-5)	0	0	0	0	0	1	1	16.7 (1/6)
Late Child (6-9)	0	0	0	0	0	1	1	16.7 (1/6)
Early Adolescent (10-14)	0	0	0	0	0	0	0	0 (0/6)
Middle Adolescent (15-17)	0	0	0	0	0	0	0	0 (0/6)
Late Adolescent (18+)	0	0	0	0	1	0	1	16.7 (1/6)
Total								
Age Category	Male	Probable Male	Ambiguous	Probable Female	Female	Undetermined	Total	% of Sample (n=55)
Early Child (1-5)	1	0	0	0	0	1	2	3.6 (2/55)
Late Child (6-9)	0	0	0	0	1	1	2	3.6 (2/55)
Early Adolescent (10-14)	0	1	1	0	0	2	4	7.3 (4/55)
Middle Adolescent (15-17)	1	1	0	2	2	1	7	12.7 (7/55)
Late Adolescent (18+)	0	0	0	0	1	0	1	1.8 (1/55)

** The ambiguous category contains individuals with observable sex features but who could not be classified with certainty. The undetermined category contains individuals that were too young to undergo a sex estimation (<15) and individuals with insufficient sex features.*

Table 4.3 *Crude and true fracture prevalence across sites by age categories and fracture location.*

Collection	Age Category	Individual		Element															
				Fibula		Humerus		Cranial Vault		Zygomatic		Rib		Cervical Vertebra		Thoracic Vertebra		Lumbar Vertebra	
		n/N	CP (%)	n/N	TP (%)	n/N	TP (%)	n/N	TP (%)	n/N	TP (%)	n/N	TP (%)	n/N	TP (%)	n/N	TP (%)	n/N	TP (%)
Arnhem (ARJB)	Early Child (1-5)	0/10	0	0/3	0	0/12	0	0/3	0	0/4	0	0/164	0	0/24	0	0/58	0	0/27	0
	Late Child (6-9)	0/3	0	0/2	0	0/5	0	0/2	0	0/3	0	0/38	0	0/16	0	0/21	0	0/10	0
	Early Adolescent (10-14)	2/5	40	0/9	0	0/8	0	0/3	0	0/5	0	0/77	0	0/29	0	0/53	0	7/25	28
	Middle Adolescent (15-17)	5/8	62.5	0/11	0	0/16	0	0/7	0	0/12	0	0/167	0	0/56	0	17/94	18.1	5/34	14.3
	Late Adolescent (18+)	0/0	-	0/0	-	0/0	-	0/0	-	0/0	-	0/0	-	0/0	-	0/0	-	0/0	-
Eindhoven (EHV-CK)	Early Child (1-5)	1/3	33.3	0/1	0	1/5	20	0/2	0	0/3	0	0/28	0	0/10	0	0/14	0	0/6	0
	Late Child (6-9)	1/2	50	0/0	-	0/3	0	0/2	0	1/4	25	0/36	0	0/13	0	0/18	0	0/3	0
	Early Adolescent (10-14)	1/4	25	0/3	0	0/5	0	0/0	-	0/0	-	0/57	0	0/7	0	1/27	3.7	3/12	25
	Middle Adolescent (15-17)	1/2	50	0/1	0	0/4	0	0/1	0	0/2	0	0/35	0	0/8	0	0/18	0	1/8	12.5
	Late Adolescent (18+)	0/0	-	0/0	-	0/0	-	0/0	-	0/0	-	0/0	-	0/0	-	0/0	-	0/0	-
Alkmaar (GRK)	Early Child (1-5)	0/6	0	0/5	0	0/8	0	0/6	0	0/10	0	0/87	0	0/35	0	0/36	0	0/14	0
	Late Child (6-9)	0/3	0	0/4	0	0/6	0	0/3	0	0/6	25	0/56	0	0/21	0	0/35	0	0/15	0
	Early Adolescent (10-14)	1/2	50	1/4	25	0/4	0	0/1	0	0/2	0	0/0	-	0/0	-	0/0	-	0/0	-
	Middle Adolescent (15-17)	1/1	100	0/2	0	0/2	0	1/1	100	0/2	0	0/0	-	0/0	-	0/0	-	0/3	0
	Late Adolescent (18+)	0/0	-	0/0	-	0/0	-	0/0	-	0/0	-	0/0	-	0/0	-	0/0	-	0/0	-
Zwolle (ZW-87)	Early Child (1-5)	1/2	50	0/3	0	0/4	0	0/1	0	0/2	0	0/48	0	3/7	42.9	2/19	10.5	0/10	0
	Late Child (6-9)	1/1	100	0/1	0	0/2	0	0/1	0	0/2	0	3/16	18.8	0/2	0	0/0	-	0/0	-
	Early Adolescent (10-14)	0/1	50	0/1	0	0/2	0	0/1	0	0/1	0	0/0	0	0/0	-	0/3	0	0/1	0
	Middle Adolescent (15-17)	0/1	0	0/2	0	0/2	0	0/1	0	0/2	0	0/6	0	0/1	0	0/7	0	0/1	0
	Late Adolescent (18+)	1/1	100	0/2	0	0/2	0	0/1	0	0/2	0	1/24	4.2	0/0	-	0/1	0	0/0	-
All Collections	Early Child (1-5)	2/21	9.5	0/12	0	1/29	3.4	0/12	0	0/19	0	0/327	0	3/76	3.9	2/127	1.6	0/57	0
	Late Child (6-9)	2/9	22.2	0/7	0	0/16	0	0/8	0	1/15	6.7	3/16	18.8	0/52	0	0/74	0	0/28	0
	Early Adolescent (10-14)	4/12	33.3	1/17	5.9	0/19	0	0/5	0	0/8	0	0/0	0	0/36	0	1/83	1.2	10/38	26.3
	Middle Adolescent (15-17)	7/12	58.3	0/16	0	0/24	0	1/10	10	0/18	0	0/6	0	0/65	0	17/119	14.3	6/46	13
	Late Adolescent (18+)	1/1	100	0/2	0	0/2	0	0/1	0	0/2	0	1/24	4.2	0/0	-	0/1	0	0/0	-
Totals		16/55	29.1	1/54	1.9	1/90	1.1	1/36	2.8	1/62	1.6	4/373	1.1	3/229	1.3	20/404	5	16/169	9.5

n = number of individuals with fracture; N = total number of individuals
CP = crude prevalence (number of fractures by individual); TP = true prevalence (number of fractures by skeletal element)

4.2.1 Vertebral Fractures

Vertebral fractures were the most common type of fracture across all collections, accounting for 33/47 (70.2%) of the observed fractures and affecting 10/55 (18.2%) individuals. Vertebral fractures occurred overwhelmingly in the individuals from Arnhem (ARJB) and Eindhoven (EHV-CK), with only a single higher status individual (ZW-87 235) exhibiting spinal trauma. All but one individual (EHV-CK S2918) exhibited fractures in more than one vertebra, affecting primarily the thoracic and lumbar levels. True prevalence of fracture by spinal level is available in Table 4.3. The majority of fractures affecting the vertebrae are compression fractures (n=8) and Schmorl's nodes (n=8); co-occurrence of vertebral compression fractures and Schmorl's nodes was evident in 6 individuals. A summary of vertebrae affected by Schmorl's nodes, compression fractures, and burst fractures can be found in Table 4.4. Vertebral compression fractures are concentrated between T3-T8 and L2-L5. Schmorl's nodes are concentrated between T7-L3. A Fischer's Exact test for significance found a statistically significant association ($p<0.05$) between the presence of compression fractures and Schmorl's nodes in a single individual (see Appendix E). Due to the statistical correlation, Schmorl's nodes are counted as fractures for the purposes of this thesis and have been grouped together with the compression fractures as occurring through similar fracture mechanisms. However, the compression fractures in ZW-87 235 likely resulted through a different fracture mechanism due to their location (affecting the lower cervical and upper thoracic vertebrae) and the young age of the individual (early child), therefore, they will be analysed separately. A Fischer's Exact test for significance was also used to examine the association between vertebral fracture (discounting individual ZW-87 235) and socioeconomic status at the individual level. While there is no association between socioeconomic status and all fracture types, there is a significant correlation

between low- to mid-socioeconomic status and vertebral fractures ($p<0.05$) (see Appendix E). Reasons for this correlation will be discussed in chapter 5.

Table 4.4 *Vertebral level (thoracic (T) and lumbar (L)) with number of fractures categorized by type.*

Vertebra	Compression	Schmorl's Node	Burst
T1	0	0	0
T2	0	0	0
T3	**1**	0	0
T4	**1**	**1**	**1**
T5	**1**	0	0
T6	**1**	0	0
T7	**1**	**2**	0
T8	**1**	**3**	0
T9	0	**2**	0
T10	0	**2**	0
T11	0	**2**	0
T12	0	**2**	0
L1	**1**	**1**	0
L2	0	**2**	0
L3	**3**	**1**	0
L4	**4**	0	0
L5	**3**	**1**	0

**ZW-87 235 has been excluded due to different fracture mechanism.*

Two individuals (ARJB V1556 and ARJB V1912) presented with endplate defects (Fig. 4.2A) (see section 4.2.1.13) to the vertebrae that might be healed vertebral compression fractures but may also be the result of other processes, including normal growth and development. The endplate defects only appear in individuals from the ARJB collection, compression fractures and Schmorl's nodes likewise only appear in the ARJB and EHV-CK collections which supports the notion that the endplate defects represent healing compression fractures. Micro-CT reconstructions further support the assessment that the alterations are healing fractures (Fig. 4.2B).

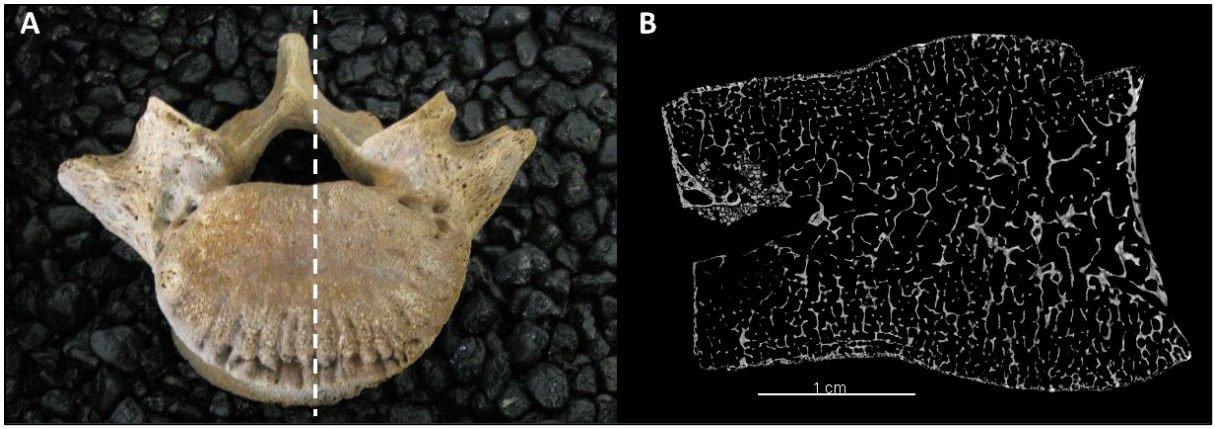

Figure 4.2 *An example of the endplate defects believed to be healed compression fractures. Image shows the gap where the endplate does not meet the anterior rim of the body. Image B shows a micro-CT slice from the same vertebrae with disorganized and thickened trabeculae underlying the fracture zone. Dotted white line in image A indicates location of micro-CT slice.*

4.2.1.1 ARJB V556

ARJB V556 is a probable male in the middle adolescent age category (14-18 years) displaying evidence for fractures to the L4 and L5 vertebrae. On L4, there is a gap between the superior endplate and the anterior edge of the vertebral body (Fig. 4.3). The edges are rounded, composed primarily of lamellar bone, though a small amount of reactive bone is still visible. There is also a small gap on the inferior endplate at the anterior edge. Endplate changes to the L4 conform to features of a healing vertebral compression fracture discussed in section 3.2.1. There is a bow-shaped depression to the superior endplate of L5 with a rounded, elevated area of bone posterior to the depression (Fig. 4.4). The bow shaped depression is filled with reactive bone. Some post-mortem damage has occurred, evidenced by the exposed trabeculae. A sagittal slice

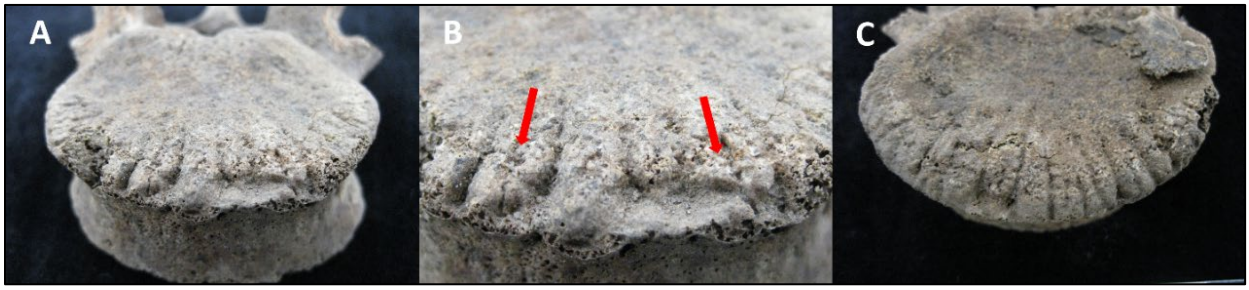

Figure 4.3 *Superior endplate (A & B) and inferior endplate (C) of L4 from individual ARJB V556. The red arrows (B) point to small areas of reactive bone.*

from the micro-CT reconstruction of the center of the L5 provides more detailed information (Fig. 4.5). The new bone formation on the surface of the compressed area is clearly visible in the reconstruction, and areas of thickened trabeculae on the anterior and posterior walls indicate ongoing healing. From this, we can extrapolate that both the anterior and posterior aspects of the vertebral body experienced compressive forces.

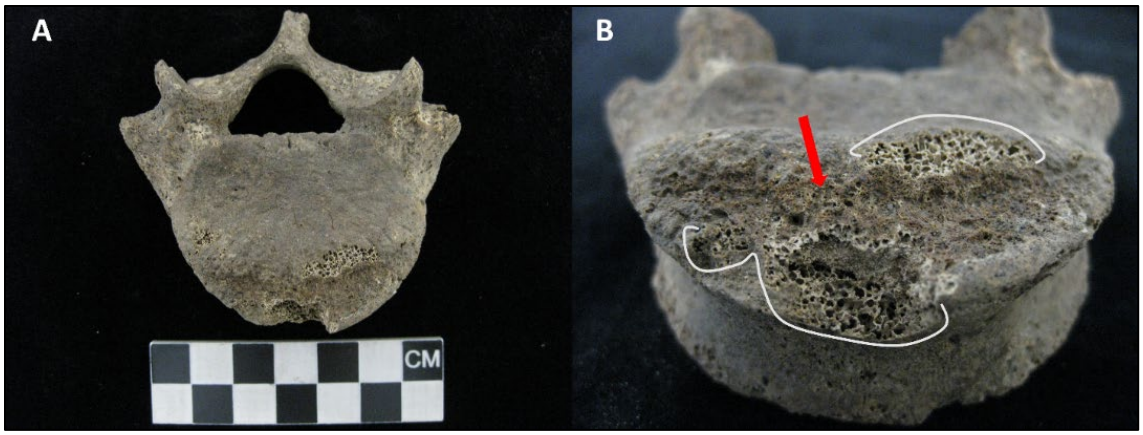

Figure 4.4 *L5 vertebra with a compression fracture from individual ARJB V556 (A), red arrows point to an area of porous, reactive bone and white lines indicate areas of taphonomic damage (B).*

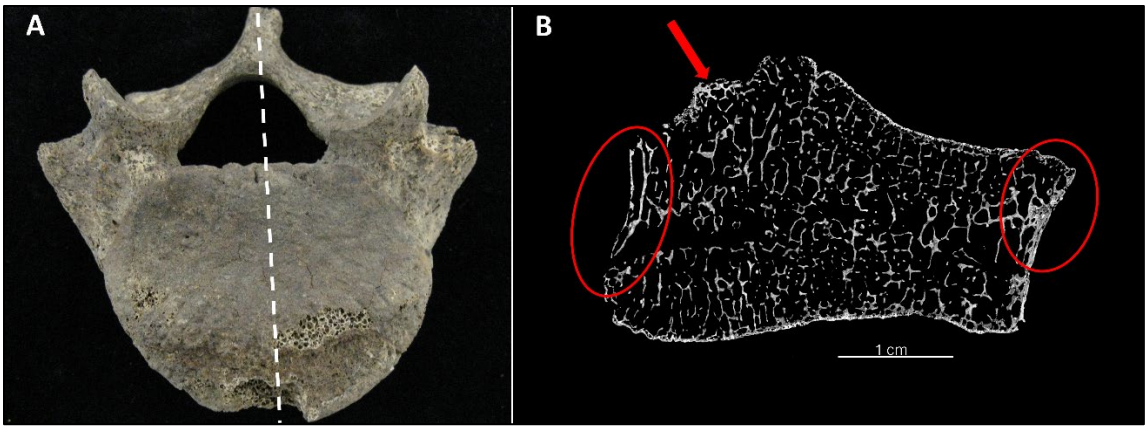

Figure 4.5 *Image of L5 vertebra with line indicating location of micro-CT slice (A), mid-sagittal micro-CT slice of L5 vertebra with a compression fracture from individual ARJB V556 (B). The red arrow points to new bone formation and the red circles show areas of thickened trabeculae. Note general thinning of the trabecular structure in image B.*

The L4 appears well-healed, with only small amounts of porous bone remaining, whereas the L5 displays large amounts of porous new bone. The injuries probably occurred in separate events as the result of continued movements resulting in spinal compression. Based on the

micro-CT data the fracture margins of the L5 appear to have sclerosis of the margin and some reactive bone. L5 conforms to stage two fracture repair with a peak post-traumatic time interval of 68.6 days (range 22-179 days) (see Table 3.3). The L4 is likely in stage five with a peak post-traumatic time interval of 147.7 days (range 29-385 days). As the estimated ranges of the post-traumatic time interval overlap, there is the possibility the injuries occurred in the same event, but this is unlikely given the remodeled nature of the L4.

4.2.1.2 ARJB V1463

Individual ARJB V1463 is a probable female in the middle adolescent category with an age estimation between 14 and 18 years. The T3 and T4 display evidence for a combination of compression fractures and Schmorl's nodes.

Figure 4.6 *Inferior endplate of T3 with a compression fracture (A), superior endplate of T4 with Schmorl's node (B), and inferior endplate of T4 with a compression fracture and Schmorl's node (C) from individual ARJB V1463.*

On the inferior surface of T3 there is a bow shaped compression fracture to the anterior aspect of the vertebral body with anterior displacement of the annular ring and upward posterior displacement of the body (Fig. 4.6A). On the superior surface of T4 there is a Schmorl's nodes with defined margins (Fig. 4.6B). On the inferior surface of the T4 there is a second compression fracture and a small Schmorl's node with an exposed trabecular floor near the posterior right edge (Fig. 4.6C). On all vertebrae, the fracture margins are defined and sharp.

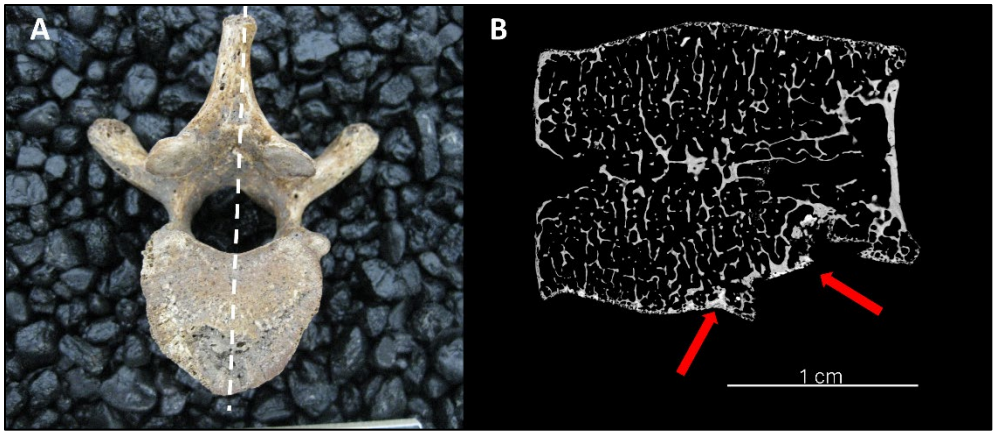

Figure 4.7 *Image of inferior T3 vertebra with line indicating the location of the micro-CT slice (A), mid-sagittal micro-CT slice of T3 vertebra from individual ARJB V1463 (B). Red arrows point to areas of sclerosis, also note decreased trabeculae in anterior body overlying fracture.*

A micro-CT reconstruction of the T3 vertebra reveals sclerosis of the endplate posterior to the fracture and to regions along the fracture margin (Fig. 4.7). There is also a significant decrease in the trabecular structure underlying the fracture. There is very little evidence of healing in any of the fractures, all three vertebrae conform to stage one with a post-traumatic time interval between 28 and 42 days.

4.2.1.3 ARJB V1556

ARJB V1556 is a probable male in the early adolescent category, with an age estimation between 12.5-15.5 years using dental development and eruption. There is evidence for fractures on the L2, L3, L4, and L5 vertebrae.

On the superior surface of the L2 there is a small Schmorl's node to the center of the endplate (Fig. 4.8). The margins are well-defined but blunted and the trabecular floor is not visible indicating some amount of remodeling, but there is a single spicule of bone projecting outward.

Figure 4.8 *Superior endplate of L2 with small Schmorl's node and beaded osseous tissue at the anterior endplate from individual ARJB V1556.*

The anterior margin of the endplate also shows the “beaded circlets of osseus tissue” (Jaffe, 1972, p. 24) consistent with normal growth and development (see section 4.2.1.11).

Figure 4.9 *Superior endplates of L3 (A), L4 (B), and L5 (C) from individual ARJB V1556, all displaying endplate defects.*

The L3 through L5 vertebrae all show defined endplate defects that exceed normal growth and development. The endplates do not meet the anterior edges of the superior bodies (Fig. 4.9). The edges of endplates are rounded and composed of lamellar bone, indicating possible well-remodeled compression fractures.

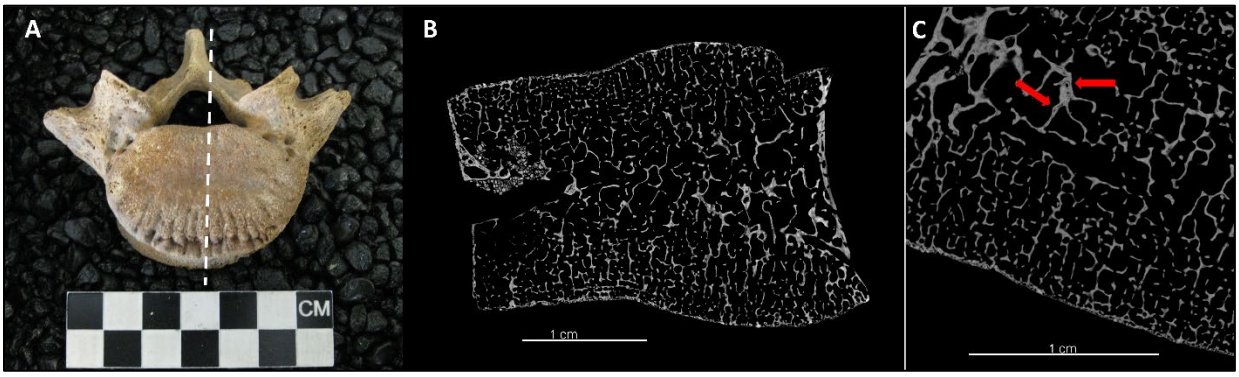

Figure 4.10 *Image of L5 vertebra with line indicating location of micro-CT slice from ARJB V1556 (A), mid-sagittal micro-CT slice of L5 vertebra (B) (note the disarranged and thickened trabeculae underling the fracture zone), micro-CT image showing mineralization defects (red arrows) consistent with vitamin D deficiency.*

The micro-CT slice reveals thickening of the anterior trabeculae and a decreased number of trabeculae (Fig. 4.10A-B) in the anterior body. Mineralization defects consistent with vitamin

D deficiency (Brickley, 2024) were also noted in the micro-CT images (Fig. 4.10C). The compression fractures on the L2, L3, L4, and L5 are all in similar stages of remodeling, fitting the stage five category of fracture repair. The post-traumatic time interval is approximately 147.7 days. The intrusion fracture might have occurred slightly nearer to the time of death as indicated by the defined margins; it is likely in stage four with a post-traumatic time interval estimate of 76.3 days.

4.2.1.4 ARJB V1583

Individual ARJB V1583 is middle adolescent with an age estimation of 16–18 years using epiphyseal fusion. Sex is undetermined. They presented with Schmorl's nodes to T7, T8, T9, T10, T11, and T12, all affecting the inferior endplates.

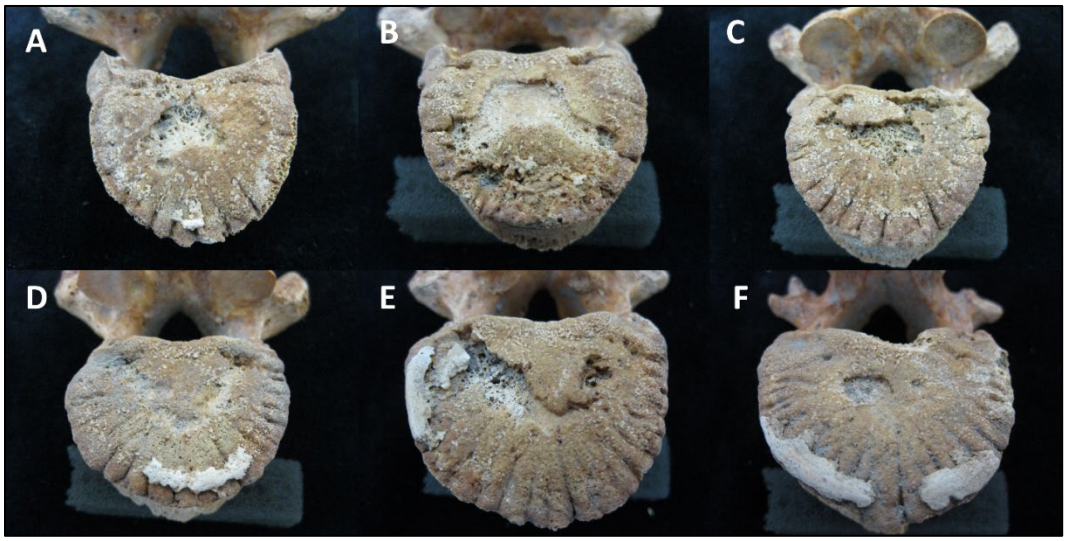

Figure 4.11 *Vertebrae from ARJB V1583. Inferior endplate of T7 (A) with Schmorl's node and new bone on the trabecular floor, inferior endplate of T8 (B) with shallow, central Schmorl's node and healing compression fracture, inferior endplate of T9 (C) with Schmorl's node and exposed trabecular floor, inferior endplate of T10 (D) with healing Schmorl's node, inferior T11 (E) with a Schmorl's node and new bone on fracture margin, and inferior T12 (F) with a small Schmorl's node.*

The inferior endplate of T7 displays an irregularly shaped Schmorl's node with defined fracture margins and an exposed trabecular floor (Fig. 4.11A). Reactive bone overlays portions of the exposed trabeculae. On the inferior endplate of T8, there is a wide, shallow Schmorl's

node with an irregular shape (Fig. 4.11B). The trabecular floor is only visible at the lateral edges of the depression. There is also a minor compression fracture to the anterior margin and a Schmorl's node on the left side. There is a small amount of new bone formation on both the Schmorl's node and compression fracture. On the inferior surface of T9 there is an irregularly shaped Schmorl's node with defined edges and an exposed trabecular floor (Fig. 4.11C). The margins show some evidence of blunting and there is new bone formation on the floor of the depression. The T10 has a U-shaped Schmorl's node on the inferior surface, crossing the entire width of the vertebral body (Fig. 4.11D) with signs of remodelling. The inferior endplate of T11 has a long, deep Schmorl's node (Fig. 4.11E). Near the center, the depression shows remodeling, but in the posterior section there is an exposed trabecular floor with some new bone formation visible along the left margin. The 12 has a small, shallow Schmorl's node with defined margins (Fig. 4.11F).

In all cases the fracture margins appear blunted, and there is new bone formation on T7, T8, and T9. These fractures probably occurred around the same time. Rounding of the fracture margins and the presence of woven bone indicates the fractures are in stage two of repair with a post-traumatic time interval of approximately 68.6 days. The T10 and T11 both show signs of remodeling placing them between stage four and five with a post-traumatic time interval of 76.3-147.7 days. The small areas of exposed trabecular bone on the T11 may indicate ongoing compression in this region of the spine or re-injury.

4.2.1.5 ARJB V1827

ARJB V1827 is a female in the middle adolescent category with an age estimation between 15 and 17 years using epiphyseal fusion, dental development and eruption gave an age range of 16 to 18 years. Vertebrae with evidence of fracture includes T4 through T12.

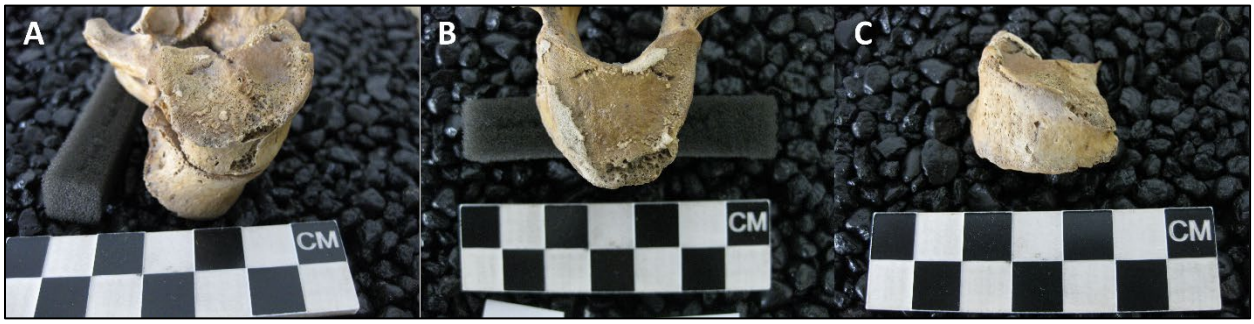

Figure 4.12 *Inferior endplate of T4 (A) with partially healed burst fracture along midline, superior endplate of T5 (A) with a compression fracture to the anterior margin, anterior view of T6 (C, superior up) showing wedge fracture of left aspect, from individual ARJB V1827.*

The inferior endplate of T4 displays a possible burst fracture through the midline between the anterior and posterior margins (Fig. 4.12A); however, there is additional taphonomic damage to the anterior body which makes it difficult to determine if the fracture penetrated the entire body. The surface of the endplate is porous with some reactive bone formation near the anterior aspect, and the margins of the fracture are elevated along the midline. The superior endplate of the T5 vertebra has a compression fracture concentrated on the left side (Fig. 4.12B) with anterior displacement of the annular ring. Extensive porosity indicating a possible hematoma (Maat & Mastwijk, 2000) was present at the superior endplate of T6. A hematoma is not considered a fracture and therefore not included in the prevalence results, but likely occurred as a result of trauma. The left side of the T6 body has been crushed, creating a wedge (Fig. 4.12C). The pedicles fractured post-mortem.

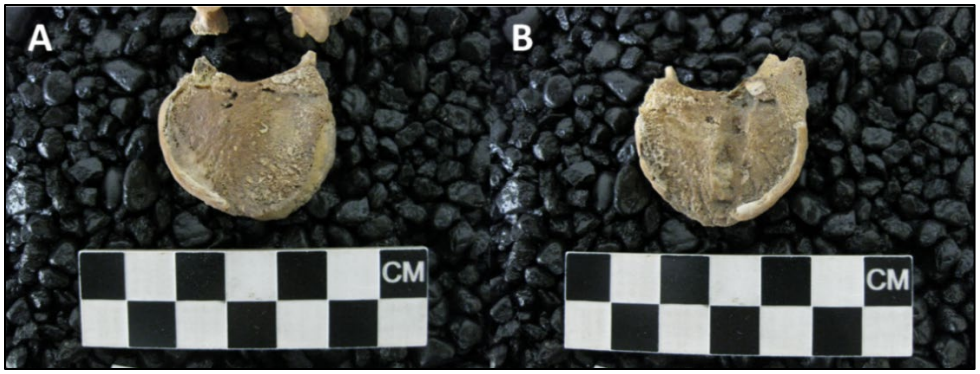

Figure 4.13 *Superior endplate of T7 (A) with porosity and new bone formation consistent with hematoma, inferior endplate of T7 (B) with linear depression and compression fracture from individual ARJB V1827.*

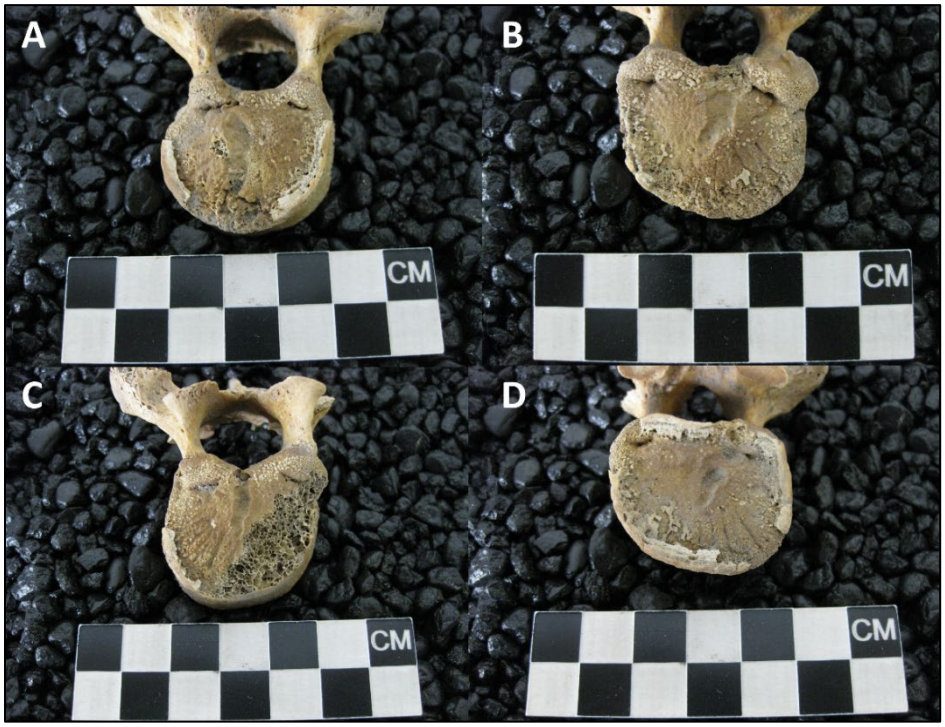

Figure 4.14 *Superior endplate of T8 (A) with linear depression, Schmorl's node, and compression fracture, inferior endplate of T8 with linear depression and compression fracture (B), superior endplate of T9 with linear depression and Schmorl's node (C), inferior endplate of T9 with linear depression and Schmorl's node (D), from individual ARJB V1827.*

The superior endplate of the T7 has porosity and new bone formation possibly indicating a hematoma, with disruption to the apophyseal ring (Fig. 4.13A). The inferior surface of the T7 has a linear Schmorl's node on the endplate (Fig. 4.13B) and a compression fracture to the anterior right margin, disrupting the apophyseal ring. There remains some porous, reactive bone

on the compressed regions of bone but both show remodeling. The pedicles fractured post-mortem. On the superior T8, the endplate has a linear depression with a shallow Schmorl's node near the anterior margin (Fig. 4.14A). There is also a compression fracture to the anterior margin that has displaced the annular ring. There is reactive, porous bone along the Schmorl's node and over the cortical bone where the compression fracture is located. The inferior endplate of the T8 displays evidence for a compression fracture to the anterior margin (Fig. 4.14B), there is porous new bone formation and disruption of the apophyseal ring along the anterior margin. There is also a shallow, linear depression in the center of the body that progresses into an Schmorl's node on the posterior margin near the midline. The superior T9 has a shallow, linear depression on the endplate that progresses into a shallow Schmorl's node at the posterior margin (Fig. 4.14C). Unfortunately, the surface has largely been destroyed by post-mortem damage. The inferior T9 endplate likewise has a shallow linear depression that progresses into a Schmorl's node at the posterior margin (Fig. 4.14D). There is disruption to apophyseal ring, but this appears to be post-mortem as there is no evidence of an underlying fracture. The superior endplate of the T10 does not have pathological changes, but the inferior endplate has a large Schmorl's node to the anterior portion, posterior to the apophyseal ring which is not anteriorly displaced (Fig. 4.15A). Additionally, there is an elevation in the center of the body where the bone has been displaced upward as a result of the anterior compression. The elevation has a small depression in the center. There is woven bone covering the exposed trabeculae on the anterior fracture. The superior endplate of T11 has a Schmorl's node to the anterior and right side of the body (Fig. 4.15B). The underlying trabeculae are exposed and presents with some new bone formation. There is also a Schmorl's node to the center of the body, though some post-mortem damage has

affected the margins. A large piece of the endplate is nearly separated by a deep, groove-like

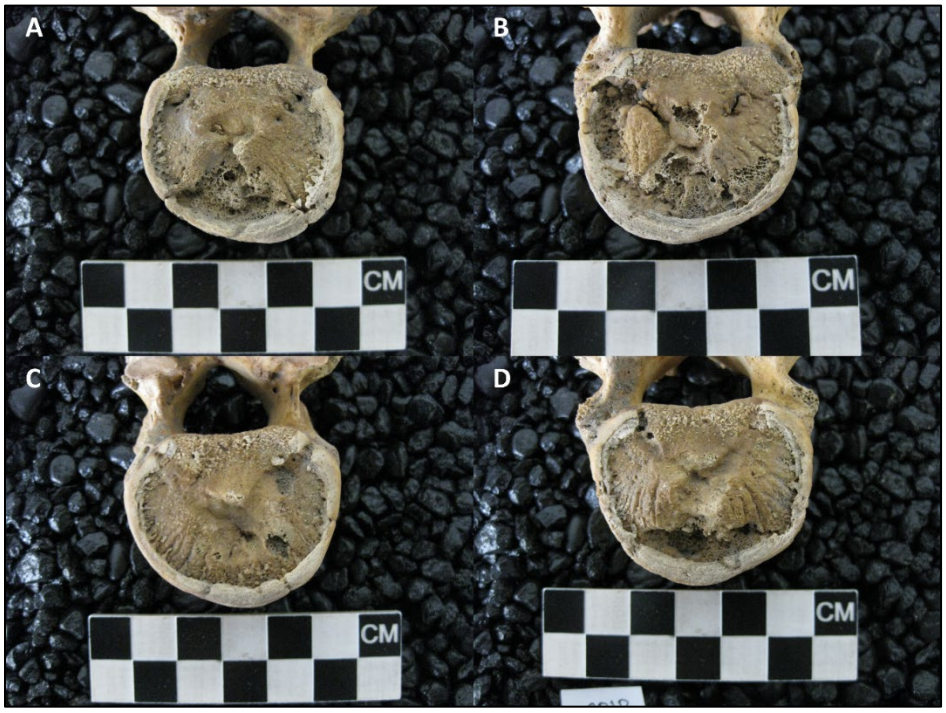

Figure 4.15 *Inferior endplate of T10 (A), superior endplate of T11 (B), inferior endplate of T11 (C), superior endplate of T12 (D) with Schmorl's nodes, from individual ARJB V1827.*

depression moving between the right-side and central intrusion fractures. The inferior T11 endplate has a U-shaped depression in the center of the body, which is deep at the center and becomes shallower laterally (Fig. 4.15C). There is a small, deep Schmorl's node on the right, anterior aspect and a small, shallow one on the right, posterior aspect. The superior T12 has an anterior fracture with a deep Schmorl's node into the trabecular structure (Fig. 4.15D). As with the T11, there is an elevation in the center of the body caused by the displacement of bone. There is a U-shaped depression running through the elevation that progresses into a small Schmorl's node on the left side. The elevation in the center of the body fits into the depression on the inferior surface of the T11. A micro-CT slice of T11 shows a small amount of sclerosis on the margins of the herniation to the inferior endplate (Fig. 4.16).

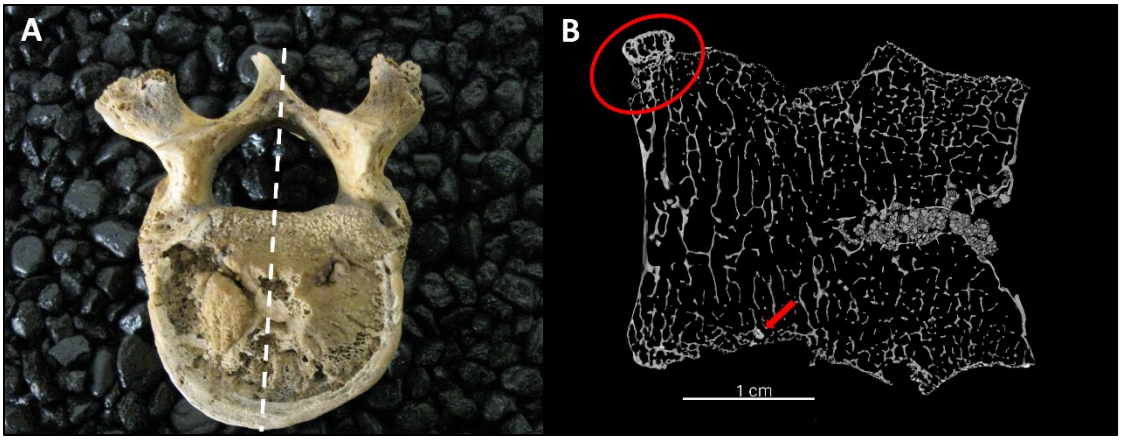

Figure 4.16 *Image of T11 vertebra with line showing location of micro-CT slice from ARJB V1827 (A), sagittal micro-CT slice (B), note the fusing apophyseal ring (red circle) and small region of sclerosis (red arrow).*

Pathological changes to the vertebrae are probably in part the result of congenital fusion of the left inferior and superior articular facets and the neural arches of the T4 and T5 vertebrae (Fig. 4.17A), resulting in mild, S-curve scoliosis (Fig. 4.17B) (Lee et al., 2022). There is a pseudo-articular surface between the articular facets on the right side. Congenital fusion of vertebrae is characterised by smoothly conjoined surfaces of the vertebral bodies, laminae, and/or spinous processes (Titelbaum, 2020), whereas traumatic fusion generally features uneven contours, ossified tissues, and degenerative changes. The smooth cortical surface on the laminae of T4 and T5 indicate fusion is likely congenital.

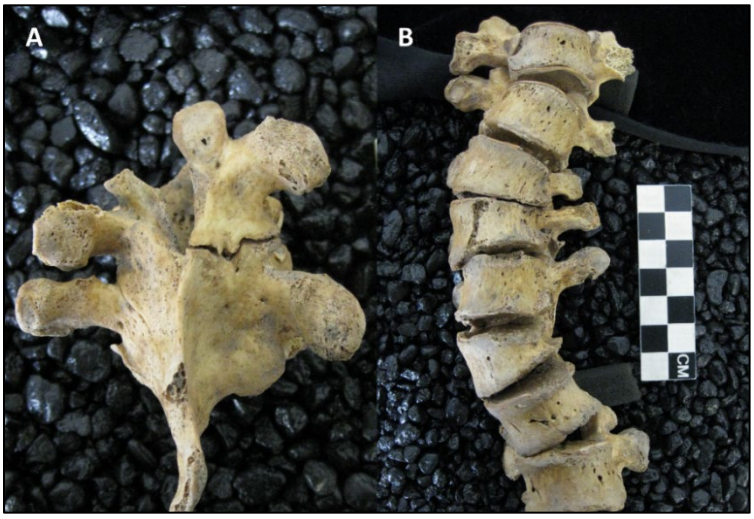

Figure 4.17 *Congenital fusion of the left articular facets and neural arches T3 and T4 vertebrae (A) from individual ARJB V1827, with false articular surface between right articular facets. Associated mild S-curve scoliosis (B) between T1 and T8 from individual ARJB V1827.*

A post-traumatic time interval is difficult to establish due to the extant of the injuries, however, porous new bone is present

on nearly every element and the fracture margins are still well-defined. Most likely, these fractures occurred around the same time and were in the earlier stages of callus formation adhering to stage two and a post-traumatic time interval estimate of approximately 68.6 days. However, the reactive bone may also reflect the chronic nature of the scoliosis and increased mechanical loading of the spine.

4.2.1.6 ARJB V1912

ARJB V1912 is a probable female in the middle adolescent category with an age estimation between 15 and 17 years using epiphyseal fusion and 15 to 17.5 years using dental development and eruption. Evidence indicates possible healed compression fractures to L3, L4, and L5.

Figure 4.18 *L3 (A), L4 (B), and L5 (C) vertebrae from individual ARJB V1912 with endplate defects.*

The anterior endplate on the superior surface of the L3 displays defined endplate defects (Fig. 4.18A) wherein the endplate does not meet the anterior edge of the body. The superior endplate of the L4 likewise does not meet the anterior edge of the body, but the defect is more distinct (Fig. 4.18B). The endplate is composed of lamellar bone and the margins are rounded. L5 has the most severe endplate defect, there is a large gap between the superior endplate and the anterior edge of the body (Fig. 4.18C). As with the L3 and L4, the margins are rounded and composed of lamellar bone.

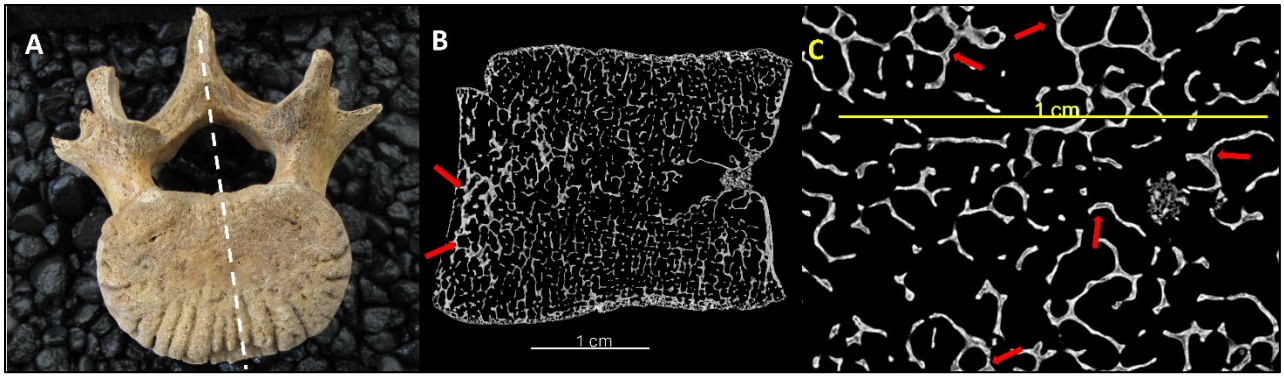

Figure 4.19 *Image of L4 vertebra from ARJB V1912 with white line showing location of micro-CT slice (A), mid-sagittal micro-CT slice with red arrows pointing to thickened anterior trabeculae (B), and mineralization defects (red arrows) consistent with vitamin D deficiency (C).*

A micro-CT reconstruction of the L4 reveals there is no decrease in the number of trabeculae at the anterior aspect of the body, with only slight thickening of the trabeculae in comparison to the rest of the body (Fig. 4.19B), potentially indicative of an advanced stage of fracture repair. Mineralization defects consistent with vitamin D deficiency (Fig. 4.19C) are visible in a transverse micro-CT slice. The possible compression fractures on the, L3, L4, and L5 are all in stage five of fracture repair, with a post-traumatic time interval of approximately 147.7 days.

4.2.1.7 ARJB V1945

Individual ARJB V1945 is an early adolescent with an age estimation between 12.5 and 16.5 years using dental development and eruption. The sex estimation is ambiguous as a result of mixed male and female traits. They presented with a series of Schmorl's nodes to the L1, L2, and L3 vertebrae.

On the superior endplate of the L1 there is a small, shallow Schmorl's node near the center of the vertebral body (Fig. 4.20A). The floor is filled entirely with reactive bone. The superior endplates of the L2 and L3 also have small, shallow Schmorl's nodes with reactive new bone filling the depressions (Fig. 4.20B-C). The L1 has a minor, partially healed Schmorl's node

to the inferior L1 and L2 has a partially healed Schmorl's node to the inferior surface. Based on the degree of healing the lumbar vertebrae are in stage three of fracture repair, with a post-traumatic time interval of approximately 68.6 days.

Figure 4.20 *Superior endplates of L1 (A), L2 (B), and L3 (C) vertebrae from individual ARJB V1945 with small, partially healed Schmorl's nodes.*

4.2.1.8 EHV-CK S2918

EHV-CK S2918 is the only individual to present with a single vertebral fracture. Identified as female by DNA testing, she is a middle adolescent with an age estimate between 14 and 16 years using epiphyseal fusion. The dentition was not preserved.

The inferior endplate of the L5 vertebrae displays a linear Schmorl's node that has penetrated the cortical surface at the posterior margin and anterior right margin (Fig. 4.21). The trabecular floor is visible at the posterior margin, there is no sign of reactive bone formation.

Figure 4.21 *Inferior endplate of T12 from individual EHV-CK S2918 with a linear depression and small Schmorl's node.*

Micro-CT data is not available for this element, and without knowing if sclerosis has occurred the stage of fracture repair could be

anywhere between stage two and four. Therefore, the post-traumatic time interval is between 68.6 to 76.3 days.

4.2.1.9 EHV-CK S3507

EHV-CK S3507 is an early adolescent individual of undetermined biological sex with an age range between 13 and 16 years. Age is based on epiphyseal fusion as no dentition was recovered. Fractures are evident on the T8, L1, L3, and L4.

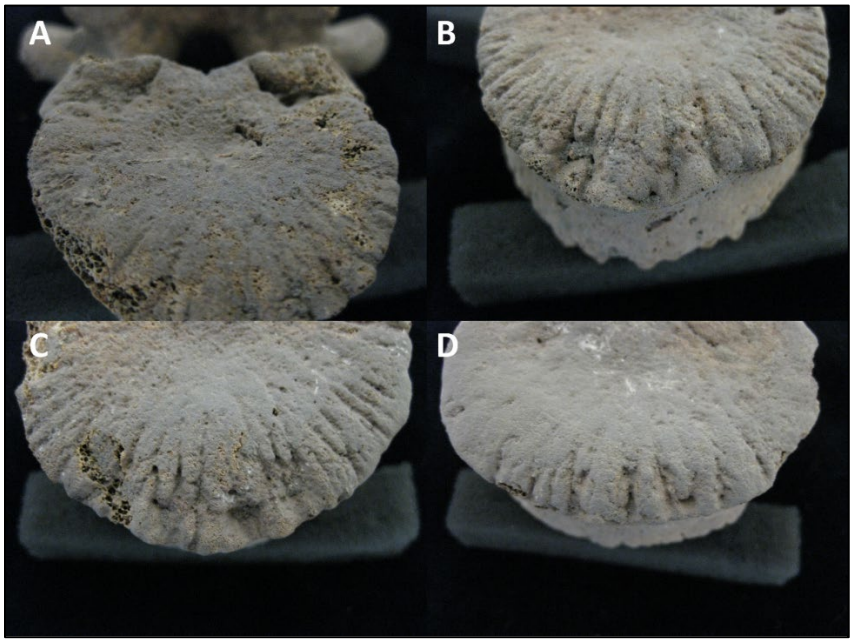

Figure 4.22 *Superior T8 (A) with small Schmorl's node, superior L1 (B) with healing compression fracture, superior L3(C) with healing compression fracture, and minor morphological changes to superior L5 (D) from individual EHV-CK S3507.*

The T8 has a Schmorl's node to the center of the superior endplate with a small region of exposed trabeculae (Fig. 4.22A). The T9 and T10 both have small depressions in the superior and inferior endplates but as there is no discontinuity in the cortical surface they have not been counted as fractures. The superior L1 endplate has irregular morphological changes to the anterior endplate (Fig. 4.22B). While the margins are rounded, they are also uneven, with a 'ruffled' appearance. The superior L3 endplate has similar irregular depressions on the anterior

margin (Fig. 4.22C). The margins are rounded but stepped, with uneven elevation, and there appears to be a small amount of woven bone present. The anterior changes in both L1 and L3 are consistent with healing compression fractures. Post-mortem damage has resulted in exposed trabeculae on the right side of the anterior aspect. The superior endplate of L4 has only minor alterations, with small gaps between the endplate and the anterior margin (Fig. 4.22D). The margins on the endplate are rounded and the elevation is more even than the L1 or L3. The L2 was too damaged to assess.

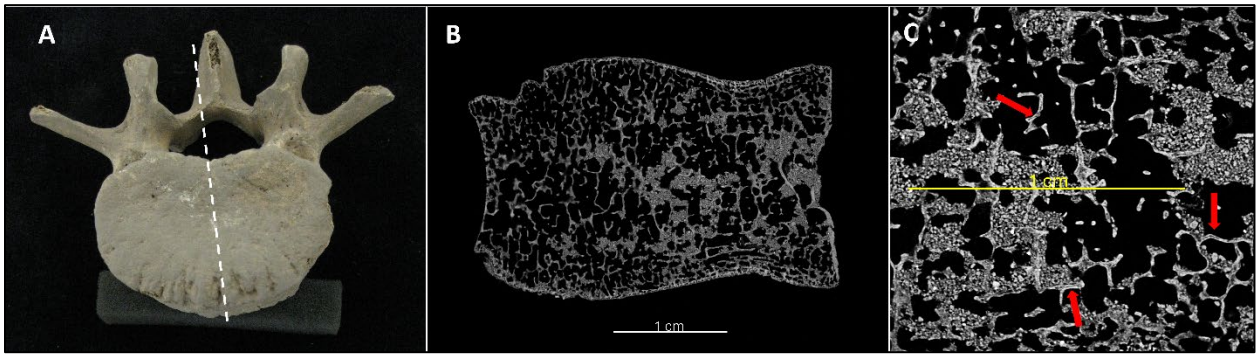

Figure 4.23 *Image of L4 vertebra from EHV-CK S3507 with white line showing the location of the micro-CT slice (A), sagittal micro-CT slice from L4 vertebrae showing thinning and loss of trabeculae in the anterior body (B) and mineralization defects (C) (red arrows) consistent with vitamin D deficiency.*

Micro-CT imaging reveals a significant loss of trabeculae in the anterior body (Fig. 4.23), however, there is also significant soil deposition from the burial environment which may have impacted the number of trabeculae. Mineralization defects consistent with vitamin D deficiency (Brickley, 2024) were also noted in the micro-CT images (Fig. 23C).

The uneven surface elevations of the endplate margins on L1 and L3, combined with porous bone visible on L3, indicate they may be in an earlier stage of fracture repair than L5 that has smoother, remodeled endplate margins. The L3 and L4 therefore are estimated to be in either stage two or stage three of fracture repair, with a post-traumatic time interval of approximately

68.6 days. The L5 is in stage five of fracture repair with a post-traumatic time interval of 147.7 days.

4.2.1.10 ZW-87 235

The individual from Zwolle presented with a unique pattern of pathological lesions, affecting the cervical and thoracic levels. Individual ZW-87 235 is an early child, aged 3-5 years based on dental development and eruption, with a total of five fractures affecting the C4, C5, C6, T1, and T2. Compression fractures to the vertebral bodies occurred on the C4, C5, T1, and T2. The C5 and C6 have healing crush fractures to the left transverse processes. The inferior vertebral body of the C3 has a porous surface consistent with a hematoma (Maat & Mastwijk, 2000) during life, although this is not counted as a fracture. Macroscopic examination revealed discontinuity of the cortical surface with exposed trabecular floors and new bone formation.

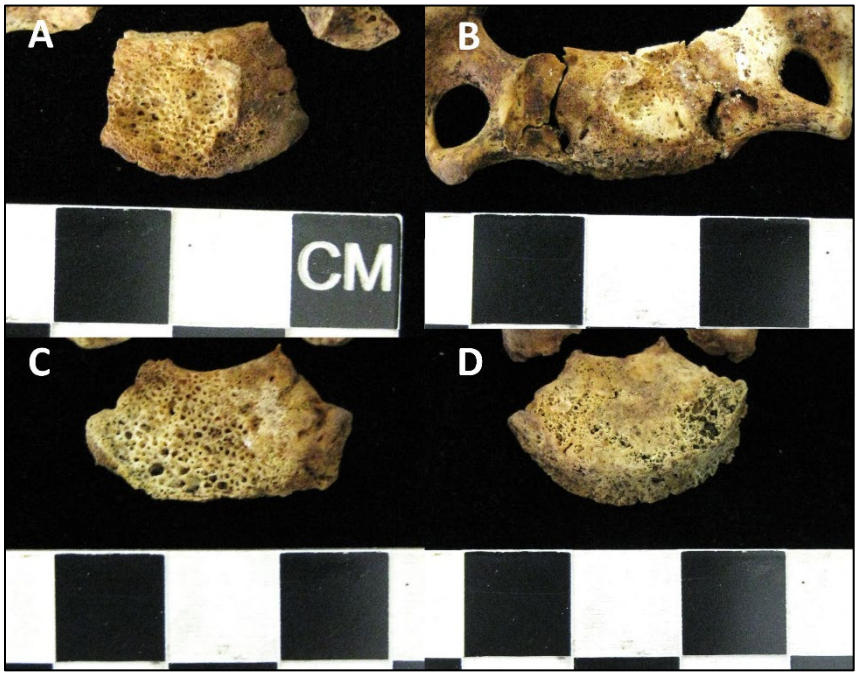

Figure 4.24 *Inferior C4 centrum (A) with a compression fracture to left side with raised margin, superior C5 centrum (B) with a Schmorl's node, inferior T1 (C)centrum with severe compression fracture to left aspect, superior T2 (D) with minor compression fracture to left aspect from individual ZW-87 235.*

The C4 has a large compression fracture to the inferior vertebral surface with exposed trabecular floor and a lip of raised bone near the midline and a small amount of woven bone along the posterior aspect (Fig. 4.24A). The C5 has a fracture to the superior vertebral body resembling a Schmorl's node (Fig. 4.24B). The cortical surface has been depressed, revealing the trabeculae, and there is a raised bony platform in the center surrounding the depression. The remaining cortical surface shows increased porosity. A small area of eburnation was noted anterior to the depression. The inferior vertebral body of the T1 shows a compression fracture concentrated on the left side (Fig. 4.24C). The cortical surface is nearly entirely absent and only a small amount of new bone formation is evident along the right margin. The superior endplate of the T2 has a compression fracture concentrated on the left anterior aspect with exposed trabecular floor (Fig. 4.24D). There are also areas of exposed trabeculae along the right aspect, but it is difficult to determine if this ante- or post-mortem.

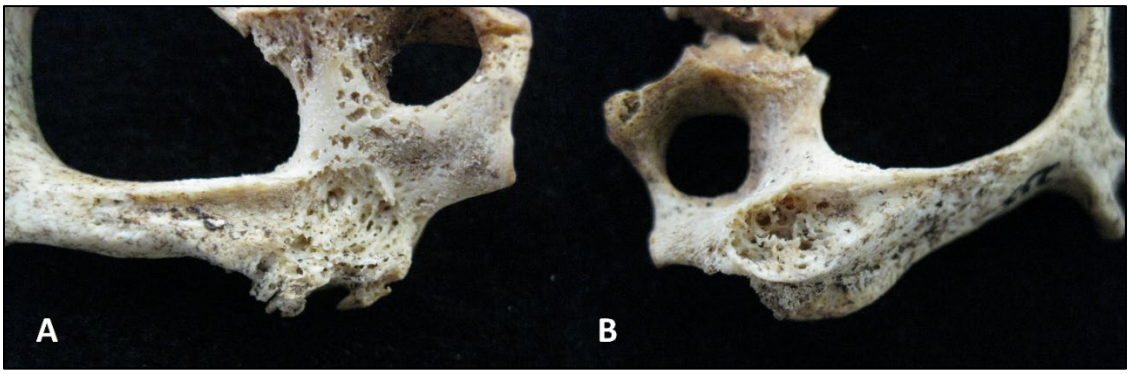

Figure 4.25 *Crush fracture to left transverse process of C5 vertebra (A) with new bone formation and left superior articular facet of C6 vertebra (B) with new bone formation from individual ZW-87 235.*

The left transverse process of the C5 shows evidence of being crushed, extending from the mid point of the laminae through the inferior articular facet to the edge of the vertebral body (Fig. 4.25A). The area has a sheet of new bone formation with spicules projecting off the articular facet. There is also some new bone formation on the superior aspect of the pedicle.

Matching the damage to the transverse process of the C5, the C6 vertebrae shows evidence of crushing to the superior, left transverse process (Fig. 4.25B). The surface of the articular facet is concave, with new bone filling the space, and small projecting osteophytes of new bone on the lateral surface of the lamina and around the pedicle.

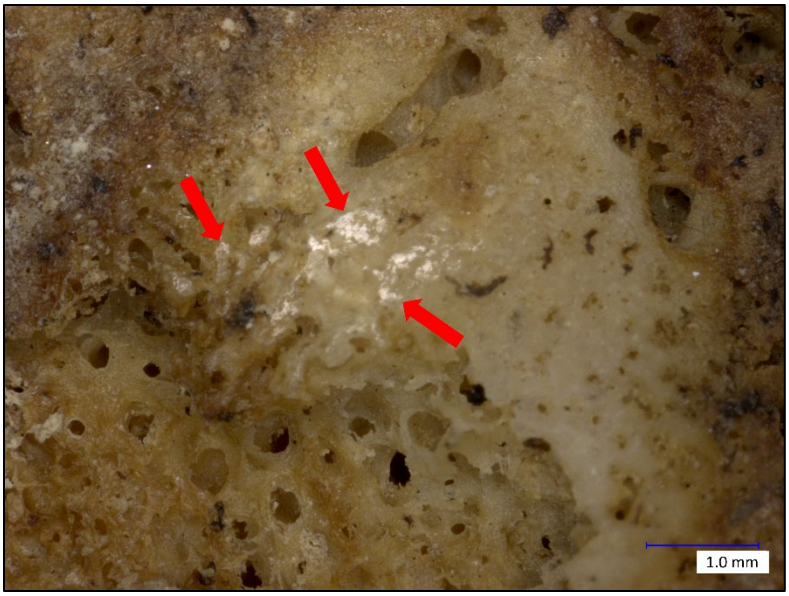

Figure 4.26 *Microscopy image at 20x magnification of the superior endplate of C5, the red arrows point to the region of eburnation from individual ZW-87 235.*

Microscopy images highlighted an area of eburnation on the superior endplate of the C5 (Fig. 4.26). The micro-CT reconstruction only shows the new bone formation along the fracture margins and along the transverse process (Fig. 4.27). There is no obvious thinning of the trabecular structure.

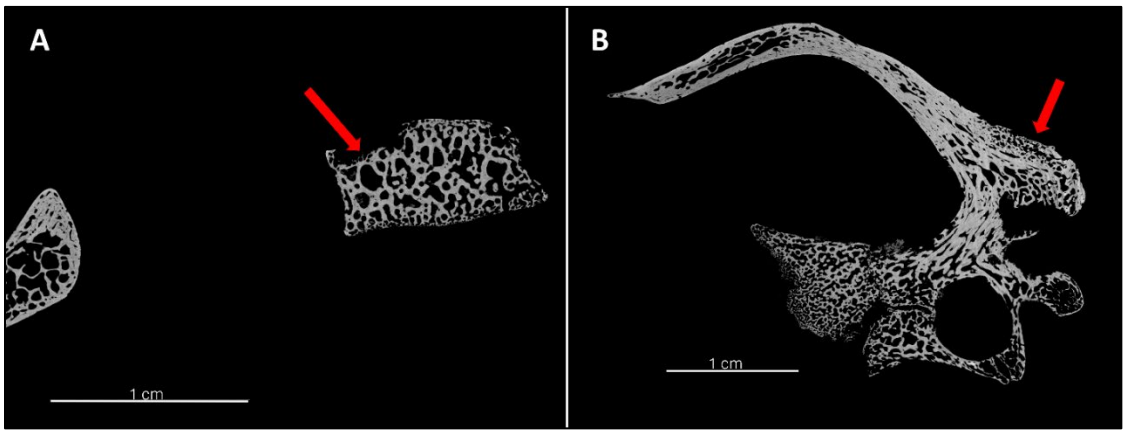

Figure 4.27 *Mid-sagittal micro-CT slice of C5 (A) with arrow pointing to area of new bone formation and transverse micro-CT slice of C5 (B) wit arrow pointing to new bone formation on the transverse process, from individual ZW-87 235. Note the lack of thinned trabeculae or cloaca in the trabecular structure.*

The location of the fractures, bordering the cervicothoracic junction, and young age of the individual indicates this example of spinal trauma occurred through a different process than that affecting the other individuals in this study. Pathological lesions resulting in lytic lesions to the vertebrae, including tuberculosis (TB), brucellosis, and osteomyelitis have been ruled out as possible diagnoses. Extra pulmonary tuberculosis may affect the spine, resulting in lytic lesions with little to no new bone formation and marked osteoporosis of the affected bone (Lewis, 2011; Waldron, 2009). In adults, lesions generally affect the anterior vertebral body in the lower thoracic and lumbar vertebrae (Roberts & Buikstra, 2019), but in children, infection may begin at the intervertebral disk and extend to the body. Lewis (2011) states that infection of the cervical vertebrae is rare but may occur. The location of the lesions in ZW-87 235 on the superior and inferior vertebral endplates in the cervical and upper thoracic vertebrae with no involvement of the anterior body, the presence of reactive new bone, and the lack of other skeletal lesions related to tuberculosis infection indicates TB is an unlikely diagnosis. Roberts and Buikstra (2019) state that in adults, brucellosis similarly affects the lower thoracic and lumbar vertebrae and presents with focal, lytic lesions to the vertebral bodies but in children brucellosis infection rarely affects the spine. Lytic lesions generally affect the anterior, superior margin of the vertebral body with a sclerotic new bone formation extending around the margin (Robert & Buikstra, 2019). Lesions of the cervical and thoracic vertebrae in a young child are not compatible with a diagnosis of brucellosis. Finally, vertebral osteomyelitis is more common in adults than children (Waldron, 2009). Osteomyelitis may be difficult to differentiate from tuberculosis and brucellosis but involves increased new bone formation in addition to focal, lytic lesions. Osteomyelitis may increase the size of a bone and cloacae may form as drainage canals for pus (Waldron, 2009). The affected vertebrae in ZW-87 235 do not show an increase in size or differences in

morphology. The fractured cortical surfaces reveal a trabecular floor, which is more consistent with a compression fracture than a cloaca. Finally, the new bone formation is localized primarily to the transverse process of the C5 with little generalized reactive bone. The lesions are more consistent with fractures resulting from high-velocity trauma, such as a fall from a height, than osteomyelitis.

There is minimal evidence for healing, with only small amount of reactive new bone, placing it in stage two of fracture repair. For the young child category, the post-traumatic time interval is 22-35 days. The presence of eburnation on C5 indicates the injury likely occurred at least 13 days prior to time of death (Mant et al., 2019; Todd and Iler, 1927).

4.2.1.11 Differential Diagnoses of the Multiple Vertebral Fractures

Several pathological conditions can result in lesions to the vertebral endplates and must be considered in a differential diagnosis. Acute trauma will be difficult to distinguish from fractures resulting from repeat movement and mechanical loading and therefore will not be a focus of discussion, however, multiple epiphyseal dysplasia, tuberculosis, Scheuermann's disease, and normal growth and development are considered. Multiple epiphyseal dysplasia and tuberculosis do not adhere to the lesions described in the present thesis and have therefore been ruled out. Normal growth and development have likewise been ruled out, as the endplate defects identified in this study (see section 4.2.1) are too extensive and are therefore likely the result of pathology. Fractures and Scheuermann's disease remain the most likely explanations, however, a definite diagnosis of Scheuermann's disease, following the clinical criteria, cannot be established, therefore the vertebral lesions are classified as fractures.

Multiple epiphyseal dysplasia (MED) is a genetic condition that presents in early childhood and affects ossification of the epiphyses in the long bones (Briggs et al., 2019). MED

has been noted to occasionally affect the spine, potentially resulting in irregularities of the anterior superior and inferior borders of the vertebral bodies, anterior rounding or wedging of the vertebrae resembling Scheuermann's kyphosis, and an increase in the presence of Schmorl's nodes (Briggs et al., 2019; Hulvey & Keats, 1969). The description of spinal abnormalities closely resembles the findings in the present study; however, MED also results in other skeletal abnormalities, including small ossification centers with irregular contours, abnormalities in the shape of long bone metaphyses, and shortened limb length (Briggs et al., 2019; Hulvey & Keats, 1969). Clubfoot, coxa vara, and genu varum may also be present (Briggs et al., 2019). No other skeletal abnormalities were noted in the individuals with vertebral anomalies, decreasing the likelihood of MED as being the causative factor of the described vertebral pathologies. Additionally, the incidence of MED is approximately one in every 10,000 births, which does not fit with the high number of individuals with vertebral lesions noted here.

Lesions indicative of extra pulmonary tuberculosis affecting the spine were discussed in section 4.1.2.12 in association with individual ZW87 235. Many of the characteristics that led to the exclusion of TB as a diagnosis for the cervical lesions also apply to the remainder of the individuals displaying evidence of vertebral lesions. While the anterior endplates have been affected, none of the individuals display lytic lesions to the anterior body which are generally associated with TB infection. There is also evidence of healing in the form of woven and lamellar bone for all individuals, which does not conform to a diagnosis of TB. There are also no other lesions to indicate a pulmonary infection, indicating TB is an unlikely diagnosis.

Scheuermann's disease, also known as Schuermann's kyphosis or juvenile kyphosis, is a condition characterized by anterior collapse and wedging of the lower thoracic spine resulting in kyphosis (increased curvature) affecting adolescents aged 12–17 years (Jaffe, 1972; Lewis,

2018). There are two forms of Scheuermann's disease, the classical presentation is recognized by anterior wedging of at least 5 degrees in 3 or more adjacent vertebrae, combined with central Schmorl's nodes, and endplate defects (Gustavel & Beals, 2002; Mansfield & Bennett, 2023). The atypical form of Scheuermann's disease is characterized by endplate irregularities in one or two vertebrae, anterior Schmorl's nodes, but no anterior wedging (Gustavel & Beals, 2002). Histological examination may also reveal irregular mineralization (Mansfield & Bennet, 2023). The primary cause of Scheuermann's kyphosis is prolapse of the intervertebral disk into the anterior vertebral body (Jaffe, 1972; Lewis, 2018). Scheuermann's disease primarily affects the thoracic region at T9 and T10 (Type-I kyphosis) and the thoracic-lumbar junction (Type-II kyphosis) (Lewis, 2018; Mansfield & Bennett, 2023), only rarely does kyphosis occur in the cervical region (Jaffe, 1972). Scheuermann's disease often heals without intervention but may cause growth delays in the cartilage endplate (Lewis, 2018), which may explain the endplate defects seen in ARJB V1556 and ARJB V1912. The endplate defects also affect three continuous vertebrae in both individuals but without anterior wedging. Of the remaining seven individuals with vertebral fractures, none have three or more continuously affected vertebrae. ARJB V556 and ARJB V1463 have two adjacent vertebrae affected (L4 and L5 and T3 and T4 respectively), though neither of the affected regions is good match for Scheuermann's disease. EHV-CK S3507 likely has four adjacent vertebrae that have been affected, but because the L2 was too damaged to assess, only compression fractures affecting the L1, L3, and L4 can be confirmed. The atypical presentation is a possible diagnosis, as Scheuermann's disease is also found in association with Schmorl's nodes (Gustavel & Beals, 2002; Mansfield & Bennett, 2023), which appears in 6/7 individuals with compression fractures. However, a diagnosis of Scheuermann's disease cannot be confirmed for any individuals, therefore, "compression fracture" will continue to be used to

refer to anterior crushing of the vertebral endplate. But Scheuermann's disease remains a possible diagnosis for the vertebral trauma in five cases (ARJB V566, ARJB V1463, ARJB V1556, ARJB V1912, EHV-CK S3507) in the present study. While there is a possible genetic component to Scheuermann's disease (Mansfield & Bennett, 2023), nutritional and mechanical factors also play a role in the development of the condition.

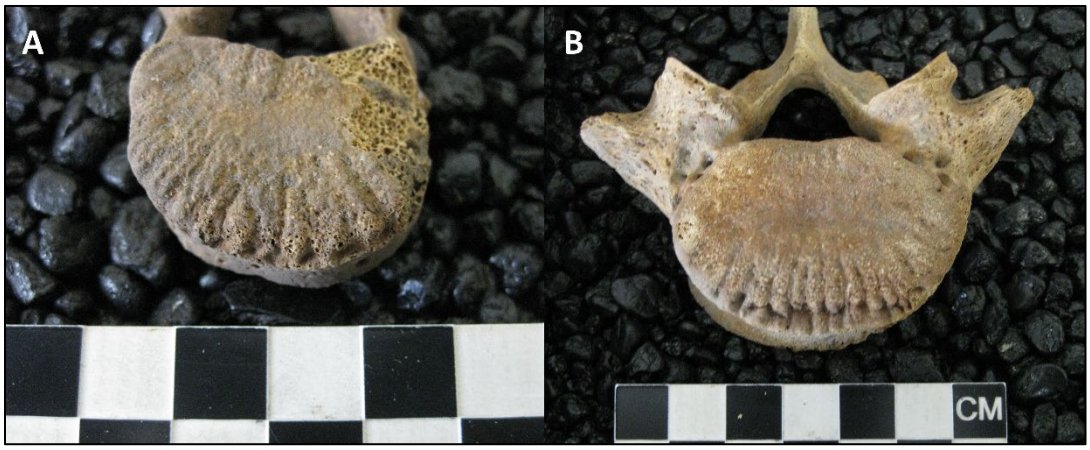

Figure 4.28 *Normal growth and development (A) in the form a beaded osseus circlet from EHV-CK S1834 compared to an endplate defect (B) from ARJB V1556.*

The morphological variations seen in ARJB V1556, ARJB V1912, may also be related to normal growth and development. In the developing spine, a thick plate of hyaline cartilage covers the vertebral endplates, ending in the cartilaginous marginal ring which attaches in a groove extending around the upper and lower border of the developing body (Jaffe, 1972, p. 26). The secondary ossification center for the marginal ring appears around 7-9 years of age, and by 12 years forms a complete bony ring separated from the endplate by a thin layer of cartilage (Jaffe, 1972). At approximately 14-15 years of age, blood vessels disrupt the remaining cartilage between the marginal ring and the endplate, resulting in destruction of the cartilage. The ossification centers along the endplate may appear as "beaded circlets of osseus tissue" (Jaffe, 1972, p. 24) (Fig. 4.28A). The macroscopic appearance of normal growth and development seen

in two individuals (ARJB V1437 & EHV-CK S1834) does not conform to the changes seen in ARJB V1556 and ARJB V1912 (Fig. 4.28B). The extreme morphological variations present in these two individuals is unlikely then to be the result of normal growth development. But they may be abnormal attachment points for cartilage resulting from a combination of normal growth and development and pathological conditions affecting ossification, including metabolic disorders and mechanical stress (Kushchayev et al., 2018; Lotz et al. 2013). Small endplate defects are difficult to observe radiographically, and so the incidence in modern adolescents is largely unknown (Lotz et al., 2013).

4.2.2 Long Bone Fractures

Only two ante-mortem fractures to long bones were detected, the left humerus from individual EHV-CK S2567 and the right fibula from individual GRK V59. The crude prevalence of long bone fractures is 2/55 individuals or 3.6%. The true prevalence for each skeletal element can be found in Table 4.3.

4.2.2.1 EHV-CK S2567

Individual EHV-CK S2567 falls into the early child category, aged 2-5 years based on dental development and eruption, and identified as male through DNA analysis (see section 3.1.2). Macroscopic examination of the left humerus revealed an ante-mortem fracture to the proximal shaft (Fig. 4.29A).

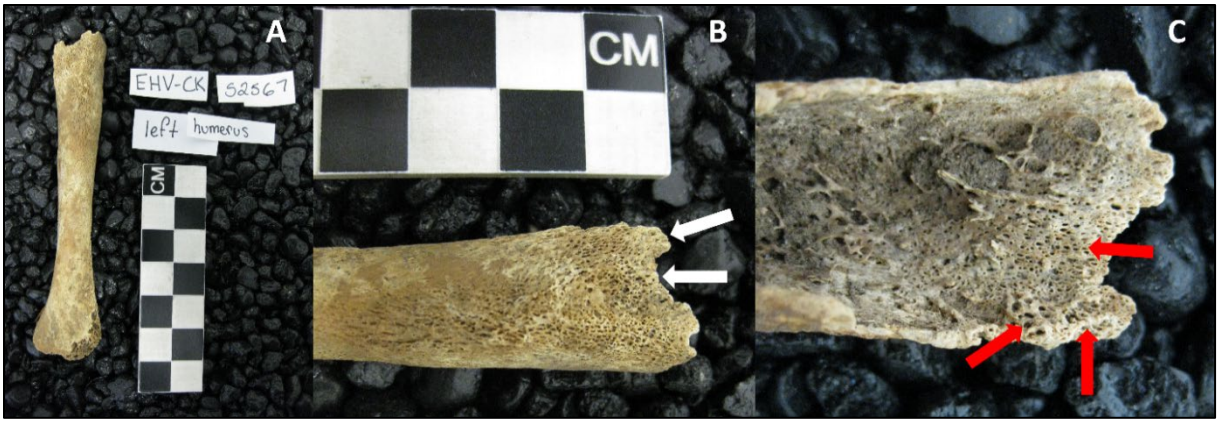

Figure 4.29 *Left humerus with proximal shaft fracture (A) from individual EHV-CK S2567. Image B shows the fracture margin viewed the anterior aspect; white arrows indicate rounded fracture margins. Image C shows the endosteal surface viewed from the posterior aspect; red arrows indicate areas of new bone formation.*

While some postmortem damage has occurred, the fracture margins on the anterior aspect are rounded with new bone formation (Fig. 4.28B). The surrounding cortical bone is thin with severe porosity and new bone formation on both the external and internal surfaces (Fig. 4.29B-C). The new bone formation on the fracture margins is visible via microscopy (Fig. 4.30A) as is the layering of new bone on the endosteal surface (Fig. 4.30B-C). Post-mortem damage to the posterior shaft precludes the ability to assess the type of fracture, though it may have been transverse or greenstick. Directionality is likewise unknown. The rounded fracture margins, porosity, and small amount of new bone formation adheres to stage one of fracture repair and provides a post-traumatic time interval of approximately 15 to 35 days.

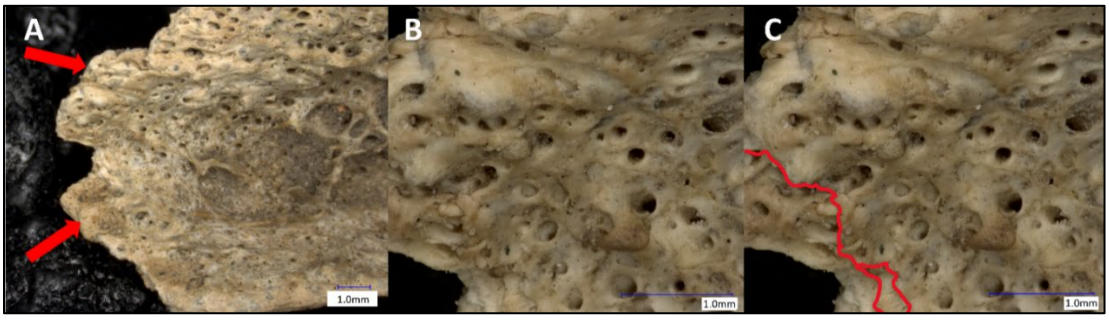

Figure 4.30 *Microscopic images of new bone formation on left humerus from individual EHV-CK S2567. Interior cortical surface at 20x magnification with new bone on the margins (red arrows) (A), internal cortical surface at 100x magnification (B), internal cortical surface at 100x magnification with red lines marking layers of new bone (C).*

4.2.2.2 GRK V59

Individual GRK V59 is an early adolescent, aged 10-12 years based on dental development and eruption. A sex estimation was not undertaken due to their young age. They presented with a suspected fracture to the shaft of the right fibula (Fig. 4.31A).

Macroscopic examination revealed a rounded elevation on the anterior surface and a build up of potential new bone on the internal surface (Fig. 4.31B-C). The cortex on the exterior surface has been removed, likely through taphonomic processes, but there is no evidence of new

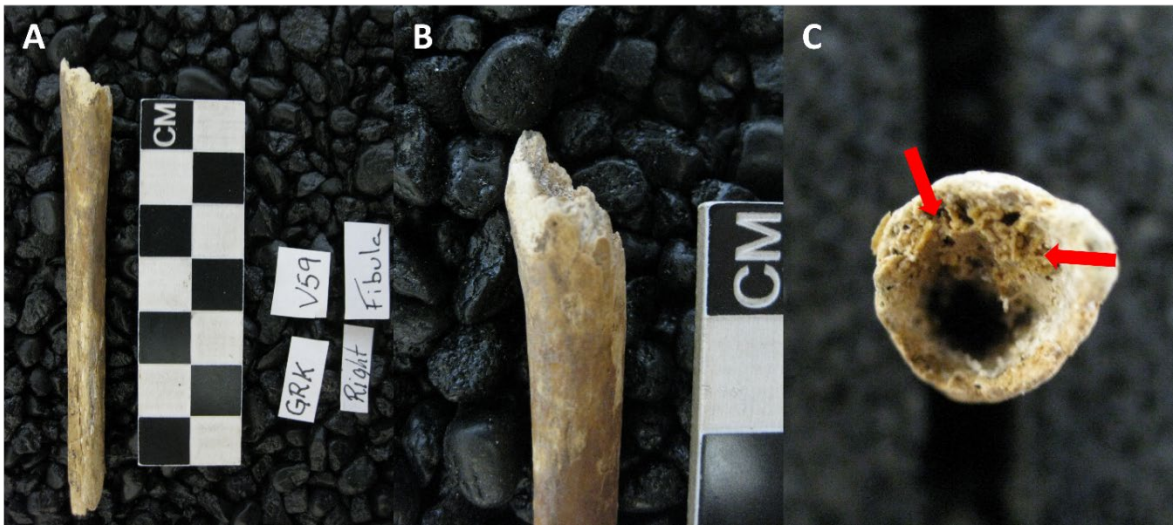

Figure 4.31 *Fracture to right fibula from individual GRK V59 (A), rounded external cortical surface (B), and a mass in the medullary cavity (C).*

bone formation on the remaining external surface and the cortical bone appears to be well remodeled. The fracture margins are light in color indicating a post-mortem break; however, the build up of suspected new bone in the marrow cavity (Fig. 4.31C) warranted attention and the bone underwent micro-CT scanning to investigate the internal structure. Slices from the micro-CT reconstruction (Fig. 4.32) showed the build up is in fact bone tissue, with porous new bone visible around the trabeculae. There are two possibilities, either the fibula represents a well healed fracture with secondary callus and the remaining build up of bone in the medullary cavity

is the remnants of the endosteal callus that were slowly being resorbed, or the fracture occurred above the remaining section of bone and damage made the bone more susceptible to taphonomic processes, meaning the fractured portion did not preserve. The medullary cavity is generally reestablished during the bone remodeling stage (stage five), so either option is a possibility. The micro-CT images also revealed mineralization defects (Fig. 4.32B) consistent with vitamin D deficiency (Brickley, 2024).

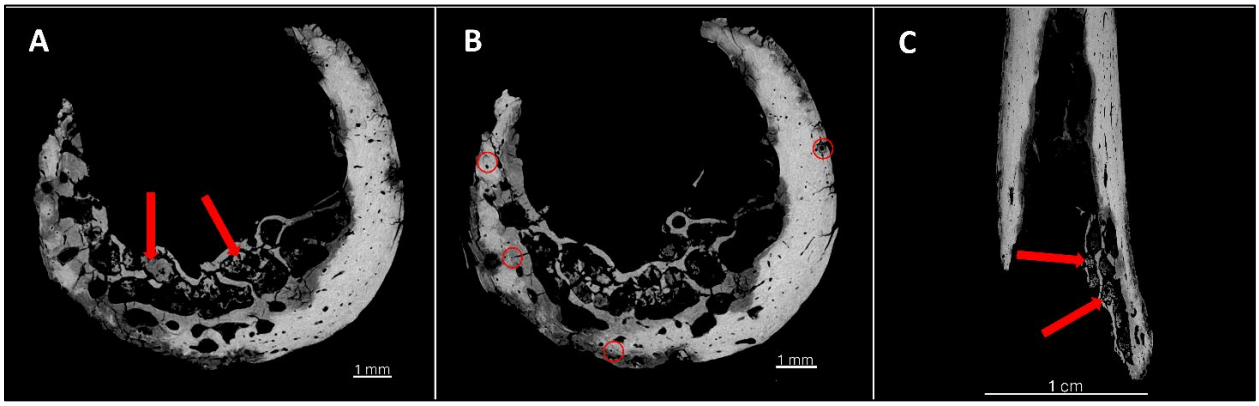

Figure 4.32 *Transverse micro-CT images of the right fibula from individual GRK V59 showing fracture callus (A, red arrows), mineralization defects (B, red circles), and a sagittal slice showing the same fracture callus (C, red arrows).*

The stage of fracture repair for the first option conforms to stage five with a post-traumatic time interval greater than 49 days. If the fracture occurred in the absent section of bone, the stage of fracture repair is unknown, and an estimation of the post-traumatic time is not possible.

4.2.3 Cranial Fractures

Two individuals presented with cranial fractures. Individual EHV-CK S979 has a fracture to the left zygomatic and GRK V512 has a remodelled compression fracture to the frontal bone. The crude prevalence of cranial fractures is 2/55 individuals or 3.6%. The true prevalence for each skeletal element can be found in Table 4.3.

4.2.3.1 EHV-CK S979

EHV-CK S979 was identified as female through DNA analysis (see section 3.1.2), and falls into the late child category, aged 6-9 years based on dental development and eruption. Macroscopic examination identified a hairline fracture to the orbital surface of the left zygomatic (Fig. 4.33).

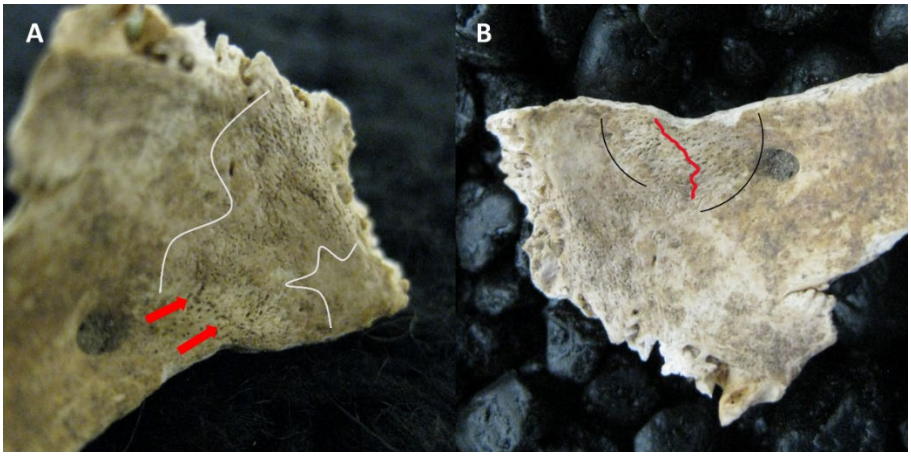

Figure 4.33 *Remodeled fracture to left zygomatic from individual EHV-CK S979. The fracture line is indicated by the red arrows, white lines outline area of reactive bone (A). Fracture line (red line) and remodeled bone outlined by black lines (B).*

Partially remodeled new bone covers the fracture line on the orbital surface near the frontal process. While the cortex has been damaged postmortem, there is a small but noticeable depression on the anterior surface of the zygomatic directly inferior to the hairline fracture. The micro-CT reconstruction revealed a small, superficial fracture line beneath the new bone formation (Fig. 4.34). Based on the depression in the bone at the base of the fracture line, the fracture may have been the result of blunt force trauma (Lovell, 1997). The presence of lamellar bone covering the fracture line indicates the fracture is in stage three of repair, with a post-traumatic time interval of approximately 91 days.

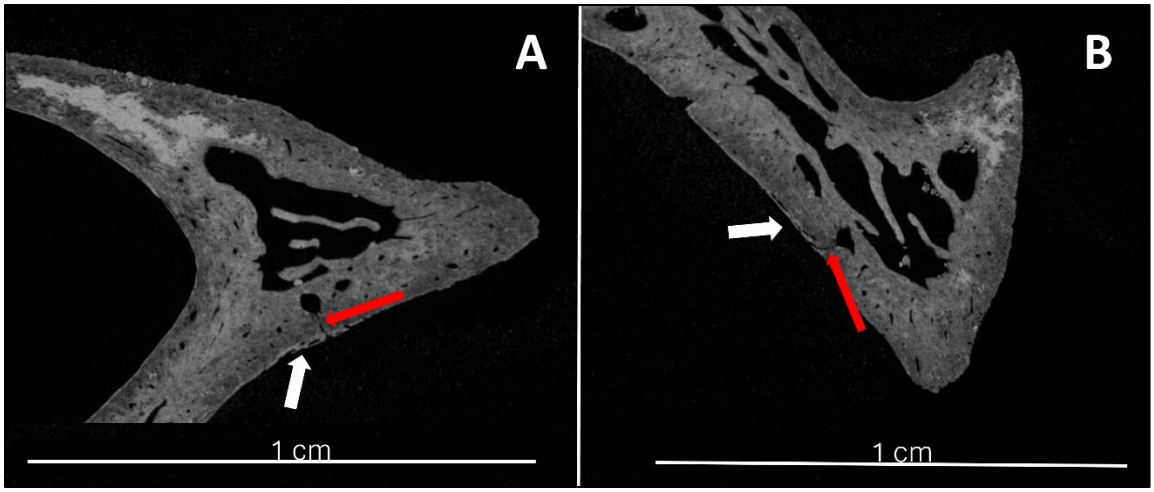

Figure 4.34 *Micro-CT slice of left zygomatic from individual EHV-CK S979.Coronal view (A) and lateral view (B). The red arrows point to the fracture line and the white arrows indicate new bone formation.*

4.2.3.2 GRK V512

GRK V512 is a 16-year-old, male individual in the middle adolescent category, identified through a burial record. He presented with a well healed, depressed cranial fracture to the frontal squama above the right orbit (Fig. 4.35A). The lesion is concave with a coarse surface texture composed of lamellar bone suggesting remodelling. The ellipsoid depression measures 21mm at the longest point and 7mm at the widest point. The margins of the depression are rounded but well-defined. There is only a single lesion evident on the cranium.

Figure 4.35 *Depression indicative of a remodeled compression fracture to the frontal from individual GRK V512 outlined in red (A). A close-up image of the depressed, healed cranial fracture showing definition of the margins (B).*

Botham (2019) explains that healed depressed cranial lesions may result from fracture, lytic lesions, neoplasms, and cranial cysts. However, according to the criteria established by Botham (2019), the lesion is highly consistent with a healed fracture. The shape and location of the lesion are only "consistent with" a cranial fracture, but the rounded margins, evidence of a bony reaction, and singular lesion fall into the "highly consistent with" category (Botham, 2019). Beveling could not be determined due to the remodelled nature of the lesion. The cranium was also intact, precluding the ability to conduct a micro-CT scan or to examine the endocranial surface. Based on the shape and remaining region of depressed bone, the fracture likely resulted from blunt-force trauma.

There is limited information detailing the timing of cranial fracture repair (Partiot et al., 2020). However, in a forensic case involving a 7-year-old child, Walker et al. (1997) noted five trephined holes on the frontal and parietal related to a surgery three months previously. Signs of healing included well consolidated new bone surrounding the margins but there was no bridging of the holes (Walker et al., 1997). In a similar case study of a 16-year-old adolescent, Sauer and Dunlap (1985) noted two well-healed burr holes from a surgical procedure five years previously. In this case, one hole was covered by remodeled bone and the other showed remodeled bone around the margins of the open hole (Sauer & Dunlap, 1985). Considering these data, and the fracture repair rates in Table 3.3, the cranial depression fracture is in stage five with a likely minimum post-traumatic time interval of 147.7 days.

4.2.4 Rib Fractures

Only two individuals presented with ante-mortem rib fractures, both from the Zwolle collection. ZW-87 8 presented with one rib fracture and ZW-87 67 presented with three rib fractures. The crude prevalence is 2/55 or 3.6%. The true prevalence can be found in Table 4.3.

4.2.4.1 ZW-87 8

ZW-87 8 is a 19-year-old female, identified via burial record, and the only individual in the late adolescent category. Macroscopic examination revealed a fracture to the left twelfth rib with a partially remodeled fracture callus at the midshaft (Fig. 4.36A). There was probable delayed union of the shafts based on remodeling of the fracture margin (Brickley & Buckberry, 2015). The anterior shaft was not recovered. The rib was also likely dislocated at the time of fracture and displaced anteriorly. The fracture callus has a distinct boney projection on the cranial surface, which matches a downward boney projection on the caudal surface of the eleventh rib (Fig. 4.36C). The boney spicule on the eleventh rib is likewise composed of partially remodeled woven bone and is located near the midshaft (Fig. 4.36B), indicating rib 12 was displaced anteriorly before the formation of the fracture callus. The combination of fracture and dislocation indicate the injury likely resulted from blunt force.

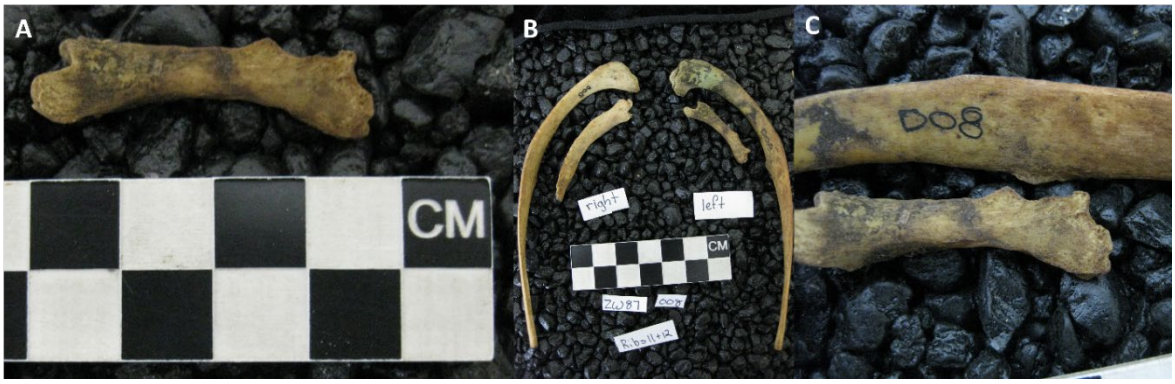

Figure 4.36 *Head and partial shaft of fractured left twelfth rib from individual ZW-87 8 (A) (rib head is on the left and the partially remodeled fracture callus is right), location of the left twelfth rib in comparison to right, supporting an anterior dislocation (B), and boney projection on the inferior surface of rib 11 that aligns with the callus on rib 12 (C).*

The macroscopic appearance of the fracture callus adheres to stage three with a post-traumatic time interval of approximately 68.6 days. There are no bone spicules or post-mortem breaks in the callus indicating bridging with the anterior shaft. There is no eburnation or porosity to indicate non-union (Brickley & Buckberry, 2015), however, non-union remains a possibility.

4.2.4.2 ZW-87 67

ZW-87 67 is an 8.5–10-year-old, based on dental development and eruption, in the late child category. Sex estimation was not undertaken. Macroscopic examination revealed three fractured lower ribs on the left side. Because not all ribs were present the exact rib number could not be determined, therefore, they are referred to as rib A, B, and C.

Figure 4.37 *Left rib A from individual ZW-87 67 with fracture to shaft and small woven bone callus. The red arrow points to a patch of eburnation on the visceral fracture margin.*

Rib A sustained a fracture to the midshaft, and there is a sheet of woven bone on the visceral surface (Fig. 4.37). The posterior fracture margins are straight and sharp while the anterior fracture margins are jagged and overlap. It is unknown whether the callus broke during life or in the post-mortem environment, however, eburnation on the anterior fracture margins indicates a possible period of delayed union. On the posterior surface, there is only a small sheet of new bone formation. Ribs B and C both sustained fractures to the neck (Fig. 4.38). The fracture margins are sharp, though both posterior and anterior margins are jagged. The rib heads were not recovered. There is a small amount of new bone on the visceral surface of the shaft anterior to the fractures on both ribs, again the callus has been partially removed either during life or post-deposition. Rib B has no new bone on the posterior surface while rib C has a small sheet. There is a small patch of eburnation on the internal cortical surface of the anterior aspect of rib B and eburnation on the external cortical surface of the visceral shaft of rib C. The location

of the fractures and stages of repair indicate the individual likely experienced a single event of blunt force trauma.

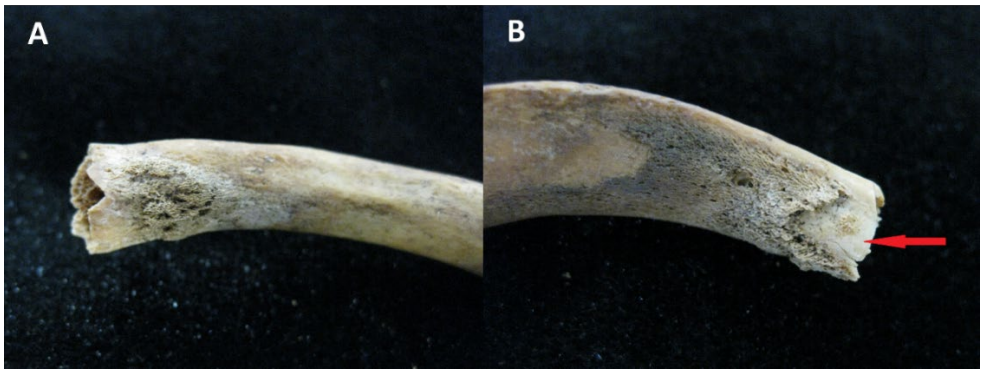

Figure 4.38 *Left rib B (A) and rib C (B) from individual ZW-87 67 with fractures to the neck and small woven bone calluses. The red arrow points to a patch of eburnation on the visceral fracture margin.*

The reactive bone on the fracture margins indicates ZW-87 67 is in stage two of fracture repair, with a post-traumatic time interval of 28-42 days. The presence of eburnation on the fracture margins indicates a post-traumatic time interval of at least 13 days (Todd & Iler, 1927), but may also indicate delayed union or non-union (Brickley & Buckberry, 2015; Mant et al., 2019). However, this timeline may have been complicated by underlying health conditions (see section 5.2.2). As a result, there is uncertainty regarding the estimated timing of the fracture prior to death.

4.2.5 Unconfirmed Cases

Several individuals displayed pathological changes potentially resulting from fracture, but which could not be confirmed macroscopically, and micro-CT imaging was not undertaken. These cases have not been included in the fracture prevalence but warrant some attention due to their relationship to the limitations of the present study, which is discussed in section 4.2.6.

4.2.5.1 ARJB V1368

A probable female between the ages of 14 and 18 years, based on epiphyseal fusion, ARJB V1368 displays evidence for 6 morphological anomalies affecting T8, T9, T10, T12, L1, and L3. These all take the form of possible depression fractures without discontinuity to the surface of the endplates, but where the trabeculae below the bowl-shaped depression may be fractured (Brinckmann et al., 1988). Thoracolumbar border shifting occurred, with T12 taking on the articular facets of a lumbar vertebra.

Figure 4.39 *Inferior endplate of T8 vertebrae from ARJB V1368 with bowl-shaped depression.*

There are bowl-shaped depressions on the central endplates of T8-T10 and T12-L1 and L3. The depression is on the inferior surface of T8 (Fig. 4.39), T9 and T10 have bowl-shaped depressions on both superior and inferior endplates (Fig. 4.40). T12 has the deepest central depression located on the superior endplate. The depression on L1 is also on the superior surface and has well defined margins. L3 has a depression on the superior surface. Unfortunately, micro-CT imaging was not undertaken for these vertebrae, therefore fractured trabeculae beneath the cortical surface

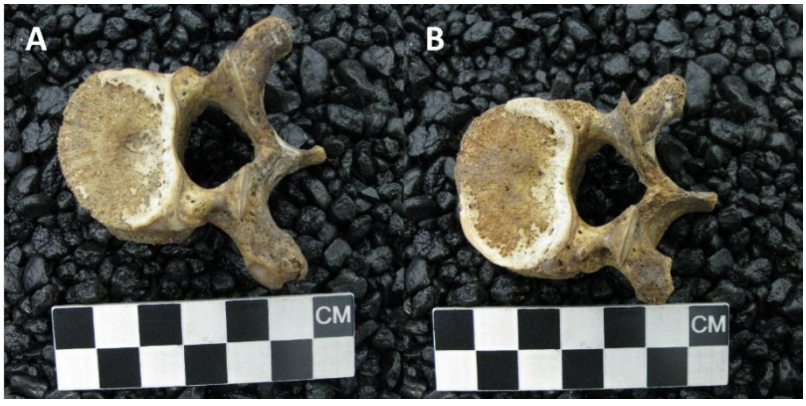

Figure 4.40 *Superior endplates of T9 (A) and T10 (B) vertebrae from ARJB V1368 with bowl-shaped depressions.*

could not be confirmed. Alternatively, the lesions may be well-remodelled Schmorl's nodes affecting the central endplates.

4.2.5.2 ARJB V1632

ARJB V1632 is an early child aged 10.5 months to 1.5 years based on dental development and eruption. There is a ridge of new bone formation on the distal left humerus that could be evidence of a healing physeal fracture (Figure 4.41A); however, taphonomic processes have resulted in extensive damage to the distal humerus.

Figure 4.41 *Distal left humerus from ARJB V1632 with bone spicules on posterolateral aspect.*

There is a spicule of reactive bone, measuring 0.5 cm, on the posterolateral surface beginning above where the olecranon process would be located and projecting laterally (Fig. 4.41B). The medial and central distal end have been destroyed by taphonomic processes. In modern populations physeal factures account for 15-30% of all injuries in children below 16 years of age (Levine et al., 2023). Physeal fractures may involve just the cartilage or extend through the cartilage into the metaphysis, potentially resulting in partial detachment of the metaphysis from the diaphysis (corner or bucket-handle fracture) (Meyers & Marquart, 2023; Lewis, 2018). The area of damaged bone matches the general description of a Salter-Harris type II or IV physeal fracture, wherein the fracture extends into the metaphysis (Levine et al., 2023; Salter & Harris, 1963). Reactive bone may indicate the presence of fracture repair. Unfortunately, a definitive diagnosis cannot be

reached due to the extent of the taphonomic damage and because the epiphysis was not available for examination.

4.2.5.3 EHV-CK S1834

Individual EHV-CK S1834 is an early adolescent of undetermined biological sex and an age range of 11 to 15 years, based on epiphyseal fusion as the dentition was not available. They presented with morphological changes to a left rib that may be the result of a well healed fracture.

An unnumbered lower left rib shows a deep depression on the posterior, vertebral end adjacent to the tubercule (Fig. 4.42A-B). The edges are smooth and composed of lamellar bone. On the visceral surface there is a small, linear defect resembling a fracture line.

Figure 4.42 *Lower left rib with possible healed fracture from EHV-CK S1834, posterior surface (A & B) and visceral surface (C).*

The edges are ragged (Fig. 4.42C) but composed of lamellar bone as indicated by microscope image (Fig. 4.43). There is a total of 16 ribs available for individual EHV-CK S1834, eight left and eight right, but only a single rib exhibits morphological changes matching the above description, indicating the defect is unlikely to be

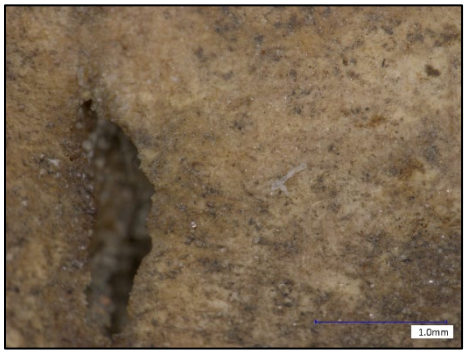

Figure 4.43 *Microscopy image at 100x magnification of linear groove on visceral surface.*

the result of a rugose muscle attachment. Instead, the depression and remaining linear defect may be the result of a well-healed fracture to the rib neck. Changes in the internal bone structure are unknown as micro-CT analysis was not undertaken.

4.2.6 Issues in the Identification of Fractures in Developing Bone

The methodological problems inherent in the identification of fractures in developing bone (see section 2.5.5) are equally relevant to the present research. This research did not identify any of the most common types of fracture affecting developing bone (torus/buckle, greenstick, and physeal) (see section 2.5.1). This is likely due to the subtle nature of these types of fractures. In greenstick fractures, the loose attachment of the periosteum often results in a large hematoma but with limited evidence of a fracture line (Lewis, 2018, p. 92). A wide variety of conditions may result in widespread new bone formation, and without the use of additional imaging technologies, a greenstick fracture is unlikely to be detected. Torus/buckle fractures can likely only be identified through macroscopic examination by a slight bulge in the cortical surface. Lewis (2018, p. 93) states that no clear examples have been identified in the archaeological record. Lastly, physeal fractures may not impact bone (Lewis, 2018, p. 95; Salter & Harris, 1963), and any chondral injury will not be evident in dry bone. Additionally, without complications physeal injuries undergo rapid fracture repair (Lewis, 2018, p. 95), resulting in a narrow window of time during which they would be visible. There was one suspected physeal fracture in this thesis (see section 4.2.5.2), but this could not be confirmed, reinforcing the inability for current paleopathological methods to identify specific fracture types in developing bone. More bioarchaeological research on the appearance of fracture types that are unique to developing bone is required.

While a combined approach using macroscopic, microscopic, and micro-CT analyses was applied to increase the chances of identifying fractures, it is the opinion of the author that only fractures occurring within a small window in the timeline of fracture repair were identified. The majority of fractures in the present study involved some degree of macroscopically visible healing in the form of woven or lamellar bone, providing an obvious, outward indication that a fracture had occurred. However, not all stages of healing are visible macroscopically in dry bone. Without some outward indication of fracture, additional imaging was not undertaken. Examples of fracture likely occurring on the extreme ends of the spectrum can be found in the unconfirmed cases section (see section 4.3.5). The morphological change seen in the rib of EHV-CK S1834 may represent a well healed fracture to the neck. However, without the application of imaging technologies to examine the inner trabecular structure, a fracture cannot be ascertained with any confidence. An increased rate of healing in young individuals is likely to mask the true prevalence of fracture in children and adolescents, and while micro-CT imaging may provide more information, without justification the cost of imaging methods continues to be prohibitive to paleopathological analysis.

Effects of taphonomy on developing bone combined with a fracture occurring near to the time of death are potentially masking a traumatic injury to the humeral metaphysis of ARJB V1632. The individual was between 10.5 months and 1.5 years of age at the time of death, an age during which the bones are incredibly vascular and porous. While a spicule of reactive new bone indicates some type of pathology, damage to the metaphyseal surface and medial aspect of the distal humerus prevented proper analysis. Given the current limitations of methods and technologies in the field of paleopathology, the recognition of fractures in poorly preserved remains from individuals undergoing growth and development is likely to remain an issue and

may have resulted in cases of fracture being overlooked in the present study. For the above stated reasons, there is a high likelihood that fractures occurring very near to the time of death, those that were very well remodeled, and those that were affected by taphonomic processes were missed during analysis, meaning the prevalence presented here may be an underestimate.

4.3 Summary

A total of 55 children and adolescents were examined for this study. Macroscopic, microscopic, and micro-CT analysis resulted in the identification of 47 fractures in 16/55 individuals for a combined crude prevalence of 29.1%. Microscopic and micro-CT imaging provided additional information unavailable through macroscopic analysis alone and played a significant role in the determination of ante-mortem fractures. A summary of the results of crude fracture distribution by element, age category, and biological sex is available in Table 4.5.

Table 4.5 *Summary table with crude fracture prevalence (fracture per individual) by element, age category, and biological sex.*

Summary of Crude Fracture Prevalence					
Crude Fracture by Element		**Crude Fracture by Age Category**		**Crude Fracture by Biological Sex**	
Cervical Vertebrae	1/55	Early Child	2/21	Male	2/4
Thoracic Vertebrae	5/55	Late Child	2/9	Probable Male	2/5
Lumbar Vertebrae	6/55	Early Adolescent	4/12	Ambiguous	1/1
Humerus	1/55	Middle Adolescent	7/12	Probable Female	2/3
Fibula	1/55	Late Adolescent	1/1	Female	4/5
Cranial Vault	1/55			Undetermined	5/37
Zygomatic	1/55				
Ribs	2/55				

The most fractures were identified in middle adolescent individuals, followed by early adolescents, and both males and females were relatively equally affected. A summary of the individuals with observed fractures and stage of repair is plotted in Table 4.6. There is no discernable pattern between biological sex, age, and stage of fracture repair. There are also three cases of suspected fracture that could not be confirmed as micro-CT analysis was not undertaken.

Table 4.6 *Summary of all observed fractures with individual number, estimated biological sex, age category, and repair stage estimate.*

Summary of Observed Fractures				
Individual	**Sex**	**Age Category**	**Fracture**	**Repair Stage**
ARJB V556	Probable Male	Middle Adolescent	L4, L5	2, 5
ARJB V1463	Probable Female	Middle Adolescent	T4, T5	1
ARJB V1556	Probable Male	Early Adolescent	L2, L3, L4, L5	5
ARJB V1583	Undetermined	Middle Adolescent	T7, T8, T9, T10, T11, T12	2, 4 to 5
ARJB V1827	Female	Middle Adolescent	T4-T12	2?
ARJB V1912	Probable Female	Middle Adolescent	L3, L4, L5	5
ARJB V1945	Ambiguous	Early Adolescent	L1, L2, L3	3
EHV-CK S979	Female	Late Child	L. Zygomatic	3
EHV-CK S2567	Male	Early Child	L. Humerus	1
EHV-CK S2918	Female	Middle Adolescent	L5	2 to 4
EHV-CK S3507	Undetermined	Early Adolescent	T8, L1, L3, L4	2 to 3, 5
GRK V59	Undetermined	Early Adolescent	R. Fibula	5?
GRK V512	Male	Middle Adolescent	Frontal	5
ZW-87 8	Female	Late Adolescent	L. Rib 12	3
ZW-87 67	Undetermined	Late Child	Lower L. Ribs A, B, C	2
ZW-87 235	Undetermined	Early Child	C4, C5, C6, T1, T2	2

Vertebral fractures accounted for most of the observed fractures (10/16 individuals), and thoracic and lumbar compression fractures and Schmorl's nodes accounted for 90.0% (9/10) of all fractures to the spine. There is a significant correlation between the presence of vertebral compression fractures and Schmorl's nodes in the same individual ($p<0.05$). While there is no association between socioeconomic status and fractures in general, there is a significant correlation between vertebral fractures (compression and Schmorl's nodes) and mid- to low-socioeconomic status ($p<0.05$). In the following chapter, this correlation will be discussed in terms of lifeways and social determinants of health. The pattern of fractures, especially in the lower-class cemeteries, can aid in understanding the social roles and activities during life.

Chapter 5 Discussion

The aims of this study were to examine ante-mortem fractures in children and adolescents (1–20 years) resulting from direct and in-direct force, underlying pathology, and stress 1) to investigate childhood and adolescent fracture prevalence from post-medieval urban centers in the Netherlands; 2) to explore how fracture prevalence relates to age, biological sex, and socioeconomic status; and 3) to determine what the patterning of fractures can tell us about the activities, social roles, and risk-factors for children and adolescents. This study found an overall crude prevalence of ante-mortem fractures to be 29.1%. Analysis revealed a total of 46 fractures affecting 16 individuals and were primarily identified by the presence of ongoing healing (see chapter 4 for full results). While all age categories, and both males and females, experienced fractures, vertebral fractures in adolescents of lower socioeconomic status were the only clear pattern to emerge. The pattern of vertebral fractures, including compression fractures and Schmorl's nodes, is likely related to activity, social roles, and lifeways in adolescence.

5.1 Fracture Prevalence and Patterns

5.1.1 Overall Fracture Prevalence

The crude fracture prevalence across all four sites is 29.1% (16/55). The crude prevalence of fracture for each site is as follows: Arnhem 26.9% (7/26), Eindhoven 36.4% (4/11), Alkmaar 16.7% (2/12), and Zwolle 50.0% (3/6). Prevalence between archaeological material and clinical data can be difficult to compare (Wood et al., 1992), as clinical studies rarely present their data according to the age/biological sex categories commonly used in bioarchaeology (Brickley et al., 2020, p. 153). Additionally, clinical data is often reported as incidence as opposed to prevalence. Cumulative incidence refers to the risk (probability) of developing a particular condition within a given time frame, whereas prevalence represents the number of people with a condition at a

given point in time (Suchmacher & Geller, 2021). Clinical estimates of fracture incidence vary between studies, by geographic location, age range, and between males and females, with a cumulative incidence typically reported between 42%-64% for boys and 27%-40% for girls below 17 years of age (Boyce & Gafni, 2011; Cooper et al., 2004; Valerio et al., 2010). While the reporting measures are different, the 29.1% crude prevalence of fractures occurring between 1 and 20 years of age in this thesis fits within the clinical risk estimate that 1 in 3 modern individuals under the age of 17 years will experience a fracture (Cooper et al., 2004; Hedström et al., 2010; Herdea et al., 2023). Lewis (2014) posited that because the primary causes of fracture in modern contexts (sports injury, vehicular accident) are unlikely to have existed in the past, the types and prevalence of childhood and adolescent fractures in the past would also be expected to differ. The finding that the crude prevalence of fractures in four, urban post-medieval Dutch communities approaches modern cumulative incidence indicates that while the mechanisms of fracture risk may have changed over space and time, young individuals in the past likewise participated in activities that exposed them to fracture risk.

The comparison of the findings related here to other archaeological contexts is difficult due to the limited number studies examining childhood and adolescent trauma. Confounding this issue is the different research questions, data collection strategies, methods, and reporting used in each respective study. Despite this, the findings presented by other authors have been compiled in Table 5.1 to offer comparison. Research examining intentional violence (e.g. warfare) have not been included because the aims of this research focus on the everyday lives of children and adolescents. The overall crude prevalence (CP) found in the analysis for this thesis is generally higher than those seen in other archaeological sites where the examination of fractures in young individuals has been undertaken (see Table 5.1), even when Schmorl's nodes are considered

separately (CP=25.5% for fracture; CP=14.5% for Schmorl's nodes), likely as a result of the combined assessment methods and aims of the research. However, the reported prevalence of fractures in young people from archaeological contexts has been increasing over time, which may be related to a combination of increased interest in childhood and adolescence and the availability of new investigative technologies.

Table 5.1 *Comparative analysis of childhood and adolescent fracture prevalence from archaeological contexts.*

Author(s)	Age Range	Site	Sample	CP	Female CP	Male CP	SN INCL[1]	SN CP
Langlois, 2024	1 – 20 years	Netherlands 1650 – 1850 CE	N=55	29.1%	66.7% (n=9)	50% (n=8)	Yes	14.5%
Lewis, 2016	6.6 – 25 years	Medieval England 900 – 1550 CE	N=3,983	6.4% (Urban)	6.2% (Urban)	12.8% (Urban)	No	10.8% (Urban)
Lewis, 2016	6.6 – 25 years	Medieval England 900 – 1550 CE	N=629	4.6% (Rural)	9.2% (Rural)	4.1% (Rural)	No	2.4% (Rural)
Connell et al., 2012	6 – 17 years	St. Mary Spital 1120 – 1539 CE	N=892	3.6%	---	---	No	9.9%
Scott et al., 2023	16 – 25 years	Fortress of Louisburg 1730 – 1770 CE	N=11	27.3%	---	---	No[2]	62.5%
Van de Vijver, 2019	<18 years	Mechelen & Antwerp, Belgium 15 – 18th c. CE	N=135	13.3%	---	---	No	---
Shapland et al., 2016	14 – 25 years	Medieval England 900 – 1600 CE	N=314	---	3.8% (Vertebral Fractures Only)	3.4% (Vertebral Fractures Only)	No	29.8% (Females) & 40.3% (Males)
Lewis, 2010	<17 years	Poundbury Camp	N=364	3.6%	---	---	No	---
Djurić et al. (2010)	ranging between eruption of the second molar to closure of the long bone epiphyses	Stara Torina 800 – 1200 CE	N=81	2.5%	---	---	No	0.0%
Gowland et al., 2023	8 – 20 years	Fewston, North Yorkshire 19th c.	N=154	0.65%	---	---	---	---
Gowland et al., 2018	<20 years	Britain 19th c.	N=181	0.55%	---	---	---	---

[1] Schmorl's nodes (SN) reported as part of the overall crude prevalence.
[2] Poor preservation led to a reduced sample size.
--- Not available

Lewis (2016) examined fracture prevalence in children and adolescents and found an overall crude prevalence of 6.4% (n=3,983) in urban populations, a significantly lower prevalence than reported in this thesis. However, her comparatively low result may be due to the use of secondary data, including published and unpublished field reports, where the careful analysis of child and adolescent remains for fracture may not have been an aim of the original research. Additionally, Lewis (2016) states that many of the reports date to a time before the advancement of paleopathological methods and the availability of imaging technologies. Connell et al., (2012) reported an overall crude prevalence of fractures of 2.0% (7/348) for individuals aged 6-11 years and 4.6% (25/544) for the 12-17 years category. No fractures were found in individuals below 6 years of age. The reported numbers are the result of a site analysis, and as a result, careful examination of the remains of children and adolescents for fractures was likely not undertaken. Only the most obvious cases would have been recorded and included in the reported prevalence. Research questions also play an important role in reported fracture prevalence. Scott et al. (2023) conducted an intentional trauma analysis of adolescent and adult males from the Fortress of Louisberg, Nova Scotia, Canada, and found a crude prevalence of fractures for adolescents of 27.3%, a comparable prevalence to the findings in this thesis. Similarly, van de Vijver (2019) purposely examined trauma and reported crude prevalence of fracture to be 3.3% (2/61) and 21.6% (16/74) in two collections from Antwerp and Mechelen, Belgium for a combined prevalence of 13.3%. Shapland et al. (2016) did not assess all traumatic injuries but made note of activity markers including vertebral fractures and Schmorl's nodes in their analysis of adolescents (14-25 years) from medieval England. They reported a prevalence of vertebral fractures of 3.8% and 3.4% for females and males, respectively, and prevalence of Schmorl's nodes of 29.8% and 40.3% for females and males. The remaining archaeological studies

examining fracture prevalence in children and adolescents (Table 5.1) report significantly lower prevalence, reasons for these differences are unknown but may be related to methods of analysis (macroscopic versus a combined approach), preservation, intent of the research, or lifestyle factors for the different communities.

5.1.2 Fracture Prevalence by Age, Biological Sex, and Socioeconomic Categories

Fracture prevalence by age category is as follows: early child 9.5% (2/21), late child 22.2% (2/9), early adolescent 30.8% (4/13), middle adolescent 63.6% (7/11), late adolescent 100% (1/1). Fractures spanned every age category but the crude prevalence of fractures among adolescent individuals (12/25=48.0%) is markedly higher than that of the late and early child categories (4/30=13.3%). The late adolescent category has been excluded from further analysis due to small sample size (n=1). Crude fracture prevalence by biological sex produced no statistically significant differences, although fractures were present in females (6/9=66.7%) slightly more often than males (4/8=50%). The crude prevalence of trauma in the low and mid- to low-socioeconomic sites of Arnhem and Eindhoven is 26.9% (7/26) and 36.4% (4/11), respectively. Crude prevalence is the mid- to high-socioeconomic sites of Alkmaar and Zwolle is 16.7% (2/12) and 50% (3/6), respectively.

In clinical work, the location of pediatric fractures tends to vary according to skeletal maturation and age-specific activities, with fracture incidence steadily increasing with age through puberty (Hedström et al., 2010; Mathison & Agrawal, 2010; Valerio et al., 2010). Clinical studies (Cooper et al., 2004; Mathison & Agrawal, 2010; Valerio et al., 2010) have found that in children aged two to five years, injuries to the long bones often result from engaging in new activities such as learning to walk, running, and falling. Injuries to the distal radius and ulna, the humerus, the clavicle, and skull are more common during this age range. As

age increases, fractures to the lower limbs, feet, hands, and ribs also increase. Unfortunately, the number of fractures found in the present study is too small to allow for analysis of fracture location by age. Notably, analysis for this thesis did not identify any of the fracture types common in developing bone (physeal, torus/buckle, and greenstick fractures) (see sections 2.5.1 and 4.2.6). There was one suspected physeal fracture (section 4.2.5.2), but this could not be confirmed as micro-CT imaging was not undertaken.

Clinical pediatric studies have identified the peak in fracture incidence to occur during the adolescent period between approximately 11 and 15 years of age (Boyce & Gafni, 2011; Cooper et al., 2004; Hedström et al., 2010), as activity patterns and exposure to risk-factors change. A higher prevalence of fracture in adolescents is also commonly reflected in archaeological material (Connell et al., 2012; Dittmar, 2021; Lewis 2016; Penny-Mason & Gowland, 2014; van der Vijver, 2019), and is posited to potentially be related to changes in activity, with the adolescents beginning to take on adult social roles (Penny-Mason & Gowland, 2014; van der Vijver, 2019). The accumulation of trauma over the life course may be playing a role in higher fracture prevalence among adolescents, as both GRK V512 (see section 4.2.3.2) and GRK V59 (see section 4.2.2.2) present with well healed fractures; however, the majority of fractures (7/25) in the early and middle adolescent age categories occurred near the time of death (below stage five of fracture repair). As a result, the fractures likely reflect engagement with new activities during the adolescent period as opposed to accumulated trauma.

The finding that males and females experienced fractures at relatively similar fracture prevalence indicates that both engaged in activities with risk of fracture. This differs somewhat from modern studies of childhood and adolescent fracture, where males tend to experience fractures more often than females (Cooper et al., 2004; Hedström et al., 2010; Naranje et al.,

2016; Valerio et al., 2010). Archaeological studies examining trauma have found mixed results regarding fracture prevalence between males and females. In a study of adolescents in rural and urban contexts in medieval England, Lewis (2016) found that in urban populations, males had a crude prevalence of 12.8% for fracture compared to females at 6.2%. However, in the rural populations, females had a higher crude prevalence (9.2%) compared to males (4.1%) (Lewis, 2016). Connell et al. (2012) reported a higher prevalence of fractures in males compared to females across all adult age categories and time periods, unfortunately, sex estimations were not undertaken for the adolescent individuals. Further comparison is limited as sex estimations were not undertaken by Van der Vijver (2019) and Scott et al. (2023) did not assess females.

Differing levels of preservation between the sites investigated in the current study probably affected the ability to detect fractures. However, the crude prevalence of trauma is slightly higher in the combined lower socioeconomic sites of Arnhem and Eindhoven 30.6% (11/36) as compared to the higher socioeconomic sites of Alkmaar and Zwolle 27.8% (5/18). However, this difference is not statistically significant. Of note, the high crude prevalence in Zwolle may be skewed by small sample size and potentially biased by which remains were kept onsite at Leiden University, impacting the overall results. A higher fracture prevalence in lower socioeconomic communities was reported by Lewis (2016) and Van de Vijver (2019), both of whom posit lifeways as the largest contributing factor to increased fracture prevalence. Lifeways may likewise explain the differences in prevalence between sites in this study and are discussed in section 5.2.

5.1.3 Pattern of Vertebral Fractures in Adolescents, Activity, and Social Roles

Only a single, clear relationship emerged from the analyzed data: vertebral fractures, including vertebral compression fractures and Schmorl's nodes, in adolescent individuals of mid-

to low-socioeconomic status. The true prevalence of Schmorl's nodes affecting the thoracic and lumbar vertebrae is 3.0% (17/573) affecting eight individuals (CP=14.5%). The true prevalence of vertebral compression fractures affecting the thoracic and lumbar vertebrae is 3.3% (19/573) affecting seven individuals (CP=12.7%). All affected individuals were early and middle adolescents from the lower socioeconomic collections. Of the 13 adolescents from Arnhem, seven presented with vertebral fractures (53.8%) and 2/6 (33.3%) adolescents in Eindhoven. A single mid- to upper-class individual, ZW-87 235, exhibited evidence for vertebral fractures resulting from a different mechanism, but no other individuals from the upper-class collections exhibited vertebral fractures. Amongst the lower-class collections, vertebral fractures more commonly occurred in the middle adolescent category (6/10=60.0%), followed by the early adolescent category (3/9=33.3%) (see full results in section 4.2.1), conforming to the above stated peak occurrence of fracture in adolescence related to changes in activities and social roles. The pattern of fractures affecting the thoracic and lumbar vertebrae is notable as it allows for the consideration of activities associated with specific age and socioeconomic groups. Fracture mechanisms and associated activities and lifeways will be discussed in section 5.2.

The finding of fractures in adolescent spines is not unique to the present analysis, and the prevalence is generally comparable to the findings in this study. Lewis (2016) found an overall crude prevalence of fractures in the spine to be 8.2% (24/294), with urban females (14.9%) displaying more spinal fractures than urban males (7.9%). From St. Mary Spital, 106/1027 non-adults (<18 years) displayed evidence of spinal joint diseases for a crude prevalence of 10.3% affecting the 6-11 (n=3) and 12-17 (n=103) year age categories (Connell et al., 2012). Within the 12–17-year category, Schmorl's nodes were the most common form of vertebral trauma, affecting 9.9% of individuals (103/1027 individuals). Schmorl's nodes were likewise considered

separately by Scott et al. (2023), and while vertebral preservation was poor leading to a small sample size, the crude prevalence of Schmorl's nodes was 62.5%. In an examination of adolescents (14-25 years) from three medieval sites in England, Shapland et al. (2016) found an overall crude prevalence of vertebral fracture of 3.9% for females and 3.4% for males. Schmorl's nodes had a crude prevalence of 29.8% for females and 40.3% for males. While van der Vijver (2019) states there is no evidence of fracture, they reported an overall crude prevalence of vertebral trauma (consisting of porosity to the surface of the endplate, porous depressions, and endplate changes) of 8.5% from Antwerp and Mechlen, Belgium. Maat and Mastwijk (2000) examined spinal trauma in two Dutch collections from Gorinchem and Breda (n=44), dating between 1455-1572 and the 17th c. to 1824 CE respectively. They identified healed avulsion and compression fractures to the vertebral column in a total of 11 adult individuals (7 males and 4 females). Of the 11 individuals affected, they identified three as having spinal injuries that occurred during youth, identifiable by the fact that the mechanisms of the fracture type can only occur in developing vertebrae due to the lack of fused apophyseal ring.

5.1.3.1 Sample Size and the Osteological Paradox

The correlation between the presence of vertebral fractures and mid- to low-socioeconomic status must be considered through the lens of sample size and alongside the osteological paradox. The lower socioeconomic collections of Arnhem and Eindhoven combined (n=37) contain a greater number of individuals than the combined upper socioeconomic collections (n=18) of Alkmaar and Zwolle. The greater number of individuals in the lower socioeconomic collections likely resulted in a higher chance of detecting fractures, contributing to the increased crude prevalence seen in these collections. Additionally, of the adolescent individuals present in the upper socioeconomic collections none had an adequate number of

vertebrae available for analysis, likely impacting the correlation of vertebral fracture presence with low- to mid-socioeconomic status. Additional research examining a larger sample size, with equal representation of low- and upper-class individuals, is required to verify the findings presented in this thesis.

The presence of vertebral stress fractures with lower socioeconomic status must also be considered alongside the osteological paradox. The osteological paradox states that we do not have a sample of all the individuals at risk for disease and trauma (Wood et al., 1992), we only have those who died. It is possible that vertebral fractures occurred in the upper socioeconomic individuals, but factors unrelated to the fractures predisposed the lower-class individuals to an increased mortality risk. As a result, vertebral fractures may have been present in adolescents from the upper social classes but were not visible because the individuals survived into adulthood. This may be confounded by a smaller sample of upper socioeconomic status individuals in the analyzed pool, and the small number of preserved vertebrae within this sample. This situation would result in a false positive correlation between lower socioeconomic status and vertebral fractures. However, Wood et al. (1992) also says that lesions present on the bones of individuals who died young may also be considered as highly selective for lesions associated with increased mortality risk. In clinical literature, there is an association between vertebral compression fractures and increased mortality risk (Lau et al., 2008; Son et al., 2023; Zohar et al., 2023). Jalava et al. (2003) found that mortality rates were 3- to 6-fold higher across all age groups (28–88 years) in osteoporotic patients with vertebral fracture compared to those without vertebral fracture. A second study examining the association between vertebral compression fractures and mortality in all ages by Kim et al. (2023) found that the risk of mortality following vertebral fracture was highest amongst the youngest age cohort they examined (20-29 years) and

decreased with each successive age group. While reasons for the increased mortality risk are not well understood, Kim et al. (2023) posit it may be because the vertebral fractures in the younger age cohorts are more likely the result of traumatic accident. While mortality risk following vertebral fracture in pediatric populations has been found to be low (Babu et al., 2017; Bansal et al., 2019), the estimated post-traumatic time interval for the vertebral fractures place 7/9 cases as occurring near the time death, suggesting a relationship between mortality and vertebral fracture in this study, though the exact mechanisms cannot be determined. Moving forward, increased attention to vertebral trauma in young individuals from archaeological contexts is warranted to better understand the relationship between fracture, lifeways, and mortality risk.

5.2 Lifeways, Social Determinants of Health, and Fracture Risk

Aspects of lifeways impact an individual's fracture risk by exposing them to different hazards. Social determinants of health (SDH) are defined as non-biological factors that influence health outcomes and play an important role in health inequities (Marmot, 2005; Marmot & Wilkinson, 2000; Raphael, 1990, 2000; World Health Organization, 2024). Education, socioeconomic status, and employment may adversely affect health by exposing people to increased fracture risk through activities, and the development of other pathological conditions related to social contexts. Additional biological factors, such as age and biological sex, may likewise influence health. The following sections examine possible lifestyle factors, both biological and social, that may have exposed younger individuals in 17th to 19th century Dutch society to fracture risk and resulted in the relationship between vertebral fractures and mid- to low-class adolescents.

5.2.1 Labour and Apprenticeships for Children and Adolescents

Strenuous labour may explain the correlation of mid- to low-socioeconomic status with vertebral fractures. The aetiology of Schmorl's nodes is multifactorial, with axial compression and torsion of the spine playing a crucial role in combination with other factors (see section 2.5.2.2). Likewise, compression fractures are associated with axial compression and hyperflexion/hyperextension of the spine (see section 2.5.2.1). It is possible the young people examined here engaged in occupations or activities involving axial loading and torsion, hyperextension, and/or hyperflexion affecting the spine such as strenuous labour.

In an extensive study of child labour in the Netherlands, van Nederveen Meerkerk and Schmidt (2008) traced child labour to at least the 17th century, where children and adolescents participated in industry through apprenticeships and labor for pay. Adulthood in post-medieval Netherlands was legally recognized between 21 and 25 years of age (Blom et al., 2021; van Nederveen Meerkerk & Schmidt, 2008), but the age of transition to specific adult social roles varied. Women could marry without parental permission at 20 years and men at 25, and labourers only received adult wages after 20 years of age. However, adolescents over 17 years of age were often denied residence in orphanages and were instead expected to work and take care of themselves (van Nederveen Meerkerk & Schmidt, 2008).

Industriousness and work were prized virtues in the Dutch Republic (Schmidt, 2011; Smit, 2014, p. 506). Occupational training or wage labour served as an educational tool that prepared children for future employment. However, child labour was also often required for the survival of the household in lower income families (Smit, 2014, p. 506) and was desirable for the state as it reduced the necessity of poor relief. Thousands of children in pre-industrial Netherlands were engaged in wage labour. In the city of Tilburg in 1810, over a quarter of all

children were registered as having an occupation, making up a total of 18% of the workforce (van Nederveen Meerkerk & Schmidt, 2008). Children from orphanages began work between eight and nine years of age, but archival records indicate children as young as six could be employed in various occupations. Children beginning apprenticeships, and those whose parents did not require poor relief, were on average older, beginning work between 12 and 14 years of age (Schalk, 2017; van Nederveen Meerkerk & Schmidt, 2008). Types of apprenticeships varied: an apprentice could receive payment in the form of a wage or room and board or, the apprentice could pay the master for the training received (Martini & Bellavitis, 2014). Schalk (2017) states that wages were related to skill level and productive capacity: in the first couple years, an apprentice received lower wages, but as their skills developed their wages increased and surpassed those of lower skilled occupations. Workhouses, established from the late 16th century onward, also provided additional work opportunities to the poor (Schmidt, 2011).

While occupational options and the significance of child/wage labour varied according to age, sex, and socioeconomic background, van Nederveen Meerkerk and Schmidt (2008) and Schalk (2017) state that the majority of children and adolescents worked in the industrial sector. The textile industry offered the most opportunities for young people, males and females worked in reeling, spinning, and carding positions. Girls could also be employed weaving, knitting, and making lace. During childhood, males and females performed much the same type of labour, but around 14 years of age, boys were presented with the opportunity to transition to higher-skilled positions outside of the textile industry, including carpentry, tailoring, leatherworking, glassmaking, and shipbuilding. Options for girls were more limited, encompassing only the garment industry and domestic services (Schmidt, 2011). Most females remained in unskilled or low-skilled sectors, resulting in a gendered division of labour through middle adolescence into

adulthood. Consequently, females often remained in the workhouses longer than their male counterparts. The number of males registered, compared to females, drops significantly after 16-17 years of age; likely because the opportunity for better work became more readily available for males of this age. It is important to note, child labour was not always registered (van Nederveen Meerkerk & Schmidt, 2008) and admittance to orphanages was often restricted to the children of craftsmen (Schalk, 2017), meaning lower socioeconomic children and adolescents, who did not gain employment through formal institutions such as orphanages, may have been engaged in more unskilled, labour-intensive industries than those described here. Children below 12 years of age were banned from engaging in wage labour and apprenticeships following the Van Houten Law of 1874 that emerged in response to the public outcry over the exploitative nature of child labour (Smit, 2014, p. 27).

In a series of letters, William Dodd (1968) described the experiences of factory workers, including children, in early 19th century textile factories in Leeds, England. Dodd details the observations of the Leeds Infirmary surgeon Samuel Smith, who noted the impact of work in a textile factory on the skeletal system. He states that the long hours standing (14–16 hours a day) caused the arch of the foot to collapse and damage to the ligaments in the ankles and knees resulting in the ankles either pronating or supinating and genu varum (bow leggedness). He further noted that disease and deformities of the spine were a common consequence of factory work. All these deformities were noted in people who worked a variety of positions within the textile factory, including spinning, but were more extreme in those individuals who began working at a young age. Dodd (1968) likewise relates his own experiences as a child labourer working as a piecer in a cotton mill, a common occupation for younger children. The role of the piecer was to feed cardings of fabric onto spindles for the spinner. A piecer was required to stand

with one leg forward, bearing the majority of their weight, and transfer the cardings using a torsional or sidelong movement of the torso, then rub the carding on a rough canvas to feed it onto the spindle. The processing of raw materials in the textile factory required manual labour in the form of lifting bales of flax or wool, but often it was the long hours standing and repetitive motions affecting the joints, that caused the most serious deformities.

Vertebral compression fractures and Schmorl's nodes are only present in individuals from the lower socioeconomic collections, supporting documentary evidence that poor children engaged in labour beginning at a young age. The youngest age category to show vertebral fractures is in early adolescence (10-14 years), with individual ARJB V1945 who has an age estimation between 12.5-16.5 years. The middle adolescent category (15-18 years) contains the largest number of individuals with vertebral compression fractures (n=7). The affected age categories conform to the ages at which young people in the Netherlands would be expected to be engaging in wage labour. The comparable prevalence of vertebral trauma in males and females also supports the idea of wage labour, as both boys and girls in the lower socioeconomic classes were expected to work and performed similar tasks involving strenuous labour and repetitive motions affecting the spine.

Scheuermann's disease remains a possible diagnosis for the vertebral fractures in the adolescent age categories (see section 4.2.1.13) and is strongly associated with mechanical loading of the spine while standing (Lewis, 2018; Mansfield & Bennett, 2024). Type-II Scheuermann's disease, affecting the thoracolumbar junction, is also known as "apprentices' spine" due to the relationship of the disease with heavy lifting and muscular activity (Lewis, 2018, p. 257). Consequently, even if Scheuermann's disease is the cause for the compression fractures and Schmorl's nodes in adolescents in this study, the finding of child and adolescent

labour remains valid. However, vertebral compression fractures resulting from mechanical loading and strenuous activity cannot be distinguished from those resulting from acute trauma. In modern populations, the most common cause of compression fractures in young individuals is falls from a height, vehicular accidents, and sports injuries (Clark & Letts, 2001; Saul & Dresing, 2018; Sayama et al., 2014) (see section 2.5.2.1). However, given the high prevalence of compression fractures, labour remains the most likely explanation, though acute trauma such as a fall from a height cannot be ruled out as the cause of the spinal fractures in this thesis.

Strenuous labour has also been identified as a potential cause of vertebral trauma in adolescents, including Schmorl's nodes, in other archaeological studies. Van der Vijver (2019) reported similar results to the findings in this study, where vertebral lesions were present in individuals from the lower socioeconomic cemetery at Mechlen, Belgium and none in the upper-class individuals from Antwerp. She likewise suggests that socioeconomic background and wage labour led to increased exposure to mechanical strain and fracture risk for the lower socioeconomic individuals (van der Vijver, 2019). Scott et al. (2022), who also reported a high prevalence of Schmorl's nodes in adolescent individuals (Table 5.1), posited lifestyle factors associated with the upkeep of the military fortress, including manual labour, as leading to the high prevalence of fractures and Schmorl's nodes in adolescents at the Fortress of Louisberg, Canada. Lewis (2016) likewise related vertebral trauma, including spondylolysis and Schmorl's nodes, in adolescent individuals to strenuous labour and occupation. Both lesion types affected males and females and more commonly occurred more in urban populations (Lewis, 2016). Shapland et al. (2016) believed the high prevalence of vertebral trauma in adolescent females during the medieval period in England is related to labour, as urban females displayed a higher crude prevalence compared to their rural counterparts. The high prevalence of Schmorl's nodes

in adolescent individuals from St. Mary Spital have also been suggested to be the result of increased strenuous activity in these groups (Connell et al., 2012, p. 76).

The presence of Schmorl's nodes in adolescent individuals of mid- to low-socioeconomic status in the present study probably reflects occupational health and socioeconomic activities. The association of both vertebral compression fractures and Schmorl's nodes with hyperflexion/extension and axial loading/torsion of the spine supports documentary evidence that children and adolescent individuals in the post-medieval Netherlands engaged in strenuous labour. The industrial sector offered the most employment opportunities during the post-medieval period in the Netherlands. In addition to the textile industry, the largest economic sectors in Arnhem included the production of tobacco, shoemaking, and the paper industry. In the 17-18th centuries in Eindhoven, the brewing and pottery industries dominated (Alumni Meeting Eindhoven, 2023; Casna & Schrader, 2022; Nijkamp & Goede, 2003). During this time, urbanization and industrialization led to rising class divisions and increasing social inequalities (van Zanden, 1995; van Zanden & van der Berg, 1993). Social determinants likely resulted in the necessity for young, lower-class individuals to engage in wage labour and strenuous activity as a survival strategy, exposing them to increased fracture risk and associated health inequities. The prevalence and pattern of vertebral trauma in the analyzed collections sheds light on the lifeways and social contributions of young individuals in the past.

5.2.2 Underlying Disease State & Contribution of Nutritional Deficiencies

Pathological conditions and nutritional deficiencies can contribute to increased fracture risk via reduced bone mineral density (BMD) (see section 2.5), including decreased bone formation and loss of existing bone tissue (Boyce & Gafni, 2011; Brickley et al., 2020, pp. 136-137; Follis et al., 1950; Park et al., 1935). There is evidence that several of the individuals

analyzed in the present study had underlying pathologies that may have influenced their skeletal integrity and fracture risk.

According to Boyce and Gafni (2011), vertebral compression fractures in younger individuals are rare unless a pre-existing condition compromises the integrity of bone, with low BMD being the largest contributing factor in both adults and children. Due to difficulties inherent in assessing nutrient efficacy in humans (Lappe & Heaney, 2012), clinical studies examining the association between vitamin D and calcium deficiency on bone health report mixed findings (see section 2.5.2.1). However, vitamin D and calcium deficiency have been associated with decreased BMD in modern, clinical studies (Boyce & Gafni, 2011; Herdea et al., 2023). Vitamin D deficiency has been shown to increase cortical porosity in bone (Sundh et al., 2016), leading to heightened skeletal fragility due to bone loss and compromised structural integrity. Higher age has been found to be a risk-factor in vitamin D deficiency and increased cortical porosity may occur transiently during the adolescent period related to rapid growth (Parfitt, 1994; Wang et al., 2010). Under-mineralization of bone during the early stage of the pubertal growth spurt may likewise have played a role in the development of vertebral fractures in the adolescent age categories in the present study. There is a period of delay of approximately eight months between peak growth velocity and peak BMD (Boyce & Gafni, 2011; Parfitt, 1994), during which time there is increased cortical weakness in bone. In a study of modern populations by Boyce & Gafni (2011), the under-mineralization of bone during the adolescent period was associated with the fracture incidence peak between 11-15 years of age. Mineralization defects, consistent with vitamin D deficiency (Brickley, 2024), were identified in the micro-CT reconstructions of three adolescent individuals with vertebral compression

fractures (ARJB V1556, ARJB V1912, EHV-CK S3507), indicating they may have been at an increased risk for fracture as a result of an underlying metabolic condition.

Rapid growth and hormonal changes during the adolescent period results in heightened calcium requirements (Mesías et al., 2011). Cortical porosity, decreased BMD, and inadequate mineralization of bone resulting from calcium homeostasis is a potential consequence of insufficient calcium during periods of rapid growth (Cooper et al., 2016; Mesías et al., 2011; Welsh & Brickley, 2023). Osteoporosis plays a significant role in the development of vertebral compression fractures in modern populations (see section 2.5.2.1). In addition to the mineralization defects visible in ARJB V1556, ARJB V1912, EHV-CK S3507, micro-CT reconstructions reveal less trabecular bone than expected in three individuals (ARJB V556, ARJB V1463, ARJB V1827), a possible sign of osteoporosis (Brickley et al., 2020, p. 129). Thinning of the trabecular structure may be related to decreased bone density resulting from insufficient calcium and/or vitamin D leading to skeletal fragility and increased fracture risk.

Mineralization defects and zones of improper mineralization consistent with vitamin D deficiency (Brickley et al., 2020; Brickley & Morgan, 2023) were also identified in the micro-CT reconstruction of GRK V59, the early adolescent individual with a fracture to the right fibula. Additionally, EHV-CK S2567, the early child with a fracture to the left humerus, displays biomechanical deformities in the form of bowing of both femora and the left tibia and fibula (right tibia and fibula are absent) and a band of IGD in the deciduous second mandibular molar (Cooke et al., 2023) highly consistent with healed rickets. Vitamin D and calcium deficiencies have the potential to heighten skeletal fragility via reduced BMD and increased cortical porosity (Cooper et al., 2016; Parfitt, 1994; Sundh et al., 2016; Wang et al., 2010). While the evidence in this study is limited, there is a possibility that metabolic conditions and nutritional deficiencies

related to limited sun exposure and/or insufficient diet led to increased skeletal fragility for the analyzed individuals.

ZW87 67 displayed evidence for additional pathological conditions that may have increased their skeletal fragility. Evidence points to ZW-87 67 having both congenital syphilis and scurvy at the time of death (Langlois et al., manuscript in preparation). Both scurvy and congenital syphilis (CS) affect collagen production, a critical component of bone (Fain, 2005; Koliou et al., 2022; Noordin et al., 2012; Stubbs et al., 2022). Decreased BMD is a potential outcome of co-occurring scurvy and congenital syphilis. Localized osteopenia has been noted in clinical cases of congenital syphilis in conjunction with unexplained fractures (Koliou et al., 2022; Stubbs et al., 2022) and scurvy results in osteopenia affecting both the cortical and trabecular structures (Fain, 2005; Noordin et al., 2012). Osteopenia resulting from chronic and/or co-occurring conditions probably resulted in increased fracture risk and contributed to the three lower left thoracic rib fractures. In cases of severe vitamin C deficiency, the body may be unable to produce new bone (Brickley et al., 2020, p. 50), which may have delayed the formation of a primary, woven bone callus, resulting in delayed union and eburnation on the fracture margins.

Restricted access to nutritious foods and limited sun exposure may have led to increased skeletal fragility for lower-class individuals in the post-medieval Netherlands. Vitamin D is naturally occurring in fatty fish and to a lesser extant egg yolks (Brickley et al., 2020, p. 85). But van Dam (2009) states that while fish was eaten in the Netherlands, certain fatty fish such as eel and salmon were considered luxury goods and only available to the wealthy. Dietary sources of calcium, including cheese, were readily available in the Dutch Republic. A series of famines resulting from the Little Ice Age (1550-1720) and Rinder pest (1713-1720 and 1744-1765) (Ljungqvist et al., 2024) may have decreased access to calcium-rich foods, but the groundwater

in the Netherlands contains between 40mg/l and 100mg/l of naturally occurring calcium (Huisman et al., 1998). While evidence for nutritional deficiencies and metabolic conditions is limited in the present study, the lower socioeconomic status of many of the individuals displaying evidence for fracture may have led to malnutrition and increased skeletal fragility. Metric evaluations of BMD were not undertaken for this thesis, so a diagnosis of osteopenia or osteoporosis is not possible, but decreased BMD related to malnutrition and metabolic conditions should still be considered as a possible factor in fracture prevalence. The vertebral compression fractures and Schmorl's nodes in the adolescent individuals potentially resulted from a combination of skeletal fragility related to malnutrition or limited sun exposure and strenuous activity related to wage labour and apprenticeships. The social circumstances and lifeways of these individuals therefore resulted in negative health outcomes.

Pre-fracture health is critical for determining health, function, and survival outcomes following fracture (Neuman et al., 2014). A clinical study conducted by Whitney et al. (2019) found an increased mortality risk following low-trauma fractures in individuals with increased skeletal fragility. Zohar et al. (2023) likewise found that the higher mortality rate affecting people with vertebral compression fractures is related to decreased health prior to the occurrence of fracture. Gowland et al. (2023) found an increased mortality risk in children from 19th century England that engaged in wage labour due to hazardous conditions that resulted in malnutrition, respiratory disease, and severe growth delays. While the vertebral fractures themselves may not have led to an increased mortality rate, the social conditions that increased the likelihood of experiencing vertebral fractures may also have resulted in other health risks that increased the mortality risk for adolescent individuals in the lower socioeconomic collections. According to Dodd (1968), accidents in the textiles industries were common, leading to lost fingers, amputated

hands, and occasionally death. Dust was likewise a dangerous byproduct of textile manufacturing, and respiratory infections, including byssinosis, were common.

5.3 Future Directions

Ongoing research into childhood and adolescent health, trauma, and lifestyles contexts and risk-factors is required to improve our recognition of fractures in developing bone. The current research sheds additional light on how the systematic analysis of fractures in children and adolescents related to trauma, pathology, and stress can be used to understand prevalence and lifestyles, but more work is required. Moving forward, paleopathological analyses of fractures in developing bone and those occurring near the time of death must be improved. Medicolegal researchers currently lead the charge on investigations of pediatric trauma and post-traumatic time intervals. Using samples submitted to the University of Manchester's Osteoarticular Pathology laboratory by forensic pathologists, clinicians Naqvi et al. (2019) created a database containing histological features of fracture healing in infants for the purposes of establishing post-traumatic time intervals in cases of accidental injury and abuse. The creation of a comparative online repository containing histological images of known post-traumatic time interval skeletal traumas has been created by Isaac et al. (2022) for use in forensic contexts. The samples were drawn from a body donation program through Western Michigan University Homer Stryker M.D School of Medicine. While the majority of samples included in the database are adults, there are a number of examples taken from infants (0-3 years) and juveniles (3-16 years). However, currently only trauma affecting the cranium has been included. Using documented, unclaimed individuals from the Robert J. Terry Anatomical Skeletal Collection, Mant et al. (2019) microscopically analyzed the fracture margins in a series documented hip fractures to better facilitate the identification of perimortem fractures in the archaeological

record, although the focus was on adults. Viero et al. (2022) has examined the use of micro-CT imaging to investigate the microarchitecture of cranial bone during fracture remodeling to better gauge post-traumatic survival time in forensic cases; however, the authors have likewise focused on adults. Cappella et al. (2019), working with a documented skeletal collection from the Institute of Legal Medicine of Milan, compared X-ray, histological, and micro-CT imaging to establish a list of features for use in estimating the post-traumatic time interval for fractures. However, the study only used fractures from adult remains. Additional research on peri-mortem fractures and fracture types unique to developing bone is required to better facilitate their identification in skeletal remains in bioarchaeology.

5.4 Summary

The study of fracture prevalence and patterns across age, biological sex, and socioeconomic status offers a unique opportunity to understand the lifeways of children and adolescents in the past. The investigation of fractures in this study has provided insight into sex-based fracture risk, differences in fracture prevalence between age groups, and fracture risks in urban centers of differing socioeconomic statuses in the Netherlands from 1650 to 1850 CE. The present study reported an overall prevalence of ante-mortem fracture across all four urban collections to be 29.9%. However, crude prevalence varied between collections, with the lower socioeconomic individuals presenting a higher crude prevalence of fracture, apart from Zwolle where the high prevalence is likely biased. While females experienced fractures slightly more often than males, the difference is not statistically significant, indicating both males and females engaged in activities with fracture risk. Fractures were also found to be highest in the middle adolescent age category, followed by the early adolescent category. This finding follows

expected patterns from archaeological and clinical studies, as adolescents are exposed to a higher fracture risk as they engage in new activities.

The presence of vertebral fractures in the mid- to low-socioeconomic collections sheds additional insight on the lifeways and activities of young individuals. Manual labour led to increased risk of fracture, with malnutrition and limited sun exposure acting as potential underlying causes of increased skeletal fragility. The findings support historical evidence that children and adolescent individuals in the post-medieval Netherlands engaged in labour for pay and apprenticeships. Social determinants of health, non-biological factors that both negatively and positively influence health, play an important role in ascertaining who is at risk for disease and trauma. In this case, low socioeconomic status and employment likely resulted in negative health outcomes including increased fracture risk, metabolic conditions, and nutritional deficiencies. Social and biological, as well as underlying pathological conditions, must be considered in understanding fracture prevalence in the past. Because young individuals are more likely to be impacted by biocultural stress than adults (Lewis, 2002), examining childhood and adolescent health can increase our understanding of social practices, population health, and trends in morbidity and mortality. The present study increases our understanding of the health risks related to lifeways and social identities for young individuals in post-medieval Dutch communities.

Chapter 6 Conclusion

6.0 Conclusions

Trauma analysis in bioarchaeology has the potential to contribute important information on the activities, social identities, and lived experiences of past people (Mant et al., 2021). However, the study of childhood and adolescent trauma is under-studied compared to adults (Lewis, 2018). The current thesis focused on the analysis of ante-mortem fractures, resulting from direct and in-direct force, pathology, and stress, in children and adolescents (1–20 years of age) in skeletal collections from four urban centers (Arnhem, Eindhoven, Alkmaar and Zwolle) in the Netherlands (1650-1850 CE). Increasing urbanization and industrialization in the 17th and 18th centuries in the Netherlands resulted in rising class divisions and social inequalities (van Zanden, 1995; van Zanden & van der Berg, 1993). The findings in this thesis suggest that income, employment, and socioeconomic status differences affected health outcomes among children and adolescents, including increased skeletal fragility and increased fracture risk.

The overall prevalence of ante-mortem fractures across all four sites was 29.1% (16/55), though the prevalence varied between sites. The lower-class collections from Arnhem and Eindhoven had a prevalence of 26.9% (7/26) and 36.4% (4/11), respectively. Alkmaar had a prevalence of 16.7% (2/12), and Zwolle had 50.0% (3/6). However, the high prevalence in Zwolle may be skewed by small sample size and bias resulting from which individuals from the collection were housed onsite at Leiden University. Differing levels of preservation between the sites investigated in the current study likely impacted the ability to detect fractures, impacting the prevalence at each site as well as the overall crude prevalence. Fractures affected the long bones, ribs, cranium, and vertebrae, with the highest crude and true prevalence of fracture found in the vertebrae.

Children of all ages experienced fractures in the examined collections, but there was a peak in the occurrence of fractures in the middle adolescence age category (15-17 years) followed by early adolescence (10-14 years). The post-traumatic time interval estimates indicate that the majority of these fractures occurred near the time death. As a result, the increase in fracture prevalence during adolescence likely results from engagement with new activities and changes in social roles during adolescence, following the expected pattern for modern and archaeological populations. Females experienced fractures slightly more often than males, though the difference is not significant, indicating that both boys and girls engaged in activities with risk of fracture. Vertebral compression fractures and Schmorl's nodes were the most common type of fracture, affecting a total of ten individuals. Of these, an early child displayed evidence of traumatic injury to the cervical and upper thoracic vertebrae, potentially resulting from a fall from a height. The remaining nine individuals were adolescents of lower socioeconomic status with fractures affecting the thoracic and lumbar spine. The occurrence of vertebral compression fractures and Schmorl's nodes in the same person is statistically significant, indicating the fractures likely resulted through similar mechanisms. The development of compression fractures and Schmorl's nodes in adolescence are both influenced by health of the intervertebral disc, bone quality and quantity, and repetitive axial loading and torsion of the spine. There is also a significant correlation between vertebral fractures and lower socioeconomic status. In this case, the fractures are likely a consequence of strenuous occupations, as lower-class children and adolescents engaged in paid labour and apprenticeships as a survival strategy.

The age of majority in the post-medieval Netherlands varied between 21 and 25 years of age (van Nederveen Meerkerk & Schmidt, 2008). But adolescence was a protracted period in

which new, ‘adult’ social roles were taken on gradually over time. Individuals of low socioeconomic status were expected to work and support themselves after 17 years of age but did not receive adult wages until 20 years of age. However, paid labour and apprenticeships were common practice, serving as an educational tool and source of income, for children beginning around eight years of age (van Nederveen Meerkerk & Schmidt, 2008). It is likely that the adolescents partook in wage labour in the industrial sector as a result of their lower socioeconomic status, exposing them to increased fracture risk through hazardous working conditions and strenuous activity. Underlying skeletal fragility likely also played a role in the development of vertebral fractures. Micro-CT reconstructions revealed mineralization defects consistent with vitamin D deficiency and thin, sparse trabeculae in a number of individuals. Limited sun exposure, combined with a diet deficient in vitamin D rich foods like oily fish, was the greatest contributing factor to vitamin D deficiency in past populations (Jablonski & Chaplin, 2018; Welsh et al., 2020). Lifeways, including employment in factories and living in increasingly urbanized and industrial centers, may have contributed to limited sun exposure for the individuals analyzed here. Additionally, low socioeconomic status may have resulted in limited access to resources, resulting in nutritional deficiencies affecting bone health. Social determinants of health, or non-biological factors that influence health outcomes, played a role in determining who was at risk for fractures and impaired bone health. While paleopathologists must be careful not to directly attribute worse health outcomes to individuals with low status, the evidence presented in this thesis, combined with archival evidence on child labour practices in the Netherlands, supports the idea that young individuals of low social status in the Netherlands experienced increasing social inequalities that contributed to negative health outcomes.

The results presented here contribute additional information on the prevalence of fractures among children and adolescents across and between four post-medieval Dutch communities, as well as variations in the prevalence and types of fractures experienced between different categories of age, biological sex, and socioeconomic status. Fracture prevalence was contextualized with what is known about the communities to investigate the social roles and social age of adolescents in the Netherlands during the post-medieval period (1650-1850 CE). Additionally, the findings in this thesis provide information on the types and appearance of fractures in developing bone. While the study of fractures in developing bone presents challenges for paleopathologists, detailed examination using a combination of methods, including, macroscopic, microscopic, and micro-CT imaging, contextualized through what is known about the culture via documentary sources, is likely to contribute additional information on the lived experiences and social roles of children and adolescents in other archaeological contexts.

References

Adams, M. A., Pollintine, P., Tobias, J. H., Wakley, G. K., & Dolan, P. (2006). Intervertebral Disc Degeneration an Predispose to Anterior Vertebral Fractures in the Thoracolumbar Spine. *Journal of Bone and Mineral Research: The Official Journal of the American Society for Bone and Mineral Research*, *21*(9), 1409–1416. https://doi-org.libaccess.lib.mcmaster.ca/10.1359/jbmr.060609

Adler, C. P. (1989). [Pathologic bone fractures: Definition and classification]. *Langenbecks Archiv fur Chirurgie. Supplement II, Verhandlungen der Deutschen Gesellschaft fur Chirurgie. Deutsche Gesellschaft fur Chirurgie. Kongress*, 479–486.

Alexandru, D., & So, W. (2012). Evaluation and Management of Vertebral Compression Fractures. *The Permanente Journal*, *16*(4), 46–51.

AlQahtani, S. J. (2008). Atlas of Tooth Development and Eruption. *Barts and the London School of Medicine and Dentistry*. London, Queen Mary University of London.

Alumni Meeting Eindhoven (2023). History and Other Facts. https://ameindhoven.com/?page_id=330 (Accessed February 23, 2024).

Anderson, M. W., & Greenspan, A. (1996). Stress Fractures. *Radiology*, *199*(1), 1–12. https://doi.org/10.1148/radiology.199.1.8633129

Arts, Nico. (2019). Digging Up the Dead in Eindhoven: The Choir and Churchyard of St. Catharine's, 1200-1850. In R. Van Oosten, R. Schats, and K. Fast (Eds.), *Osteoarchaeology in Historical Context: Cemetery Research from the Low Countries* (pp. 37–68). Sidestone Press, Leiden.

Ataizi, Z. S., Aydin, H. E., Kocatürk, E., Çerezci, A., & Alatas, İ. Ö. (2018). Bone Turnover in Vertebral Fractures: Does It Effect the Decision of Surgery? *Asian Journal of Neurosurgery*, *13*(2), 357. https://doi.org/10.4103/ajns.AJNS_137_16

Aten, N. (1992). De opgraving in de Broerenkerk. In H. Clevis, T Constandse-Westermann (Eds.), *De Doden Vertellen: Opgraving in de Broerenkerk te Zwolle 1987-1988* (pp. 12–29). Kampen.

Aten, N., Clevis. H. (2019). Methods of Ageing and Sexing Human Dry Bone Put to Test. Looking Back On The 1987 - 1988 Excavations In The Broerenkerk In Zwolle. In R. van Oosten, R. Schats, K. Fast (Eds.), *Osteoarchaeology in Historical Context: Cemetery Research from the Low Countries* (pp. 167–201). Sidestone Press, Leiden.

Azzouzi, H., & Ichchou, L. (2022). Schmorl's Nodes: Demystification Road of Endplate Defects—A Critical Review. *Spine Deformity*, *10*(3), 489–499. https://doi.org/10.1007/s43390-021-00445-w

Babu, R. A., Arimappamagan, A., Pruthi, N., Bhat, D. I., Arvinda, H. R., Devi, B. I., & Somanna, S. (2017). Pediatric thoracolumbar spinal injuries: The etiology and clinical spectrum of an uncommon entity in childhood. *Neurology India*, *65*(3), 546. https://doi.org/10.4103/neuroindia.NI_1243_15

Baetsen, S. & Bitter, P. (2001). English Summary and Conclusion. In S. Baetsen (Ed), *Graven In De Grote Kerk: Het Fysisch-Antropologisch Onderzoek Van De Graven In De St. Laurenskerk van Alkmaar* (pp. 73–77). Monumentenzorg en Archeologie, Alkmaar.

Baetsen, S., & Weterings-Korthorst, L. (2013). De Menselijke Overblijfselen. In N. Arts & E. Altena (Eds.), *Een Knekelveld Maakt Geschiedenis. Het Archeologisch Onderzoek Van Het Koor En Het Grafveld van De Middeleeuwse Catharinakerk in Eindhoven, circa 1200-1850* (p. 288). Uitgeverij Matrijs.

Baker, C. E., Moore-Lotridge, S. N., Hysong, A. A., Posey, S. L., Robinette, J. P., Blum, D. M., Benvenuti, M. A., Cole, H. A., Egawa, S., Okawa, A., Saito, M., McCarthy, J. R., Nyman, J. S., Yuasa, M., & Schoenecker, J. G. (2018). Bone Fracture Acute Phase Response—A Unifying Theory of Fracture Repair: Clinical and Scientific Implications. *Clinical Reviews in Bone and Mineral Metabolism*, *16*(4), 142–158. https://doi.org/10.1007/s12018-018-9256-x

Bansal, M. L., Sharawat, R., Mahajan, R., Dawar, H., Mohapatra, B., Das, K., & Chhabra, H. S. (2020). Spinal Injury in Indian Children: Review of 204 Cases. *Global Spine Journal*, *10*(8), 1034–1039. https://doi.org/10.1177/2192568219887155

Baranto, A., Ekström, L., Hellström, M., Lundin, O., Holm, S., & Swärd, L. (2005). Fracture Patterns of the Adolescent Porcine Spine: An Experimental Loading Study in Bending-Compression. *Spine*, *30*(1), 75.

Baxter, J. E. (2008). The Archaeology of Childhood. *Annual Review of Anthropology*, *37*(1), 159–175.

Benneker, L. M., Heini, P. F., Alini, M., Anderson, S. E., & Ito, K. (2005). 2004 Young Investigator Award Winner: Vertebral Endplate Marrow Contact Channel Occlusions and Intervertebral Disc Degeneration. *Spine*, *30*(2), 167. https://doi.org/10.1097/01.brs.0000150833.93248.09

Bitter, P. (2002). *Graven En Begraven. Archeologie En Geschiedenis van De Grote Kerk Van Alkmaar*. https://dare.uva.nl/search?identifier=dacc78b0-b3fc-4e11-bf0b-b53db0471d06

Bitter, P. (2018) Buried in Alkmaar: Historical and Archaeological Research On Urban Cemeteries. In R. van Oosten, R. Schats, K. Fast, N. Arts & J. Bouwmeester (Eds.), *The Urban Graveyard: Archaeological Perspectives* (pp. 87–115). Sidestone Press, Leiden.

Blom, A. A., Schats, R., Hoogland, M. L. P., & Waters-Rist, A. (2021). Coming of age in the Netherlands: An osteological assessment of puberty in a rural Dutch post-medieval community. *American Journal of Physical Anthropology*, *174*(3), 463–478. https://doi.org/10.1002/ajpa.24161

Boos, N., Weissbach, S., Rohrbach, H., Weiler, C., Spratt, K. F., & Nerlich, A. G. (2002). Classification of Age-Related Changes in Lumbar Intervertebral Discs: 2002 Volvo Award in Basic Science. *Spine*, *27*(23), 2631.

Botham, A. D. (2019). Unthinking Empiricism and The Overdiagnosis Of Nonlethal Cranial Injuries: An Interdisciplinary Review Of Diagnostic Criteria For Healing, Depressed

Cranial Fractures. *Journal of Archaeological Science: Reports*, *27*, 101939. https://doi.org/10.1016/j.jasrep.2019.101939

Boyce, A. M., & Gafni, R. I. (2011). Approach to the Child with Fractures. *The Journal of Clinical Endocrinology and Metabolism*, *96*(7), 1943–1952. https://doi.org/10.1210/jc.2010-2546

Braveman, P., & Gottlieb, L. (2014). The Social Determinants of Health: It's Time to Consider the Causes of the Causes. *Public Health Reports*, *129*, 19–31. https://doi.org/10.1177/00333549141291S206

Brickley M. B. (2024). Commentary on: Assessing diagnostic certainty for scurvy and rickets in human skeletal remains - An update on Brickley and Morgan (2023). *American journal of biological anthropology*, e24982. Advance online publication. https://doi.org/10.1002/ajpa.24982

Brickley, M. B., & Buckberry, J. (2015). Picking Up the Pieces: Utilizing the Diagnostic Potential Of Poorly Preserved Remains. *International Journal of Paleopathology*, *8*, 51–54. https://doi.org/10.1016/j.ijpp.2014.08.003

Brickley, M., Ives, R., Mays, S. (2020). *The Bioarchaeology of Metabolic Bone Disease* (Second Ed.). Academic Press.

Brickley, M. B., & Morgan, B. (2023). Assessing Diagnostic Certainty for Scurvy and Rickets In Human Skeletal Remains. *American Journal of Biological Anthropology*, *181*(4), 637–645. https://doi.org/10.1002/ajpa.24799

Briggs M. D., Wright M. J., Mortier G. R. (2019) Multiple Epiphyseal Dysplasia, Autosomal Dominant. In: Adam M.P., Feldman J., Mirzaa G.M. (Eds) *GeneReviews* [Internet]. Seattle (WA): University of Washington, Seattle; 1993-2023. Available from: https://www.ncbi.nlm.nih.gov/books/NBK1123/

Brinckmann, P., Biggemann, M., & Hilweg, D. (1988). Fatigue Fracture of Human Lumbar Vertebrae. *Clinical Biomechanics*, *3*, i-S23. https://doi.org/10.1016/S0268-0033(88)80001-9

Buckberry, J. (2018). Techniques for Identifying the Age and Sex of Children at Death. In S. Crawford, D.M. Hadley and G. Shepherd (Eds.), *The Oxford Handbook of the Archaeology of Childhood* (pp. 55–70). Oxford University Press, Oxford.

Buikstra, J. E., Ubelaker, D. (1994). *Standards for Data Collection from Human Skeletal Remains: Proceedings of a Seminar at the Field Museum of Natural History Organized by Jonathan Haas*. Arkansas Archeological Survey.

Callaghan, J. P., McGill, S. M. (2001). Intervertebral Disc Herniation: Studies on a Porcine Model Exposed to Highly Repetitive Flexion/Extension Motion with Compressive Force. *Clinical Biomechanics*, *16*(1), 28–37. https://doi.org/10.1016/S0268-0033(00)00063-2

Calmar, E. A., Vinci, R. J. (2002). The Anatomy and Physiology of Bone Fracture and Healing. *Clinical Pediatric Emergency Medicine*, *3*(2), 85–93. https://doi.org/10.1053/epem.2002.127037

Cappella, A., de Boer, H. H., Cammilli, P., De Angelis, D., Messina, C., Sconfienza, L. M., Sardanelli, F., Sforza, C., Cattaneo, C. (2019). Histologic and Radiological Analysis on Bone Fractures: Estimation of Posttraumatic Survival Time in Skeletal Trauma. *Forensic Science International*, *302*, 109909. https://doi.org/10.1016/j.forsciint.2019.109909

Cardoso, H. F. V. (2008a). Age Estimation of Adolescent and Young Adult Male and Female Skeletons II, Epiphyseal Union at the Upper Limb and Scapular Girdle in a Modern Portuguese Skeletal Sample. *American Journal of Physical Anthropology*, *137*(1), 97–105. https://doi.org/10.1002/ajpa.20850

Cardoso, H. F. V. (2008b). Epiphyseal Union at the Innominate and Lower Limb in a Modern Portuguese Skeletal Sample, and Age Estimation in Adolescent and Young Adult Male and Female Skeletons. *American Journal of Physical Anthropology*, *135*(2), 161–170. https://doi.org/10.1002/ajpa.20717

Cardoso, H. F. V., & Ríos, L. (2011). Age Estimation from Stages of Epiphyseal Union in the Presacral Vertebrae. *American Journal of Physical Anthropology*, *144*(2), 238–247. https://doi.org/10.1002/ajpa.21394

Casna, M., Burrell, C. L., Schats, R., Hoogland, M. L. P., & Schrader, S. A. (2021). Urbanization and Respiratory Stress in the Northern Low Countries: A Comparative Study of Chronic Maxillary Sinusitis in Two Early Modern Sites from the Netherlands (AD 1626–1866). *International Journal of Osteoarchaeology*, *31*(5), 891–901. https://doi.org/10.1002/oa.3006

Casna, M., & Schrader, S. A. (2022). Urban Beings: A Bioarchaeological Approach to Socioeconomic Status, Cribra Orbitalia, Porotic Hyperostosis, Linear Enamel Hypoplasia, and Sinusitis in the Early-Modern Northern Low Countries (A.D. 1626–1850). *Bioarchaeology International*. https://doi.org/10.5744/bi.2022.0001

Clark, P., & Letts, M. (2001). Trauma to the Thoracic and Lumbar Spine in the Adolescent. *Canadian Journal of Surgery*, *44*(5), 337–345.

Cooke, A., Morgan, B., Langlois, M., Nguyen, J., Ribot, I., Waters-Rist, A., van der Merwe, A., Schats, R., & Brickley, M. (2023). *A Comparison of Micro-CT and Macroscopic Analysis of Mineralization Defects in Bones and Teeth in Children from 18th -19th century Canada and 17th -19th century Netherlands* [Poster]. American Association of Biological Anthropology, Reno, USA. https://doi.org/10.13140/RG.2.2.10713.08808

Cooper, C., Dennison, E. M., Leufkens, H. G. M., Bishop, N., & van Staa, T. P. (2004). Epidemiology of Childhood Fractures in Britain: A Study Using the General Practice Research Database. *Journal of Bone and Mineral Research, 19*(12), 1976–1981. https://doi.org/10.1359/JBMR.040902

Cooper, D. M. L., Kawalilak, C. E., Harrison, K., Johnston, B. D., & Johnston, J. D. (2016). Cortical bone porosity: What Is It, Why Is It Important, and How Can We Detect It?

Current Osteoporosis Reports, 14(5), 187–198. https://doi.org/10.1007/s11914-0160319-y

Connell, B., Jones, A. G., Redfern, R., & Walker, D. (2012). *A Bioarchaeological Study of Medieval Burials on the Site of St Mary Spital: Excavations at Spitalfields Market, London E1, 1991-2007*. Museum of London Archaeology.

Dar, G., Masharawi, Y., Peleg, S., Steinberg, N., May, H., Medlej, B., Peled, N., & Hershkovitz, I. (2010). Schmorl's Nodes Distribution in the Human Spine and its Possible Etiology. *European Spine Journal*, *19*(4), 670–675. https://doi.org/10.1007/s00586-009-1238-8

De Boer, H. H., Van Der Merwe, A. E., & Maat, G. J. R. (2013). Survival Time After Fracture or Amputation in a 19th Century Mining Population at Kimberley, South Africa. *Goodwin Series*, *11*, 52–60.

de Vries, J., & van der Woude, A. (1997). *The First Modern Economy: Success, Failure, and Perseverance of the Dutch Economy, 1500–1815* (1st ed.). Cambridge University Press. https://doi.org/10.1017/CBO9780511666841

Dittmar, J. M., Mitchell, P. D., Cessford, C., Inskip, S. A., & Robb, J. E. (2021). Medieval Injuries: Skeletal Trauma as an Indicator of Past Living Conditions and Hazard Risk in Cambridge, England. *American Journal of Physical Anthropology*, *175*(3), 626–645. https://doi.org/10.1002/ajpa.24225

Djurić, M., Janović, A., Milovanović, P., Djukić, K., Milenković, P., Drašković, M., & Roksandic, M. (2010). Adolescent Health in Medieval Serbia: Signs of Infectious Diseases and Risk of Trauma. *HOMO*, *61*(2), 130–149. https://doi.org/10.1016/j.jchb.2010.02.003

Dodd, W. (1968). *Factory System Illustrated (1st ed.)*. Routledge, London.

Donnally III, C. J., DiPompeo, C. M., & Varacallo, M. (2023). Vertebral Compression Fractures. In *StatPearls*. StatPearls Publishing. http://www.ncbi.nlm.nih.gov/books/NBK448171/

Dowdell, J., Erwin, M., Choma, T., Vaccaro, A., Iatridis, J., & Cho, S. K. (2017). Intervertebral Disk Degeneration and Repair. *Neurosurgery*, *80*(3S), S46. https://doi.org/10.1093/neuros/nyw078

Einhorn, T. A., & Gerstenfeld, L. C. (2015). Fracture Healing: Mechanisms and Interventions. *Nature Reviews. Rheumatology*, *11*(1), 45–54. https://doi.org/10.1038/nrrheum.2014.164

Fain, O. (2005). Musculoskeletal Manifestations of Scurvy. *Joint Bone Spine*, *72*(2), 124–128. https://doi.org/10.1016/j.jbspin.2004.01.007

Follis, B. H., Park, E. A. & Jackson, D. (1950). The Prevalence of Scurvy at Autopsy During the First Two Years of Age. *Bulletin of the John Hopkins Hospital, 87*, 569-91.

Frost, H. M. (1989). The Biology of Fracture Healing: An Overview for Clinicians. Part II. *Clinical Orthopaedics and Related Research*, (248), 283–293.

Glencross, B. A. (2011). Skeletal Injury Across the Life Course: Towards Understanding Social Agency. In S. C. Agarwal & B. A. Glencross (Eds.), *Social Bioarchaeology*. John Wiley & Sons, Ltd.

Glencross, B., & Stuart-Macadam, P. (2000). Childhood Trauma in the Archaeological Record. *International Journal of Osteoarchaeology*, *10*(3), 198–209.

Gowland, R. L., Caffell, A., Newman, S., Levene, A., & Holst, M. (2018). Broken Childhoods: Rural and Urban Non-Adult Health during the Industrial Revolution in Northern England (Eighteenth–Nineteenth Centuries). *Bioarchaeology International*, *2*(1), Article 1. https://doi.org/10.5744/bi.2018.1015

Gowland, R. L., Caffell, A. C., Quade, L., Levene, A., Millard, A. R., Holst, M., Yapp, P., Delaney, S., Brown, C., Nowell, G., McPherson, C., Shaw, H. A., Stewart, N. A., Robinson, S., Montgomery, J., & Alexander, M. M. (2023). The Expendables: Bioarchaeological Evidence for Pauper Apprentices in 19th Century England and the Health Consequences of Child Labour. *PLOS ONE*, *18*(5), e0284970. https://doi.org/10.1371/journal.pone.0284970

Grauer, A. (2019). Paleopathology: From Bones to Social Behavior. In M. Katzenberg & A. Grauer (Eds.), *Biological Anthropology of the Human Skeleton.* (Third Edition.). John Wiley & Sons, Inc.

Gustafson, G. & Koch, G. (1974). Age Estimation Up to 16 Years of Age Based on Dental Development. *Odontol Revy,* 25, 297-306.

Gustavel, M., & Beals, R. K. (2002). Scheuermann's Disease of the Lumbar Spine in Identical Twins. *American Journal of Roentgenology*, *179*(4), 1078–1079. https://doi-org.libaccess.lib.mcmaster.ca/10.2214/ajr.179.4.1791078

Hahn, R. A. (2021). What is a Social Determinant of Health? Back to Basics. *Journal of Public Health Research*, *10*(4). https://doi.org/10.4081/jphr.2021.2324

Halcrow, S. E., & Tayles, N. (2011). The Bioarchaeological Investigation of Children and Childhood. In S. C. Agarwal & B. A. Glencross (Eds.), *Social Bioarchaeology*. John Wiley & Sons, Ltd.

Hamanishi, C., Kawabata, T., Yosii, T., & Tanaka, S. (1994). Schmorl's Nodes on Magnetic Resonance Imaging: Their Incidence and Clinical Relevance. *Spine*, *19*(4), 450.

Hedström, E., Crnalic, S., Kullström, A., & Waernbaum, I. (2021). Socioeconomic Variables and Fracture Risk in Children and Adolescents: A Population-Based Study from Northern Sweden. *BMJ Open*, *11*(10), e053179. https://doi.org/10.1136/bmjopen-2021-053179

Hedström, E. M., Svensson, O., Bergström, U., & Michno, P. (2010). Epidemiology of Fractures in Children and Adolescents. *Acta Orthopaedica*, *81*(1), 148–153. https://doi.org/10.3109/17453671003628780

Herdea, A., Ionescu, A., Dragomirescu, M.-C., & Ulici, A. (2023). Vitamin D—A Risk Factor for Bone Fractures in Children: A Population-Based Prospective Case–Control

Randomized Cross-Sectional Study. *International Journal of Environmental Research and Public Health*, *20*(4), 3300. https://doi.org/10.3390/ijerph20043300

Hilton, R. C., Ball, J., & Benn, R. T. (1976). Vertebral End-Plate Lesions (Schmorl's Nodes) in the Dorsolumbar Spine. *Annals of the Rheumatic Diseases*, *35*(2), 127–132. https://doi.org/10.1136/ard.35.2.127

Huisman, P., Cramer, W., van Ee, G., Hooghart, J. C., Salz, H., & Zuidema, F. C. (1998). *Water in the Netherlands*. Delf: Netherlands Hydrological Society.

Hulvey, J. T., & Keats, T. (1969). Multiple Epiphyseal Dysplasia. A Contribution to the Problem of Spinal Involvement. *The American Journal of Roentgenology, Radium Therapy, and Nuclear Medicine*, *106*(1), 170–177.

Imai, K. (2015). Analysis of Vertebral Bone Strength, Fracture Pattern, and Fracture Location: A Validation Study Using a Computed Tomography-Based Nonlinear Finite Element Analysis. *Aging and Disease*, *6*(3), 180–187. https://doi.org/10.14336/AD.2014.0621

Isaac, C. V., Cornelison, J. B., Prahlow, J. A., Devota, C. J., & Christensen, E. R. (2022). The Repository of Antemortem Injury Response (REPAIR): An Online Database for Skeletal Injuries of Known Ages. *International Journal of Legal Medicine*, *136*(4), 1189–1196. https://doi.org/10.1007/s00414-021-02756-z

Islam, O., Soboleski, D., Symons, S., Davidson, L. K., Ashworth, M. A., & Babyn, P. (2000). Development and Duration of Radiographic Signs of Bone Healing in Children. *American Journal of Roentgenology*, *175*(1), 75–78. https://doi.org/10.2214/ajr.175.1.1750075

Jablonski, N. G., & Chaplin, G. (2018). The Roles of Vitamin D and Cutaneous Vitamin D Production in Human Evolution and Health. *International Journal of Paleopathology*, *23*, 54–59. https://doi.org/10.1016/j.ijpp.2018.01.005

Jaffe, H. L. (1972). *Metabolic, Degenerative, and Inflammatory Diseases of Bone and Joints*. Lea & Febiger, Philadelphia.

Jalava, T., Sarna, S., Pylkkänen, L., Mawer, B., Kanis, J. A., Selby, P., Davies, M., Adams, J., Francis, R. M., Robinson, J., & McCloskey, E. (2003). Association Between Vertebral Fracture and Increased Mortality in Osteoporotic Patients. *Journal of Bone and Mineral Research*, *18*(7), 1254–1260. https://doi.org/10.1359/jbmr.2003.18.7.1254

Judd, M. A., Roberts, C. A. (1999). Fracture Trauma in a Medieval British Farming Village. *American Journal of Physical Anthropology*, *109*(2), 229–243. https://doi.org/10.1002/(SICI)1096-8644(199906)109:2<229::AID-AJPA7>3.0.CO;2-Y

Junghanns, H. (1971). *The Human Spine in Health and Disease* (First Edition). Grune & Stratton, New York.

Karlsson, L., Lundin, O., Ekström, L., Hansson, T., & Swärd, L. (1998). Injuries in Adolescent Spine Exposed to Compressive Loads: An Experimental Cadaveric Study. *Clinical Spine Surgery*, *11*(6), 501.

Kemp, W. L. (2016). Postmortem Change and its Effect on Evaluation of Fractures. *Academic Forensic Pathology*, *6*(1), 28–44. https://doi.org/10.23907/2016.004

Kim, J. E., Koh, S. Y., Swan, H., Kazmi, S. Z., Kim, H. J., Ahn, H. S., & Hong, S. S. (2023). Incidence and Mortality of Vertebral Compression Fracture Among All Age Groups: A Nationwide, Population-based Study in the Republic of Korea. *Pain Physician*, *26*(3), E203–E211.

Koliou, M., Chatzicharalampous, E., Charalambous, M., & Aristeidou, K. (2022). Congenital Syphilis as the Cause of Multiple Bone Fractures in a Young Infant Case Report. *BMC Pediatrics*, *22*(1), 728–734. https://doi.org/10.1186/s12887-022-03789-y

Kyere, K. A., Than, K. D., Wang, A. C., Rahman, S. U., Valdivia–Valdivia, J. M., La Marca, F., & Park, P. (2012). Schmorl's Nodes. *European Spine Journal*, *21*(11), 2115–2121. https://doi.org/10.1007/s00586-012-2325-9

Kushchayev, S. V., Glushko, T., Jarraya, M., Schuleri, K. H., Preul, M. C., Brooks, M. L., & Teytelboym, O. M. (2018). ABCs of the Degenerative Spine. *Insights into Imaging*, *9*(2), 253–274. https://doi.org/10.1007/s13244-017-0584-z

Lappe, J. M., & Heaney, R. P. (2012). Why randomized controlled trials of calcium and vitamin D sometimes fail. *Dermato-Endocrinology*. https://doi.org/10.4161/derm.19833

Lau, E., Ong, K., Kurtz, S., Schmier, J., & Edidin, A. (2008). Mortality Following the Diagnosis of a Vertebral Compression Fracture in the Medicare Population. *The Journal of Bone and Joint Surgery. American Volume*, *90*(7), 1479–1486. https://doi.org/10.2106/JBJS.G.00675

Lee, G. B., Priefer, D. T., & Priefer, R. (2022). Scoliosis: Causes and Treatments. *Adolescents*, *2*(2), 220–234. https://doi.org/10.3390/adolescents2020018

Levine, R. H., Thomas, A., Nezwek, T. A., & Waseem, M. (2023). Salter-Harris Fracture. In *StatPearls*. StatPearls Publishing. http://www.ncbi.nlm.nih.gov/books/NBK430688/

Lewis, M. E. (2002). Impact of Industrialization: Comparative Study of Child Health in Four Sites from Medieval and Postmedieval England (A.D. 850–1859). *American Journal of Physical Anthropology*, *119*(3), 211–223. https://doi.org/10.1002/ajpa.10126

Lewis, M. E. (2006). *The Bioarchaeology of Children: Perspectives from Biological and Forensic Anthropology*. Cambridge: Cambridge University Press. https://doi.org/10.1017/CBO9780511542473

Lewis, M. E. (2010). Life And Death in a Civitas Capital: Metabolic Disease and Trauma in the Children from Late Roman Dorchester, Dorset. *American Journal of Physical Anthropology*, *142*(3), 405–416. https://doi.org/10.1002/ajpa.21239

Lewis, M. E. (2011). Tuberculosis in the Non-Adults from Romano-British Poundbury Camp, Dorset, England. *International Journal of Paleopathology*, *1*(1), 12–23. https://doi.org/10.1016/j.ijpp.2011.02.002

Lewis, M. E. (2014). Sticks and Stones: Exploring the Nature and Significance of Child Trauma in the Past. In C. Knüsel & M. J. Smith (Eds.), *The Routledge Handbook of the Bioarchaeology of Human Conflict*. Routledge.

Lewis, M. (2016). Work and the Adolescent in Medieval England ad 900–1550: The Osteological Evidence. *Medieval Archaeology*, *60*(1), 138–171. https://doi.org/10.1080/00766097.2016.1147787

Lewis, M. E. (2018). *Paleopathology of Children*. Academic Press.

Lewis, M. E. (2022). Exploring Adolescence as a Key Life History Stage in Bioarchaeology. *American Journal of Biological Anthropology*, *179*(4), 519–534. https://doi.org/10.1002/ajpa.24615

Lillehammer, G. (1989). A Child is Born. The Child's World in an Archaeological Perspective. *Norwegian Archaeological Review,* 22(2): 89–105.

Lotz, J. C., Fields, A. J., & Liebenberg, E. C. (2013). The Role of the Vertebral End Plate in Low Back Pain. *Global Spine Journal*, *3*(3), 153–164. https://doi.org/10.1055/s-0033-1347298

Lovell, N. C. (1997). Trauma Analysis in Paleopathology. *American Journal of Physical Anthropology*, *104*(S25), 139–170. https://doi.org/10.1002/(SICI)1096-8644(1997)25+<139::AID-AJPA6>3.0.CO;2-#

Ljungqvist, F. C., Seim, A., & Collet, D. (2024). Famines in medieval and early modern Europe—Connecting climate and society. *WIREs Climate Change*, *15*(1), e859. https://doi.org/10.1002/wcc.859

Ma, Q., Miri, Z., Haugen, H. J., Moghanian, A., & Loca, D. (2023). Significance of Mechanical Loading in Bone Fracture Healing, Bone Regeneration, and Vascularization. *Journal of Tissue Engineering*, *14*. https://doi.org/10.1177/20417314231172573

Maat, G. J. R., & Mastwijk, R. W. (2000). Avulsion Injuries of Vertebral Endplates. *International Journal of Osteoarchaeology*, *10*(2), 142–152. https://doi.org/10.1002/(SICI)1099-1212(200003/04)10:2<142::AID-OA519>3.0.CO;2-L

Madassery, S. (2020). Vertebral Compression Fractures: Evaluation and Management. *Seminars in Interventional Radiology*, *37*(2), 214–219. https://doi.org/10.1055/s-0040-1709208

Mant, M., De La Cova, C., & Brickley, M. B. (2021). Intersectionality and Trauma Analysis in Bioarchaeology. *American Journal of Physical Anthropology*, *174*(4), 583–594. https://doi.org/10.1002/ajpa.24226

Mant, M., de la Cova, C., Ives, R., & Brickley, M. B. (2019). Perimortem Fracture Manifestations and Mortality after Hip Fracture in a Documented Skeletal Series. *International Journal of Paleopathology*, *27*, 56–65. https://doi.org/10.1016/j.ijpp.2019.09.002

Mansfield, J. T., Bennett, M. (2023). Scheuermann Disease. In *StatPearls*. StatPearls Publishing. https://www.ncbi.nlm.nih.gov/books/NBK499966/

Marcus, R., Dempster, D., Bouxsein, M. (2013). The Nature of Osteoporosis. In Marcus, R., Feldman, D., Dempster, D., Luckey, M., Cauley, J. (Eds.), *Osteoporosis* (Fourth Ed., pp. 21–30). Academic Press, Amsterdam.

Marmot, M. (2005). Social Determinants of Health Inequalities. *The Lancet*, *365*(9464), 1099–1104. https://doi.org/10.1016/S0140-6736(05)71146-6

Marmot, M., & Wilkinson, R. G. (2000). *Social Determinants of Health*. Oxford University Press, Oxford.

Marsell, R., & Einhorn, T. A. (2011). The Biology of Fracture Healing. *Injury*, *42*(6), 551–555. https://doi.org/10.1016/j.injury.2011.03.031

Martini, M., & Bellavitis, A. (2014). Household economies, social norms and practices of unpaid market work in Europe from the sixteenth century to the present. *The History of the Family*, *19*(3), 273–282. https://doi.org/10.1080/1081602X.2014.933999

Martus, J. E., Mencio, G. A. (2020). Fractures of the Spine. In S. L. Frick, N. E. Green, G. A. Mencio, (Eds), *Green's Skeletal Trauma in Children* (pp. 169–211). Elsevier/Saunders.

Mathison, D. J., & Agrawal, D. (2010). An Update on the Epidemiology of Pediatric Fractures. *Pediatric Emergency Care*, *26*(8), 594–603. https://doi.org/10.1097/PEC.0b013e3181eb838d

Mattei, T. A., & Rehman, A. A. (2014). Schmorl's Nodes: Current Pathophysiological, Diagnostic, and Therapeutic Paradigms. *Neurosurgical Review*, *37*(1), 39–46. https://doi.org/10.1007/s10143-013-0488-4

Mäyränpää, M. K., Viljakainen, H. T., Toiviainen-Salo, S., Kallio, P. E., & Mäkitie, O. (2012). Impaired Bone Health and Asymptomatic Vertebral Compressions in Fracture-Prone Children: A Case-Control Study. *Journal of Bone and Mineral Research*, *27*(6), 1413–1424. https://doi.org/10.1002/jbmr.1579

McKeown, T., & Brown, R. G. (1955). Medical Evidence Related to English Population Changes in the Eighteenth Century. *Population Studies*, *9*(2), 119–141. https://doi.org/10.2307/2172162

McKeown, T., & Record, R. G. (1962). Reasons for the decline of mortality in england and wales during the nineteenth century. *Population Studies*, *16*(2), 94–122. https://doi.org/10.1080/00324728.1962.10414870

Mckeown, T., Record, R. G., & Turner, R. D. (1975). An interpretation of the decline of mortality in England and Wales during the twentieth century. *Population Studies*, *29*(3), 391–422. https://doi.org/10.1080/00324728.1975.10412707

McKinley, T. (2003). Principles of Fracture Healing. *Surgery (Oxford)*, *21*(9), 209–212. https://doi.org/10.1383/surg.21.9.209.16926

Mesías, M., Seiquer, I., & Navarro, M. P. (2011). Calcium Nutrition in Adolescence. *Critical Reviews in Food Science and Nutrition*, *51*(3), 195–209. https://doi.org/10.1080/10408390903502872

Meyers, A. L., Marquart, M. J. (2023). Pediatric Physeal Injuries Overview. In *StatPearls*. StatPearls Publishing. http://www.ncbi.nlm.nih.gov/books/NBK560546/

Miszkiewicz, J. J., & Cooke, K. M. (2019). Socio-economic Determinants of Bone Health from Past to Present. *Clinical Reviews in Bone and Mineral Metabolism*, *17*(3), 109–122. https://doi.org/10.1007/s12018-019-09263-1

Modic, M. T., & Ross, J. S. (2007). Lumbar Degenerative Disk Disease. *Radiology*, *245*(1), 43–61. https://doi.org/10.1148/radiol.2451051706

Mok, F. P. S., Samartzis, D., Karppinen, J., Luk, K. D. K., Fong, D. Y. T., & Cheung, K. M. C. (2010). ISSLS Prize Winner: Prevalence, Determinants, and Association of Schmorl Nodes of the Lumbar Spine with Disc Degeneration: A Population-Based Study of 2449 Individuals. *Spine*, *35*(21), 1944. https://doi.org/10.1097/BRS.0b013e3181d534f3

Naranje, S. M., Erali, R. A., Warner, W. C. J., Sawyer, J. R., & Kelly, D. M. (2016). Epidemiology of Pediatric Fractures Presenting to Emergency Departments in the United States. *Journal of Pediatric Orthopaedics*, *36*(4), E45–E48. https://doi.org/10.1097/BPO.0000000000000595

Naqvi, A., Raynor, E., & Freemont, A. J. (2019). Histological Ageing of Fractures in Infants: A Practical Algorithm for Assessing Infants Suspected of Accidental or Non-Accidental Injury. *Histopathology*, *75*(1), 74–80. https://doi.org/10.1111/his.13850

Neuman, M. D., Silber, J. H., Magaziner, J. S., Passarella, M. A., Mehta, S., & Werner, R. M. (2014). Survival and functional outcomes after hip fracture among nursing home residents. *JAMA internal medicine*, *174*(8), 1273–1280. https://doi.org/10.1001/jamainternmed.2014.2362

Nijkamp, P., & Goede, E. (2002). Urban development in the Netherlands: new perspectives. (Serie Research Memoranda; No. 2002-1A). *Faculty of Economics and Business Administration*, Vrije Universiteit, Amsterdam.

Noordin, S., Baloch, N., Salat, M. S., Rashid Memon, A., & Ahmad, T. (2012). Skeletal Manifestations of Scurvy: A Case Report from Dubai. *Case Reports in Orthopedics*, *2012*, 624628. https://doi.org/10.1155/2012/624628

Ogden, J. A. (2000). *Skeletal Injury in the Child* (Third Ed.). Springer, New York. https://doi.org/10.1007/b97655

Panagiotis, M. (2005). Classification of Non-Union. *Injury*, *36*(4, Supplement), S30–S37. https://doi.org/10.1016/j.injury.2005.10.008

Parfitt, A. M. (1994). The Two Faces of Growth: Benefits and Risks to Bone Integrity. *Osteoporosis International*, *4*(6), 382–398. https://doi.org/10.1007/BF01622201

Park, E. A., Guild, H. G., Jackson, D., & Bond, M. (1935). The Recognition of Scurvy with Especial Reference to the Early X-Ray Changes. *Archives of Disease in Childhood*, *10*(58), 265–294. https://doi.org/10.1136/adc.10.58.265

Partiot, C., Lepetit, A., Dodré, E., Jenger, C., Maureille, B., Liguoro, D., & Thomas, A. (2020). Cranial Trepanation and Healing Process in Modern Patients—Bioarchaeological and Anthropological Implications. *Journal of Anatomy*, *237*(6), 1049–1061. https://doi.org/10.1111/joa.13266

Pedersen, L. T., Domett, K. M., Chang, N. J., Halcrow, S. E., Buckley, H. R., Higham, C. F. W., O'Reilly, D. J. W., & Shewan, L. (2019). A Bioarchaeological Study of Trauma at Late Iron Age to Protohistoric Non Ban Jak, Northeast Thailand. *Asian Perspectives*, *58*(2), 220–249.

Penny-Mason, B. J., & Gowland, R. L. (2014). The Children of the Reformation: Childhood Palaeoepidemiology in Britain, AD 1000–1700. *Medieval Archaeology*, *58*(1), 162–194. https://doi.org/10.1179/0076609714Z.00000000035

Perry, M. A. (2005). Redefining Childhood through Bioarchaeology: Toward an Archaeological and Biological Understanding of Children in Antiquity. *Archaeological Papers of the American Anthropological Association*, *15*(1), 89–111.

Perry, M. A., & Gowland, R. L. (2022). Compounding Vulnerabilities: Syndemics and the Social Determinants of Disease in the Past. *International Journal of Paleopathology*, *39*, 35–49. https://doi.org/10.1016/j.ijpp.2022.09.002

Plomp, K. A., Roberts, C. A., & Viðarsdóttir, U. S. (2012). Vertebral Morphology Influences the Development of Schmorl's Nodes in the Lower Thoracic Vertebrae. *American Journal of Physical Anthropology*, *149*(4), 572–582. https://doi.org/10.1002/ajpa.22168

Pountos, I., & Giannoudis, P. V. (2018). Fracture Healing: Back to Basics and Latest Advances. In P. V. Giannoudis (Ed.), *Fracture Reduction and Fixation Techniques: Upper Extremities* (pp. 3–17). Springer International Publishing. https://doi.org/10.1007/978-3-319-68628-8_1

Prosser, I., Lawson, Z., Evans, A., Harrison, S., Morris, S., Maguire, S., & Kemp, A. M. (2012). A Timetable for the Radiologic Features of Fracture Healing in Young Children. *American Journal of Roentgenology*, *198*(5), 1014–1020. https://doi.org/10.2214/AJR.11.6734

Raphael, D. (1999). Health Effects of Economic Inequality: Overview and Purpose. *Canadian Review of Social Policy*, *44*, 25–40.

Raphael, D. (2000). *Social determinants of health: Canadian perspectives*. Canadian Scholars' Press and Women's Press.

Raphael, D. (2006). Social Determinants of Health: Present Status, Unanswered Questions, and Future Directions. *International Journal of Health Services*, *36*(4), 651–677. https://doi.org/10.2190/3MW4-1EK3-DGRQ-2CRF

Redfern, R. & Roberts, C. A. (2019) Trauma. In J. E. Buikstra (ed.), *Ortner's Identification of Pathological Conditions in Human Skeletal Remains* (Third Ed., pp. 211–284). Academic Press. https://doi.org/10.1016/B978-0-12-809738-0.00017-X

Reeder, M. T., Dick, B. H., Atkins, J. K., Pribis, A. B., & Martinez, J. M. (1996). Stress Fractures. *Sports Medicine*, *22*(3), 198–212. https://doi.org/10.2165/00007256-199622030-00006

Roberts, C. A. (2000). Trauma in Biocultural Perspective: Past, Present and Future Work in Britain. In M. Cox, & S. Mays (Eds.), *Human Osteology in Archaeology and Forensic Science* (pp. 337-356). Medical Media, Greenwich.

Roberts, C.A., Buikstra, J.E. (2019). Bacterial Infections. In J. E. Buikstra (Ed.). *Ortner's Identification of Pathological Conditions in Human Skeletal Remains* (Third Ed., pp. 321–439). Academic Press.

Rogers, T. L. (1999). A Visual Method of Determining the Sex of Skeletal Remains Using the Distal Humerus. *Journal of Forensic Sciences, 44*(1), 57–60.

Rogers, T. L. (2009). Sex Determination of Adolescent Skeletons Using the Distal Humerus. *American Journal of Physical Anthropology, 140*, 143–148.

Salter, R., Harris, W. (1963). Injuries Involving the Epiphyseal Plate. *Journal of Bone and Joint Surgery, 45*(3), 587–622.

Samartzis, D., Mok, F. P. S., Karppinen, J., Fong, D. Y. T., Luk, K. D. K., Cheung, K. M. C. (2016). Classification of Schmorl's Nodes of the Lumbar Spine and Association with Disc Degeneration: A Large-Scale Population-Based MRI Study. *Osteoarthritis and Cartilage*, *24*(10), 1753–1760. https://doi.org/10.1016/j.joca.2016.04.020

Sauer, N. J., Dunlap, S. S. (1985). The Asymmetrical Remodeling of Two Neurosurgical Burr Holes: A Case Study. *Journal of Forensic Science, 30*, 953–957.

Saul, D., & Dresing, K. (2018). Epidemiology of Vertebral Fractures in Pediatric and Adolescent Patients. *Pediatric Reports*, *10*(1), 7232. https://doi.org/10.4081/pr.2018.7232

Sayama, C., Chen, T., Trost, G., & Jea, A. (2014). A Review of Pediatric Lumbar Spine Trauma. *Neurosurgical Focus*, *37*(1), E6. https://doi.org/10.3171/2014.5.FOCUS1490

Scannell, B., Frick, S. L. (2020). Skeletal, Growth, Development, and Healing as Related to Pediatric Trauma. In S. L. Frick, N. E. Green, G. A. Mencio, (Eds), *Green's Skeletal Trauma in Children* (pp. 1–17). Elsevier/Saunders.

Schalk, R. (2017). From orphan to artisan: Apprenticeship careers and contract enforcement in The Netherlands before and after the guild abolition. *The Economic History Review*, *70*(3), 730–757. https://doi.org/10.1111/ehr.12422

Scheuer, L., & Black, S. M. (2004). *The Juvenile Skeleton*. Academic Press.

Schindeler, A., McDonald, M. M., Bokko, P., & Little, D. G. (2008). Bone Remodeling During Fracture Repair: The Cellular Picture. *Seminars in Cell & Developmental Biology*, *19*(5), 459–466. https://doi.org/10.1016/j.semcdb.2008.07.004

Sheen, J. R., Mabrouk, A., & Garla, V. V. (2023). Fracture Healing Overview. In *StatPearls*. StatPearls Publishing. http://www.ncbi.nlm.nih.gov/books/NBK551678/

Schmidt, A. (2011). Labour Ideologies and Women in the Northern Netherlands, c.1500-1800. *International Review of Social History*, *56*, 45–67.

Scott, A., MacInnes, S., Hughes, N., Munkittrick, T. J., Harris, A., & Grimes, V. (2023). A Bioarchaeological Exploration of Adolescent Males at the Eighteenth-Century Fortress of Louisbourg, Nova Scotia, Canada. *Bioarchaeology International*, *7*(2), 146–172. https://doi.org/10.5744/bi.2022.0007

Scott, R. M., Buckley, H. R., Domett, K., Tromp, M., Trinh, H. H., Willis, A., Matsumura, H., & Oxenham, M. F. (2019). Domestication and Large Animal Interactions: Skeletal Trauma in Northern Vietnam During the Hunter-Gatherer Da But Period. *PLOS ONE*, *14*(9), e0218777. https://doi.org/10.1371/journal.pone.0218777

Shapland, F., Lewis, M., & Watts, R. (2016). The Lives and Deaths of Young Medieval Women: The Osteological Evidence. *Medieval Archaeology*, *59*(1), 272–289. https://doi.org/10.1080/00766097.2015.1119392

Smit, C. B. A., (2014). *De leidse fabriekskinderen. Kinderarbeid, industrialisatie en samenleving in een hollandse stad, 1800-1914.* Utrecht University, Utrecht.

Son, H. J., Park, S.-J., Kim, J.-K., & Park, J.-S. (2023). Mortality Risk After the First Occurrence of Osteoporotic Vertebral Compression Fractures in the General Population: A Nationwide Cohort Study. *PLOS ONE*, *18*(9), e0291561. https://doi.org/10.1371/journal.pone.0291561

Spencer, S. D. (2012). Detecting Violence in the Archaeological Record: Clarifying the Timing of Trauma and Manner of Death in Cases of Cranial Blunt Force Trauma among Pre-Columbian Amerindians of West-Central Illinois. *International Journal of Paleopathology*, *2*(2), 112–122. https://doi.org/10.1016/j.ijpp.2012.09.007

Stubbs, L. A., Saliba, C. K., Schallert, E. K., John, S. D., Khatua, S., Valencia Deray, K. G., Stevens, A. M., & Rocha, M. E. M. (2022). A Lucky Break: A Case of a 3-Month-Old Female with a Pathologic Fracture. *Clinical Pediatrics*, *61*(1), 76–80. https://doi.org/10.1177/00099228211059039

Suchmacher, M., & Geller, M. (2021). Chapter 2—Disease frequency measures. In M. Suchmacher & M. Geller (Eds.), *Practical Biostatistics (Second Edition)* (pp. 9–15). Academic Press. https://doi.org/10.1016/B978-0-323-90102-4.00017-5

Sundh, D., Mellström, D., Ljunggren, Ö., Karlsson, M. K., Ohlsson, C., Nilsson, M., Nilsson, A. G., & Lorentzon, M. (2016). Low Serum Vitamin D is Associated with Higher Cortical Porosity in Elderly Men. *Journal of Internal Medicine, 280*(5), 496–508. https://doi.org/10.1111/joim.12514

Titelbaum, A. R. (2020). Developmental Anomalies and South American Paleopathology: A Comparison of Block Vertebrae and Co-Occurring Axial Anomalies Among Three Skeletal Samples From The El Brujo Archaeological Complex Of Northern Coastal Peru. *International Journal of Paleopathology*, *29*, 76–93. https://doi.org/10.1016/j.ijpp.2019.07.001

Todd, T. W., Iler, D. H. (1927). The Phenomena of Early Stages in Bone Repair. *Annals of Surgery*, *86*(5), 715–736. https://doi.org/10.1097/00000658-192711000-00008

Trinidad, S., & Kotagal, M. (2023). Socioeconomic Factors and Pediatric Injury. *Current Trauma Reports*, *9*(2), 47–55. https://doi.org/10.1007/s40719-023-00251-x

Ubelaker, H. (1989). The Estimation of Age at Death from Immature Human Bone. In M. Y. Iscan (Ed). *Age Markers in the Human Skeleton* (pp. 55-70). Charles C. Thomas, Springfield.

Valerio, G., Gallè, F., Mancusi, C., Di Onofrio, V., Colapietro, M., Guida, P., & Liguori, G. (2010). Pattern of Fractures Across Pediatric Age Groups: Analysis of Individual and Lifestyle Factors. *BMC Public Health*, *10*(1), 656. https://doi.org/10.1186/1471-2458-10-656

van Bath, B. H. S. (1968). Historical Demography and the Social and Economic Development of the Netherlands. *Daedalus*, *97*(2), 604–621.

van Dam, P. J. (2009). Fish for Feast and Fast Fish Consumption in the Netherlands in the Late Middle Ages. In L. Sicking and D. Abreu-Ferreira (Eds.), *Beyond the Catch*. Leiden, The Netherlands: Brill. https://doi.org/10.1163/ej.9789004169739.i-422.88

van de Vijver, K. (2019). Non-adult Fracture Patterns in Late and Post-medieval Flanders, a Comparison of a Churchyard and a Church Assemblage. *Childhood in the Past*, *12*(2), 96–116. https://doi.org/10.1080/17585716.2019.1638556

van Nederveen Meerkerk, E., & Schmidt, A. (2008). Between Wage Labor and Vocation: Child Labor in Dutch Urban Industry, 1600-1800. *Journal of Social History*, *41*(3), 717–736.

van Zanden, J. L. (1995). Tracing the Beginning of the Kuznets Curve: Western Europe during the Early Modern Period. *The Economic History Review*, *48*(4), 643–664. https://doi.org/10.2307/2598128

van Zanden, J. L., & Berg, W. J. V. D. (1993). Vier Eeuwen Welstandsongelijkheid in Alkmaar, ca 1530-1930. *Tijdschrift Voor Sociale Geschiedenis, 19*, 193-215.

Verlinden, P., & Lewis, M. E. (2015). Childhood Trauma: Methods for the Identification of Physeal Fractures in Nonadult Skeletal Remains. *American Journal of Physical Anthropology*, *157*(3), 411–420. https://doi.org/10.1002/ajpa.22732

Viero, A., Biehler-Gomez, L., Messina, C., Cappella, A., Giannoukos, K., Viel, G., Tagliaro, F., & Cattaneo, C. (2022). Utility of micro-CT for dating post-cranial fractures of known post-traumatic ages through 3D measurements of the trabecular inner morphology. *Scientific Reports*, *12*(1), 10543. https://doi.org/10.1038/s41598-022-14530-1

Viero, A., Obertová, Z., Cappella, A., Messina, C., Sconfienza, L. M., Sardanelli, F., Tritella, S., Montisci, M., Gregori, D., Tagliaro, F., & Cattaneo, C. (2021). The Problem of Dating Fractures: A Retrospective Observational Study of Radiologic Features of Fracture Healing in Adults. *Forensic Science International*, *329*, 111058. https://doi.org/10.1016/j.forsciint.2021.111058

Viner, R. M., Ozer, E. M., Denny, S., Marmot, M., Resnick, M., Fatusi, A., & Currie, C. (2012). Adolescence and the Social Determinants of Health. *The Lancet*, *379*(9826), 1641–1652. https://doi.org/10.1016/S0140-6736(12)60149-4

Waldron, Tony. 2009. *Palaeopathology*. Cambridge University Press, Cambridge. Doi:10.1017/CBO9780511812569

Walker, P. L., Cook, D. C., Lambert, P. M. (1997). Skeletal Evidence for Child Abuse: A Physical Anthropological Perspective. *Journal of Forensic Science, 42*, 196–207.

Wáng, Y., Ruiz Santiago, F., Deng, M., & Nogueira-Barbosa, M. (2017). Identifying Osteoporotic Vertebral Endplate and Cortex Fractures. *Quantitative Imaging in Medicine and Surgery*, *7*, 555–591. https://doi.org/10.21037/qims.2017.10.05

Wang, Y., Videman, T., & Battié, M. C. (2012). ISSLS Prize Winner: Lumbar Vertebral Endplate Lesions: Associations with Disc Degeneration and Back Pain History. *Spine*, *37*(17), 1490. https://doi.org/10.1097/BRS.0b013e3182608ac4

Wang, Q., Wang, X. F., Iuliano-Burns, S., Ghasem-Zadeh, A., Zebaze, R., & Seeman, E. (2010). Rapid Growth Produces Transient Cortical Weakness: A Risk Factor for Metaphyseal Fractures During Puberty. *Journal of Bone and Mineral Research, 25*(7), 1521–1526. https://doi.org/10.1002/jbmr.46

Wáng, Y., Xiáng. J. (2023). Schmorl's Node of Primarily Developmental Cause and Schmorl's Node of Primarily Acquired Cause: Two Related Yet Different Entities. *Quantitative Imaging in Medicine and Surgery*, *13*(6), 4044049–4044049. https://doi.org/10.21037/qims-23-252

Wei, X., & Cooper, D. M. L. (2023). The various meanings and uses of bone "remodeling" in biological anthropology: A review. *American Journal of Biological Anthropology*, *182*(2), 318–329. https://doi.org/10.1002/ajpa.24825

Weinkamer, R., Eberl, C., & Fratzl, P. (2019). Mechanoregulation of Bone Remodeling and Healing as Inspiration for Self-Repair in Materials. *Biomimetics*, *4*(3), 46. https://doi.org/10.3390/biomimetics4030046

Welsh, H., & Brickley, M. B. (2023). Pathology or expected morphology? Investigating patterns of cortical porosity and trabecularization during infancy and early childhood. *The Anatomical Record*, *306*(2), 354–365. https://doi.org/10.1002/ar.25081

Welsh, H., Nelson, A. J., Van Der Merwe, A. E., De Boer, H. H., & Brickley, M. B. (2020). An Investigation of Micro-CT Analysis of Bone as a New Diagnostic Method for Paleopathological Cases of Osteomalacia. *International Journal of Paleopathology*, *31*, 23–33. https://doi.org/10.1016/j.ijpp.2020.08.004

Wenger, D. R., Pring, M. E., Pennock, A. T., & Upasani, V. V. (2018). *Rang's Children's Fractures* (Fourth Ed.). Lippincott Williams & Wilkins.

White, T., Folkens, P. (2005). *The Human Bone Manual*. Elsevier Academic Press, Burlington.

Whitney, D. G., Whibley, D., & Jepsen, K. J. (2019). The effect of low-trauma fracture on one-year mortality rate among privately insured adults with and without neurodevelopmental disabilities. *Bone*, *129*, 115060. https://doi.org/10.1016/j.bone.2019.115060

Wilson, L. A. B., & Humphrey, L. T. (2017). Voyaging into the Third Dimension: A Perspective on Virtual Methods and Their Application to Studies of Juvenile Sex Estimation and the Ontogeny of Sexual Dimorphism. *Forensic Science International*, *278*, 32–46. https://doi.org/10.1016/j.forsciint.2017.06.016

Wood, J. W., Milner, G. R., Harpending, H. C., Weiss, K. M., Cohen, M. N., Eisenberg, L. E., Hutchinson, D. L., Jankauskas, R., Cesnys, G., Česnys, G., Katzenberg, M. A., Lukacs, J. R., McGrath, J. W., Roth, E. A., Ubelaker, D. H., & Wilkinson, R. G. (1992). The Osteological Paradox: Problems of Inferring Prehistoric Health from Skeletal Samples. *Current Anthropology*, *33*(4), 343–370.

World Health Organization. (2024). Social Determinants of Health. https://www.who.int/health-topics/social-determinants-of-health#tab=tab_1. Accessed February 19, 2024.

Yin, R., Lord, E. L., Cohen, J. R., Buser, Z., Lao, L., Zhong, G., & Wang, J. C. (2015). Distribution of Schmorl Nodes in the Lumbar Spine and Their Relationship with Lumbar Disk Degeneration and Range of Motion. *Spine*, *40*(1), E49. https://doi.org/10.1097/BRS.0000000000000658

Zielman, G., & Baetsen, W. A. (2020). *Wat De Nieuwe Sint Jansbeek Boven Water Bracht: Dood En Leven in Het Arnhemse Verleden: Archeologisch Onderzoek Sint Jansbeek Te Arnhem*. Weesp: RAAP Archeologisch Adviesbureau.

Zohar, A., Getzler, I., Behrbalk, E. (2023). Higher Mortality Rate in Patients with Vertebral Compression Fractures is due to Deteriorated Medical Status Prior to the Fracture Event. *Geriatric Orthopaedic Surgery & Rehabilitation*, *14*, 21514593231153106. https://doi.org/10.1177/21514593231153106

Appendix A – Individual and Fracture Recording Forms

Date: _____ Site: _____

Observer:_____ SK # _____

Juvenile Fracture Recording

Age (From Inventory): _____

Sex Estimation – Distal Humerus

Olecranon Fossa	
Trochlear Curvature	
Shape of the Trochlea	
Medial Epicondyle	

Sex Estimation – Pelvis

Ventral Arc	
Subpubic Concavity	
Ischio-Pubic Ramus	
Angle of Greater Sciatic Notch	
Depth of Greater Sciatic Notch	
Arch Criterion	

Sex Estimation – Skull

Mental Protrusion	
Anterior Dental Arcade	
Mastoid Process	
Orbital Rim	
Nuchal Crest	

Sex Estimate: _____

Sex Estimate – Notes

Date: _____ Site: _____

Observer:_____ SK # _____

Age Estimation – Epiphyseal Fusion

If element unavailable, set as ---

Epiphysis	Stage of Fusion
Proximal Humerus	---
Distal Radius	---
Iliac Crest	---
Femoral Head	---
Proximal Tibia	---
Cervical Annular Rings	---
Thoracic Annular Rings	---
Lumbar Annular Rings	---
Sacral Annular Rings	---

Age Estimate Based on Epiphyseal Fusion: _____

Age Estimation – Dental Development & Eruption

Describe state of dental development and eruption.

Age Estimate Based on Dental Development & Eruption: _____

Age Estimation – Notes

Site: ARJB SK#:

Skeletal Inventory - Presence/Absence

Element	P/A[1]
Cranial Vault	---
Left Zygomatic	---
Right Zygomatic	---

[1]Presence/absence of a feature. Absence = feature is not observable

Ribs & Spine[1]

Element	# Present
Left Ribs	
Right Ribs	
Cervical Vertebrae	
Thoracic Vertebrae	
Lumbar Vertebrae	

[1]Record as number of elements present.

Long Bones

Element	LEFT					RIGHT				
	Prox epip	Prox 1/3	Mid 1/3	Distal 1/3	Distal epip	Prox epip	Prox 1/3	Mid 1/3	Distal 1/3	Distal epip
Clavicle	---	---	---	---	---	---	---	---	---	---
Humerus	---	---	---	---	---	---	---	---	---	---
Radius	---	---	---	---	---	---	---	---	---	---
Ulna	---	---	---	---	---	---	---	---	---	---
Femur	---	---	---	---	---	---	---	---	---	---
Tibia	---	---	---	---	---	---	---	---	---	---
Fibula	---	---	---	---	---	---	---	---	---	---

* segment preservation: A = absent; <25%; 25-50%; 50-75% >75%

Notes

Date: _____ Site: _____

Observer:_____ SK # _____

Location of Fracture

(Fill in Attached Skeletal Anatomy Diagram)

Element	Location on Bone	Side

Fracture Profile

Element	Smooth/ Even Fracture Margins	Hinging	Eburnation	Hairline Fractures	Depressed Cortical Surface	Defined Fracture Line	Discoloration	Sharp Fracture Margin	Other*
	---	---	---	---	---	---	---	---	
	---	---	---	---	---	---	---	---	
	---	---	---	---	---	---	---	---	

* Describe other features in notes, detail in diagram.

--- Indicates item can't be scored.

Healing Profile

Element	Rounded Fracture Margins	NBF	Bone Bridging/ Spicules	Cortical Striations	Sclerosis of Margins	Lamellar Conversion	Pitting	Callus		Other*
								Woven	Lamellar	
	---	---	---	---	---	---	---	---	---	
	---	---	---	---	---	---	---	---	---	
	---	---	---	---	---	---	---	---	---	

* Describe other features in notes, detail in diagram.

--- Indicates item can't be scored.

Notes:

Draw Element(s) and Features of Fracture on Separate Sheet

Photo:

Date: _____ Site: _____

Observer:_____ SK # _____

Complications:

If complications are present be sure to put details in notes (e.g., if overlap note the amount of overlap, etc.)

- ☐ Malunion/Overlap
- ☐ Atrophy
- ☐ Overgrowth
- ☐ Linear/Rotational Deformity
- ☐ Altered Articular Surface
- ☐ Infection
  - ☐ Periostosis (only applies if signs of trauma)
  - ☐ Osteitis/Osteomyelistis
- ☐ Displacement
- ☐ Angulation
- ☐ Shortening
- ☐ Premature Fusion
- ☐ Joint Degeneration

Notes – Complications

Summary

Number of Fractures	
Elements Involved	
Estimated Type of Fracture	
Estimated Time of Fracture	
X-rays Required (Y/N) (Indicate in notes which bones/elements to be radiographed)	
X-rays Completed (Y/N)	
MicroCT Required (Y/N) (Indicate in notes which elements to be scanned)	
MicroCT Completed (Y/N)	

Notes

Pertinent ☐

Appendix B – Age, Sex, and Socioeconomic Status (SES) for all Individuals

Each individual is identified by the site code and individual number. Age designation is by category (Early Child 1-5; Late Child 6-9; Early Adolescent 10-14; Middle Adolescent 15-17; Late Adolescent 18+). Sex estimation corresponds to Buikstra and Ubelaker (1994) designations of Male, Probable Male, Ambiguous, Probable Female, Female, and Undetermined. A designation of --- indicates a sex estimate was not undertaken due to the young age of the individual.

Site	SK#	Sex Estimation	Age Dental	Age Epiphyses	Age Category	SES
ARJB	V452	---	2.5-4	3-5	Early Child	Low
ARJB	V478	---	1-2	<5	Early Child	Low
ARJB	V522	---	---	12-14	Early Adolescent	Low
ARJB	V556	Probable Male	14-17	14-18	Middle Adolescent	Low
ARJB	V667	---	3.5-5	3-5	Early Child	Low
ARJB	V1057	---	6-7.5	>5	Late Child	Low
ARJB	V1112	---	5.5-7	4-5	Late Child	Low
ARJB	V1257	Probable Male	16-18	16-18	Middle Adolescent	Low
ARJB	V1258	---	8-10.5	6-12	Late Child	Low
ARJB	V1316	---	10.5m-1.5y	1-2	Early Child	Low
ARJB	V1348	---	2-4	1-4	Early Child	Low
ARJB	V1368	Probable Female	>15	14-17	Middle Adolescent	Low
ARJB	V1437	---	11-12	<16	Early Adolescent	Low
ARJB	V1463	Probable Female	14-16	14-18	Middle Adolescent	Low
ARJB	V1551	---	---	12-14	Early Adolescent	Low
ARJB	V1556	Probable Male	12.5-15.5	14-16	Early Adolescent	Low
ARJB	V1583	Undetermined	15.5-17.5	16-18	Middle Adolescent	Low
ARJB	V1632	---	10m-1.5y	---	Early Child	Low
ARJB	V1777	---	1-2	---	Early Child	Low
ARJB	V1791	---	1-2	---	Early Child	Low
ARJB	V1827	Female	16-18	15-17	Middle Adolescent	Low
ARJB	V1890	---	---	3-5	Early Child	Low
ARJB	V1912	Probable Female	15-17.5	15-17	Middle Adolescent	Low
ARJB	V1945	Ambiguous	12.5-16.5	11-14	Early Adolescent	Low
ARJB	V1980	---	4.5-6.5	3-5	Early Child	Low
ARJB	V2021.2	---	12-15	12-16	Early Adolescent	Low
EHV-CK	S979	F (DNA)	6-9	5-7	Late Child	Low to Mid
EHV-CK	S1427	Undetermined	---	12-16	Late Child	Low to Mid
EHV-CK	S1834	---	---	11-15	Early Adolescent	Low to Mid
EHV-CK	S2136	---	---	11-13	Early Adolescent	Low to Mid
EHV-CK	S2567	Male (DNA)	2-5	<7	Early Child	Low to Mid
EHV-CK	S2799	---	---	3-5	Early Child	Low to Mid

EHV-CK	S2918	Female (DNA)	---	14-16	Middle Adolescent	Low to Mid
EHV-CK	S3079	Male (DNA)	15-17	14-17	Middle Adolescent	Low to Mid
EHV-CK	S3115	PF (DNA)	3-5	3-5	Early Child	Low to Mid
EHV-CK	S3507	Undetermined	---	13-16	Early Adolescent	Low to Mid
EHV-CK	S3537	Male (DNA)	5-7	5-7	Late Child	Low to Mid
GRK	V36	Undetermined	>12.5	12-16	Early Adolescent	Mid to High
GRK	V59	---	10-12	<12	Early Adolescent	Mid to High
GRK	V63	---	1-2	---	Early Child	Mid to High
GRK	V169	---	3 (Burial Record)	3 (Burial Record)	Early Child	Mid to High
GRK	V181	---	1-2	1-2	Early Child	Mid to High
GRK	V194	Male (Burial Record)	8 (Burial Record)	8 (Burial Record)	Late Child	Mid to High
GRK	V388	---	1-2	1-2	Early Child	Mid to High
GRK	V397	---	7 (Burial Record)	7 (Burial Record)	Late Child	Mid to High
GRK	V451	---	7-9	7-12	Late Child	Mid to High
GRK	V512	Male (Burial Record)	16(Burial Record)	16(Burial Record)	Middle Adolescent	Mid to High
GRK	V532	---	1-2	1-2	Early Child	Mid to High
GRK	V877	---	2-4	2-4	Early Child	Mid to High
ZW87	4	---	13 (Burial Record)	13 (Burial Record)	Early Adolescent	Mid to High
ZW87	8	Female (Burial Record)	19 (Burial Record)	19 (Burial Record)	Late Adolescent	Mid to High
ZW87	64	Possible Female	16 (Burial Record)	16 (Burial Record)	Middle Adolescent	Mid to High
ZW87	67	---	8.5-10	<12	Late Child	Mid to High
ZW87	235	---	3-5	2-5	Early Child	Mid to High
ZW87	289	---	1-2	1-3	Early Child	Mid to High

Appendix C – Fracture Assessment

The following 3 pages present the raw data from the fracture assessment. For explanations of the acronyms, see the legend on this page.

Table A1.1 Legend explaining acronyms used in fracture assessment table.

Acronym	Meaning
Fracture Profile	
EM	Even Margins
H	Hinging
E	Eburnation
HF	Hairline Fracture
DCS	Depressed Cortical Surface
D	Discoloration
SFM	Sharp Fracture Margin
Healing Profile	
RFM	Rounded Fracture Margin
NBF	New Bone Formation
B	Bridging
CS	Cortical Striations
SM	Sclerosis of Margins
LC	Lamellar Conversion
P	Pitting
WC	Woven Callus
LC	Lamellar Callus
Complications	
M	Malunion

Location of Fracture 1					Fracture Profile 1										Healing Profile 1								Complications 1
Site	SK#	Element 1	Location 1	Side 1	EM 1	H 1	E 1	HF 1	DCS 1	DFL 1	D 1	SFM 1	RFM 1	NBF 1	B 1	CS 1	SM 1	LC 1	P 1	WC 1	LC 1	M 1
ARJB	V452	---	---	---	---	---	---	---	---	---	---	---	---	---	---	---	---	---	---	---	---	---
ARJB	V478	---	---	---	---	---	---	---	---	---	---	---	---	---	---	---	---	---	---	---	---	---
ARJB	V522	---	---	---	---	---	---	---	---	---	---	---	---	---	---	---	---	---	---	---	---	---
ARJB	V556	L5	Anterior Endp	---	Absent	Absent	Absent	Absent	Present	Present	Absent	Absent	Present	Present	Absent	Absent	Absent	Absent	Absent	Absent	Absent	Absent
ARJB	V667	---	---	---	---	---	---	---	---	---	---	---	---	---	---	---	---	---	---	---	---	---
ARJB	V1057	---	---	---	---	---	---	---	---	---	---	---	---	---	---	---	---	---	---	---	---	---
ARJB	V1112	---	---	---	---	---	---	---	---	---	---	---	---	---	---	---	---	---	---	---	---	---
ARJB	V1257	---	---	---	---	---	---	---	---	---	---	---	---	---	---	---	---	---	---	---	---	---
ARJB	V1258	---	---	---	---	---	---	---	---	---	---	---	---	---	---	---	---	---	---	---	---	---
ARJB	V1316	---	---	---	---	---	---	---	---	---	---	---	---	---	---	---	---	---	---	---	---	---
ARJB	V1348	---	---	---	---	---	---	---	---	---	---	---	---	---	---	---	---	---	---	---	---	---
ARJB	V1368	T8 T9 T10 T12	Vertebral Bod	---	Absent	Absent	Absent	Absent	Present	Absent	Absent	Absent	Present	Present	Absent	Absent	Absent	Present	Absent	Absent	Absent	---
ARJB	V1437	L1 L3 L4	Anterior Endp	---	Absent	Absent	Absent	Absent	Present	Absent	Absent	Absent	Present	Absent	Absent	Absent	Absent	Present	Absent	Absent	Absent	---
ARJB	V1463	T4	Inferior Endpl	---	Absent	Absent	Absent	Absent	Present	Present	Absent	Present	Absent	Present	Absent	Absent	Absent	Absent	Absent	Absent	Absent	
ARJB	V1551	---	---	---	---	---	---	---	---	---	---	---	---	---	---	---	---	---	---	---	---	---
ARJB	V1556	L2	Superior Endp	---	Absent	Absent	Absent	Absent	Present	Present	Absent	Present	Absent	Present	Present	Absent	Absent	Absent	Absent	Absent	Absent	Absent
ARJB	V1583	T7 T8 T9 T10 T11 T12	Vertebral Bod	---	Absent	Absent	Absent	Absent	Present	Present	Absent	Present	Present	Present	Absent	Absent	Absent	Absent	Absent	Absent	Absent	Absent
ARJB	V1632	Humerus	Distal 1/3 Post	L	Absent	Absent	Absent	Absent	Absent	Absent	Absent	Absent	Absent	Present	Present	Absent	Absent	Absent	Absent	Absent	Absent	Absent
ARJB	V1777	---	---	---	---	---	---	---	---	---	---	---	---	---	---	---	---	---	---	---	---	---
ARJB	V1791	---	---	---	---	---	---	---	---	---	---	---	---	---	---	---	---	---	---	---	---	---
ARJB	V1827	T3 T10 T11 T12	Vertebral Bod	---	Absent	Absent	Absent	Absent	Present	Present	Absent	Present	Absent	Present	Present	Absent	Absent	Absent	Absent	Absent	Absent	Absent
ARJB	V1890	---	---	---	---	---	---	---	---	---	---	---	---	---	---	---	---	---	---	---	---	---
ARJB	V1912	L3 L4 L5	Superior Verte	---	Absent	Absent	Absent	Absent	Present	Present	Absent	Absent	Present	Present	Absent	Absent	Absent	Absent	Absent	Absent	Absent	Absent
ARJB	V1945	L1 L2 L3	Vertebral Bod	---	Present	Absent	Absent	Absent	Present	Absent	Absent	Absent	Present	Present	Absent	Absent	Absent	Present	Absent	Absent	Absent	Absent
ARJB	V1980	---	---	---	---	---	---	---	---	---	---	---	---	---	---	---	---	---	---	---	---	---
ARJB	V2021.2	---	---	---	---	---	---	---	---	---	---	---	---	---	---	---	---	---	---	---	---	---
EHV	S979	Zygomatic	Orbital Rim	L	Absent	Absent	Absent	Absent	Present	Absent	Absent	Absent	Absent	Present	Absent	Absent	Absent	Present	Absent	Absent	Absent	Absent
EHV	S1427	---	---	---	---	---	---	---	---	---	---	---	---	---	---	---	---	---	---	---	---	---
EHV	S1834	T11 T12	Anterior Verte	---	Absent	Absent	Absent	Absent	Present	Absent	Absent	Absent	Present	Present	Absent	Absent	Absent	Present	Absent	Absent	Absent	Absent
EHV	S2136	---	---	---	---	---	---	---	---	---	---	---	---	---	---	---	---	---	---	---	---	---
EHV	S2567	Humerus	Upper Shaft	L	Absent	Absent	Absent	Absent	Absent	Present	Absent	Present	Present	Present	Absent	Absent	Absent	Absent	Absent	Present	Absent	Absent
EHV	S2799	---	---	---	---	---	---	---	---	---	---	---	---	---	---	---	---	---	---	---	---	---
EHV	S2918	L5	Inferior Verteb	---	Absent	Absent	Absent	Absent	Present	Absent	Absent	Present	Absent	Present	Absent	Absent	Absent	Absent	Absent	Absent	Absent	---
EHV	S3079	---	---	---	---	---	---	---	---	---	---	---	---	---	---	---	---	---	---	---	---	---
EHV	S3115	---	---	---	---	---	---	---	---	---	---	---	---	---	---	---	---	---	---	---	---	---
EHV	S3507	L1 L3 L4	Vertebral Bod	---	Absent	Absent	Absent	Absent	Present	Present	Absent	Absent	Present	Present	Absent	Absent	Absent	Absent	Absent	Absent	Absent	Absent
EHV	S3537	---	---	---	---	---	---	---	---	---	---	---	---	---	---	---	---	---	---	---	---	---
GRK	V36	---	---	---	---	---	---	---	---	---	---	---	---	---	---	---	---	---	---	---	---	---
GRK	V59	Fibula	Shaft	R	Absent	Absent	Absent	Absent	Absent	Absent	Absent	Absent	Present	Present	Present	Absent	Absent	Absent	Absent	Present	Absent	Absent
GRK	V63	---	---	---	---	---	---	---	---	---	---	---	---	---	---	---	---	---	---	---	---	---
GRK	V169	---	---	---	---	---	---	---	---	---	---	---	---	---	---	---	---	---	---	---	---	---
GRK	V181	---	---	---	---	---	---	---	---	---	---	---	---	---	---	---	---	---	---	---	---	---
GRK	V194	---	---	---	---	---	---	---	---	---	---	---	---	---	---	---	---	---	---	---	---	---
GRK	V388	---	---	---	---	---	---	---	---	---	---	---	---	---	---	---	---	---	---	---	---	---
GRK	V397	---	---	---	---	---	---	---	---	---	---	---	---	---	---	---	---	---	---	---	---	---
GRK	V451	---	---	---	---	---	---	---	---	---	---	---	---	---	---	---	---	---	---	---	---	---
GRK	V512	Frontal	Squama	---	Absent	Absent	Absent	Absent	Present	Absent	Absent	Absent	Present	Absent	Absent	Absent	Absent	Present	Absent	Absent	Present	Absent
GRK	V532	---	---	---	---	---	---	---	---	---	---	---	---	---	---	---	---	---	---	---	---	---
GRK	V877	---	---	---	---	---	---	---	---	---	---	---	---	---	---	---	---	---	---	---	---	---
ZW87	4	---	---	---	---	---	---	---	---	---	---	---	---	---	---	---	---	---	---	---	---	---
ZW87	8	Rib 12	Shaft	L	Absent	Absent	Absent	Absent	Absent	Present	Absent	Absent	Present	Present	Present	Absent	Present	Absent	Absent	Present	Absent	Present Displace
ZW87	64	---	---	---	---	---	---	---	---	---	---	---	---	---	---	---	---	---	---	---	---	---
ZW87	67	Thoracic Rib A	Shaft	L	Present	Absent	Present	Absent	Absent	Present	Absent	Present	Absent	Present	Present	Absent	Absent	Absent	Absent	Present	Absent	Present
ZW87	235	Thoracic Vertebrae 1-2	Centrum	---	Absent	Absent	Absent	Absent	Present	Absent	Absent	Absent	Absent	Absent	Absent	Absent	Absent	Absent	Absent	Absent	Absent	Absent
ZW87	289	---	---	---	---	---	---	---	---	---	---	---	---	---	---	---	---	---	---	---	---	---

		Location of Fracture 2			Fracture Profile											Healing Profile 2						Complications 2
Site	SK#	Element 2	Location 2	Side 2	EM 2	H 2	E 2	HF 2	DCS 2	DFL 2	D 2	SFM 2	RFM 2	NBF 2	B 2	CS 2	SM 2	LC 2	P 2	WC 2	LC 2	M 2
ARJB	V452	---	---	---	---	---	---	---	---	---	---	---	---	---	---	---	---	---	---	---	---	---
ARJB	V478	---	---	---	---	---	---	---	---	---	---	---	---	---	---	---	---	---	---	---	---	---
ARJB	V522	---	---	---	---	---	---	---	---	---	---	---	---	---	---	---	---	---	---	---	---	---
ARJB	V556	L4	Anterior Enplat	---	Absent	Absent	Absent	Absent	Present	Present	Absent	Absent	Present	Present	Absent	Absent	Absent	Present	Absent	Absent	Absent	Absent
ARJB	V667	---	---	---	---	---	---	---	---	---	---	---	---	---	---	---	---	---	---	---	---	---
ARJB	V1057	---	---	---	---	---	---	---	---	---	---	---	---	---	---	---	---	---	---	---	---	---
ARJB	V1112	---	---	---	---	---	---	---	---	---	---	---	---	---	---	---	---	---	---	---	---	---
ARJB	V1257	---	---	---	---	---	---	---	---	---	---	---	---	---	---	---	---	---	---	---	---	---
ARJB	V1258	---	---	---	---	---	---	---	---	---	---	---	---	---	---	---	---	---	---	---	---	---
ARJB	V1316	---	---	---	---	---	---	---	---	---	---	---	---	---	---	---	---	---	---	---	---	---
ARJB	V1348	---	---	---	---	---	---	---	---	---	---	---	---	---	---	---	---	---	---	---	---	---
ARJB	V1368	L1 L3	Endplates	---	Absent	Absent	Absent	Absent	Present	Absent	Absent	Absent	Present	Absent	Absent	Absent	Absent	Present	Absent	Absent	Absent	Absent
ARJB	V1437	---	---	---	---	---	---	---	---	---	---	---	---	---	---	---	---	---	---	---	---	---
ARJB	V1463	T5	Endplates	---	Absent	Absent	Absent	Absent	Present	Present	Absent	Present	Absent	Present	Absent	Absent	Absent	Absent	Absent	Absent	Absent	Absent
ARJB	V1551	---	---	---	---	---	---	---	NN	---	---	---	---	---	---	---	---	---	---	---	---	---
ARJB	V1556	L3 L4 L5	Superior Endpla	---	Absent	Absent	Absent	Absent	Present	Present	Absent	Absent	Present	Present	Absent	Absent	Absent	Present	Absent	Absent	Absent	Absent
ARJB	V1583	---	---	---	---	---	---	---	---	---	---	---	---	---	---	---	---	---	---	---	---	---
ARJB	V1632	---	---	---	---	---	---	---	---	---	---	---	---	---	---	---	---	---	---	---	---	---
ARJB	V1777	---	---	---	---	---	---	---	---	---	---	---	---	---	---	---	---	---	---	---	---	---
ARJB	V1791	---	---	---	---	---	---	---	---	---	---	---	---	---	---	---	---	---	---	---	---	---
ARJB	V1827	T7 T8 T9 T10 T11	Endplates	---	Absent	Absent	Absent	Absent	Present	Present	Absent	Present	Present	Present	Present	Absent	Absent	Present	Absent	Absent	Absent	Absent
ARJB	V1890	---	---	---	---	---	---	---	---	---	---	---	---	---	---	---	---	---	---	---	---	---
ARJB	V1912	---	---	---	---	---	---	---	---	---	---	---	---	---	---	---	---	---	---	---	---	---
ARJB	V1945	---	---	---	---	---	---	---	---	---	---	---	---	---	---	---	---	---	---	---	---	---
ARJB	V1980	---	---	---	---	---	---	---	---	---	---	---	---	---	---	---	---	---	---	---	---	---
ARJB	V2021.2	---	---	---	---	---	---	---	---	---	---	---	---	---	---	---	---	---	---	---	---	---
EHV	S979	---	---	Right	Absent	Absent	Absent	Absent	Present	Present	Absent	Absent	Present	Absent	Absent	Absent	Absent	Absent	Absent	Absent	Absent	Absent
EHV	S1427	---	---	---	---	---	---	---	---	---	---	---	---	---	---	---	---	---	---	---	---	---
EHV	S1834	Typical (Thoracic)	Proximal	Left	Present	Absent	Absent	Absent	A	Present	Absent	Present	Present	Present	Absent	Absent	Absent	Present	Absent	Absent	Absent	Absent
EHV	S2136	---	---	---	---	---	---	---	---	---	---	---	---	---	---	---	---	---	---	---	---	---
EHV	S2567	---	---	---	---	---	---	---	---	---	---	---	---	---	---	---	---	---	---	---	---	---
EHV	S2799	---	---	---	---	---	---	---	---	---	---	---	---	---	---	---	---	---	---	---	---	---
EHV	S2918	---	---	---	---	---	---	---	---	---	---	---	---	---	---	---	---	---	---	---	---	---
EHV	S3079	---	---	---	---	---	---	---	---	---	---	---	---	---	---	---	---	---	---	---	---	---
EHV	S3115	---	---	---	---	---	---	---	---	---	---	---	---	---	---	---	---	---	---	---	---	---
EHV	S3507	T8	Endplates	---	Absent	Absent	Absent	Absent	Present	Absent	Absent	Absent	Present	Absent	Absent	Absent	Absent	Present	Absent	Absent	Absent	Absent
EHV	S3537	---	---	---	---	---	---	---	---	---	---	---	---	---	---	---	---	---	---	---	---	---
GRK	V36	---	---	---	---	---	---	---	---	---	---	---	---	---	---	---	---	---	---	---	---	---
GRK	V59	---	---	---	Absent	Absent	Absent	Absent	Present	Absent	Absent	Absent	Present	Absent	Absent	Absent	Absent	Absent	Absent	Absent	Absent	Absent
GRK	V63	---	---	---	---	---	---	---	---	---	---	---	---	---	---	---	---	---	---	---	---	---
GRK	V169	---	---	---	---	---	---	---	---	---	---	---	---	---	---	---	---	---	---	---	---	---
GRK	V181	---	---	---	---	---	---	---	---	---	---	---	---	---	---	---	---	---	---	---	---	---
GRK	V194	---	---	---	---	---	---	---	---	---	---	---	---	---	---	---	---	---	---	---	---	---
GRK	V388	---	---	---	---	---	---	---	---	---	---	---	---	---	---	---	---	---	---	---	---	---
GRK	V397	---	---	---	---	---	---	---	---	---	---	---	---	---	---	---	---	---	---	---	---	---
GRK	V451	---	---	---	---	---	---	---	---	---	---	---	---	---	---	---	---	---	---	---	---	---
GRK	V512	---	---	---	---	---	---	---	---	---	---	---	---	---	---	---	---	---	---	---	---	---
GRK	V532	---	---	---	---	---	---	---	---	---	---	---	---	---	---	---	---	---	---	---	---	---
GRK	V877	---	---	---	---	---	---	---	---	---	---	---	---	---	---	---	---	---	---	---	---	---
ZW87	4	---	---	---	---	---	---	---	---	---	---	---	---	---	---	---	---	---	---	---	---	---
ZW87	8	---	---	---	---	---	---	---	---	---	---	---	---	---	---	---	---	---	---	---	---	---
ZW87	64	---	---	---	---	---	---	---	---	---	---	---	---	---	---	---	---	---	---	---	---	---
ZW87	67	Thoracic Rib B	Neck	Left	Present	Absent	P	Absent	Present	Absent	Absent	Present	Absent	Present	Present	Absent	Absent	Absent	Absent	Present	Absent	Present
ZW87	235	Cervical Vertebra	Centrum	---	Absent	Absent	Absent	Absent	Present	Present	Absent	Present	Absent	Present	Present	Absent	Absent	Absent	Absent	Absent	Absent	Absent
ZW87	289	---	---	---	---	---	---	---	---	---	---	---	---	---	---	---	---	---	---	---	---	---

		Location of Fracture 3			Fracture Profile											Healing Profile 3							Complications 3	Summary	
Site	SK#	Element 3	Location 3	Side 3	EM 3	H 3	E 3	HF 3	DCS 3	DFL 3	D 3	SFM 3	RFM 3	NBF 3	B 3	CS 3	SM 3	LC 3	P 3	WC 3	LC 3	M 3	Elements	Pertinent
ARJB	V452	---	---	---	---	---	---	---	---	---	---	---	---	---	---	---	---	---	---	---	---	---	---	No
ARJB	V478	---	---	---	---	---	---	---	---	---	---	---	---	---	---	---	---	---	---	---	---	---	---	No
ARJB	V522	---	---	---	---	---	---	---	---	---	---	---	---	---	---	---	---	---	---	---	---	---	---	No
ARJB	V556	---	---	---	---	---	---	---	---	---	---	---	---	---	---	---	---	---	---	---	---	---	L4, L5	Yes
ARJB	V667	---	---	---	---	---	---	---	---	---	---	---	---	---	---	---	---	---	---	---	---	---	---	No
ARJB	V1057	---	---	---	---	---	---	---	---	---	---	---	---	---	---	---	---	---	---	---	---	---	---	No
ARJB	V1112	---	---	---	---	---	---	---	---	---	---	---	---	---	---	---	---	---	---	---	---	---	---	No
ARJB	V1257	---	---	---	---	---	---	---	---	---	---	---	---	---	---	---	---	---	---	---	---	---	---	No
ARJB	V1258	---	---	---	---	---	---	---	---	---	---	---	---	---	---	---	---	---	---	---	---	---	---	No
ARJB	V1316	---	---	---	---	---	---	---	---	---	---	---	---	---	---	---	---	---	---	---	---	---	---	No
ARJB	V1348	---	---	---	---	---	---	---	---	---	---	---	---	---	---	---	---	---	---	---	---	---	---	No
ARJB	V1368	---	---	---	---	---	---	---	---	---	---	---	---	---	---	---	---	---	---	---	---	---	T8 T9 T10 T12 L1 L3	Maybe
ARJB	V1437	---	---	---	---	---	---	---	---	---	---	---	---	---	---	---	---	---	---	---	---	---	L1 L3 L4	No
ARJB	V1463	---	---	---	---	---	---	---	---	---	---	---	---	---	---	---	---	---	---	---	---	---	T4 T5	Yes
ARJB	V1551	---	---	---	---	---	---	---	---	---	---	---	---	---	---	---	---	---	---	---	---	---	---	No
ARJB	V1556	---	---	---	---	---	---	---	---	---	---	---	---	---	---	---	---	---	---	---	---	---	L2 L3 L4 L5	Yes
ARJB	V1583	---	---	---	---	---	---	---	---	---	---	---	---	---	---	---	---	---	---	---	---	---	T7 T8 T9 T10 T11 T12	Yes
ARJB	V1632	---	---	---	---	---	---	---	---	---	---	---	---	---	---	---	---	---	---	---	---	---	Left Humerus	Maybe
ARJB	V1777	---	---	---	---	---	---	---	---	---	---	---	---	---	---	---	---	---	---	---	---	---	---	No
ARJB	V1791	---	---	---	---	---	---	---	---	---	---	---	---	---	---	---	---	---	---	---	---	---	---	No
ARJB	V1827	T5 T6	Endplates	---	Absent	Absent	Absent	Absent	Present	Present	Absent	Present	Absent	Present	Absent	Absent	Absent	Absent	Absent	Absent	Absent	Absent	Thoracic Vertebrae	Yes
ARJB	V1890	---	---	---	---	---	---	---	---	---	---	---	---	---	---	---	---	---	---	---	---	---	---	No
ARJB	V1912	---	---	---	---	---	---	---	---	---	---	---	---	---	---	---	---	---	---	---	---	---	L3-L5	Yes
ARJB	V1945	---	---	---	---	---	---	---	---	---	---	---	---	---	---	---	---	---	---	---	---	---	L1 L2 L3	Yes
ARJB	V1980	---	---	---	---	---	---	---	---	---	---	---	---	---	---	---	---	---	---	---	---	---	---	No
ARJB	V2021.2	---	---	---	---	---	---	---	---	---	---	---	---	---	---	---	---	---	---	---	---	---	---	No
EHV	S979	---	---	---	---	---	---	---	---	---	---	---	---	---	---	---	---	---	---	---	---	---	Zygomatic	Yes
EHV	S1427	---	---	---	---	---	---	---	---	---	---	---	---	---	---	---	---	---	---	---	---	---	---	No
EHV	S1834	---	---	---	---	---	---	---	---	---	---	---	---	---	---	---	---	---	---	---	---	---	Left Typical Rib	Maybe
EHV	S2136	---	---	---	---	---	---	---	---	---	---	---	---	---	---	---	---	---	---	---	---	---	---	No
EHV	S2567	---	---	---	---	---	---	---	---	---	---	---	---	---	---	---	---	---	---	---	---	---	Left Humerus	Yes
EHV	S2799	---	---	---	---	---	---	---	---	---	---	---	---	---	---	---	---	---	---	---	---	---	---	No
EHV	S2918	---	---	---	---	---	---	---	---	---	---	---	---	---	---	---	---	---	---	---	---	---	L5	Yes
EHV	S3079	---	---	---	---	---	---	---	---	---	---	---	---	---	---	---	---	---	---	---	---	---	---	No
EHV	S3115	---	---	---	---	---	---	---	---	---	---	---	---	---	---	---	---	---	---	---	---	---	---	No
EHV	S3507	---	---	---	---	---	---	---	---	---	---	---	---	---	---	---	---	---	---	---	---	---	L1 L3 L4 T8 T9 T10	Yes
EHV	S3537	---	---	---	---	---	---	---	---	---	---	---	---	---	---	---	---	---	---	---	---	---	---	No
GRK	V36	---	---	---	---	---	---	---	---	---	---	---	---	---	---	---	---	---	---	---	---	---	---	No
GRK	V59	---	---	---	---	---	---	---	---	---	---	---	---	---	---	---	---	---	---	---	---	---	Fibula	Yes
GRK	V63	---	---	---	---	---	---	---	---	---	---	---	---	---	---	---	---	---	---	---	---	---	---	No
GRK	V169	---	---	---	---	---	---	---	---	---	---	---	---	---	---	---	---	---	---	---	---	---	---	No
GRK	V181	---	---	---	---	---	---	---	---	---	---	---	---	---	---	---	---	---	---	---	---	---	---	No
GRK	V194	---	---	---	---	---	---	---	---	---	---	---	---	---	---	---	---	---	---	---	---	---	---	No
GRK	V388	---	---	---	---	---	---	---	---	---	---	---	---	---	---	---	---	---	---	---	---	---	---	No
GRK	V397	---	---	---	---	---	---	---	---	---	---	---	---	---	---	---	---	---	---	---	---	---	---	No
GRK	V451	---	---	---	---	---	---	---	---	---	---	---	---	---	---	---	---	---	---	---	---	---	---	No
GRK	V512	---	---	---	---	---	---	---	---	---	---	---	---	---	---	---	---	---	---	---	---	---	Frontal	Yes
GRK	V532	---	---	---	---	---	---	---	---	---	---	---	---	---	---	---	---	---	---	---	---	---	---	No
GRK	V877	---	---	---	---	---	---	---	---	---	---	---	---	---	---	---	---	---	---	---	---	---	---	No
ZW87	4	---	---	---	---	---	---	---	---	---	---	---	---	---	---	---	---	---	---	---	---	---	---	No
ZW87	8	---	---	---	---	---	---	---	---	---	---	---	---	---	---	---	---	---	---	---	---	---	Rib 12	Yes
ZW87	64	---	---	---	---	---	---	---	---	---	---	---	---	---	---	---	---	---	---	---	---	---	---	No
ZW87	67	Thoracic Rib C (8)	Neck	Left	Present	Absent	Present	Absent	Absent	Present	Absent	Present	Absent	Present	Present	Absent	Absent	Absent	Absent	Present	Absent	Present	Thoracic Ribs	Yes
ZW87	235	Cervical Vertebrae 5-6	Body and Articular F	---	Absent	Absent	Absent	Absent	Present	Present	Absent	Present	Absent	Present	Present	Absent	Absent	Absent	Absent	Absent	Absent	Absent	Cervical and Thoracic	Yes
ZW87	289	---	---	---	---	---	---	---	---	---	---	---	---	---	---	---	---	---	---	---	---	---	---	No

Appendix D – Additional Images

This supplemental data contains all the images of the macroscopic appearance of fractures and suspected fractures for all individuals. Additional micro-CT and microscopy images when available have been included. Individuals are listed in alphabetical order by collection.

D1.0 ARJB V556

Figure D1.1 - *L4 vertebrae superior endplate (A) and inferior endplate (B).*

Figure D1.2 - *L5 Vertebrae – Superior Endplate*

Figure D1.3 - *L5 Vertebrae – Superior Endplate*

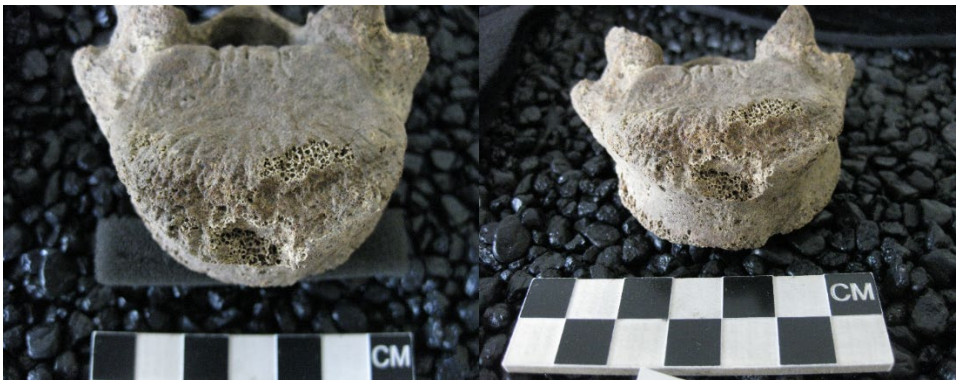

D2.0 ARJB V1368

Figure D2.1 - *T8 Vertebrae – Inferior Endplate*

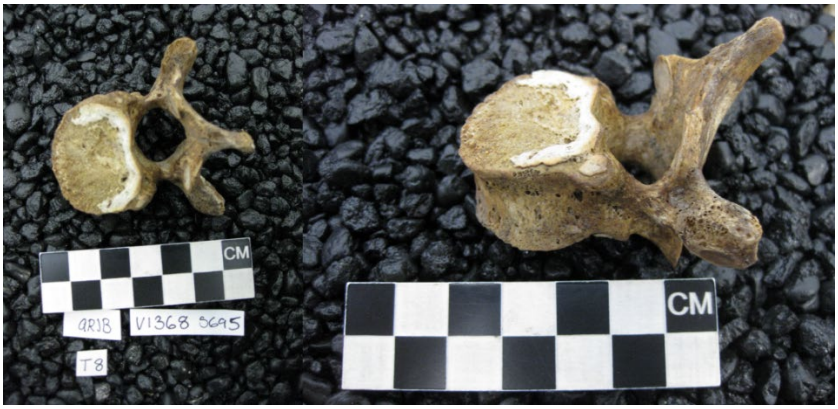

Figure D2.2 - *T9 Superior endplate (A) and T10 superior endplate (B).*

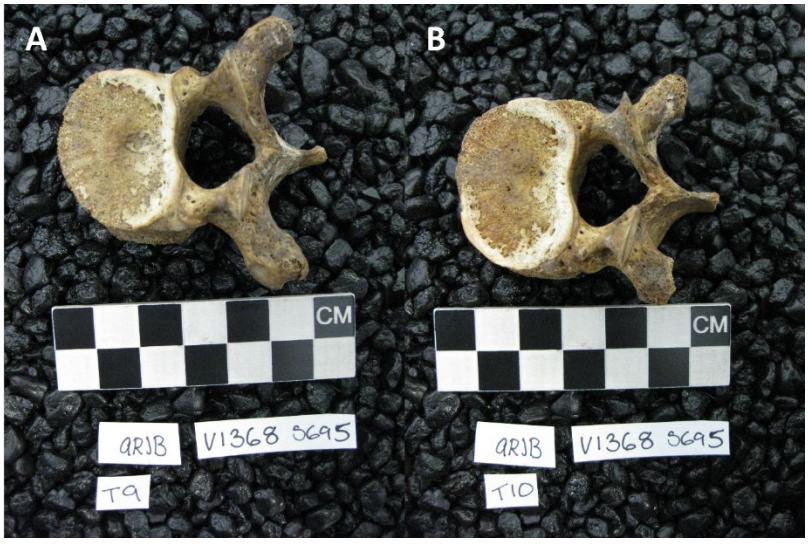

Figure D2.3 - *T12 Vertebrae – Superior Endplate*

Figure D2.4 - *L1 Vertebrae – Superior Endplate*

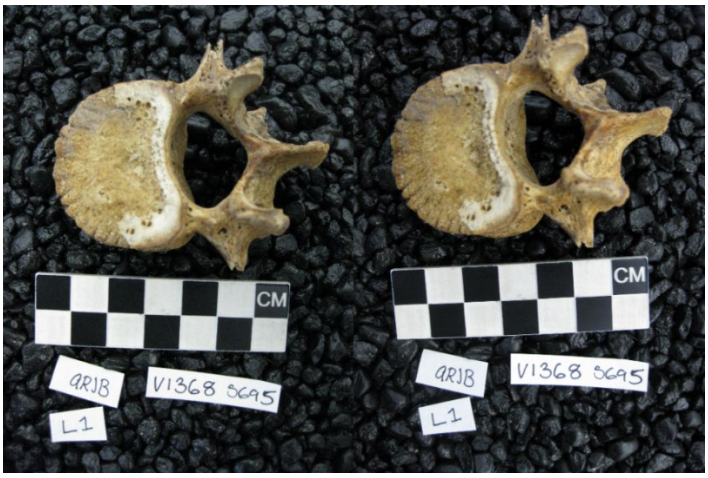

Figure D2.5 - *L3 Vertebrae – Superior Endplate*

D3.0 ARJB V1463

Figure D3.1 - *T3 Vertebrae – Inferior Endplate*

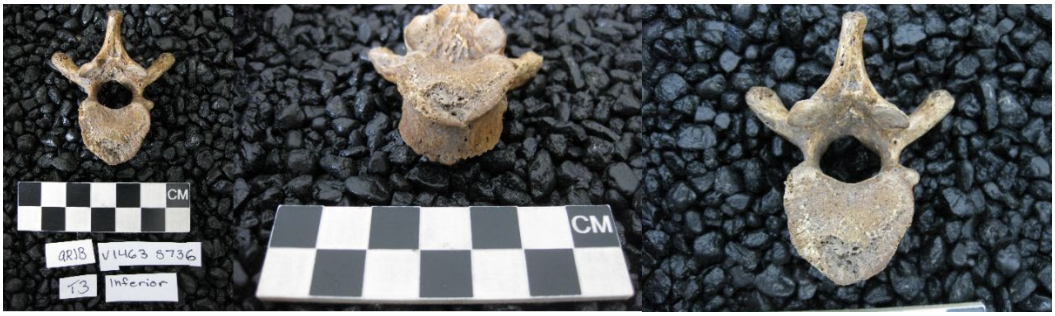

Figure D3.2 - *T4 superior endplate (A) and inferior endplate (B)*

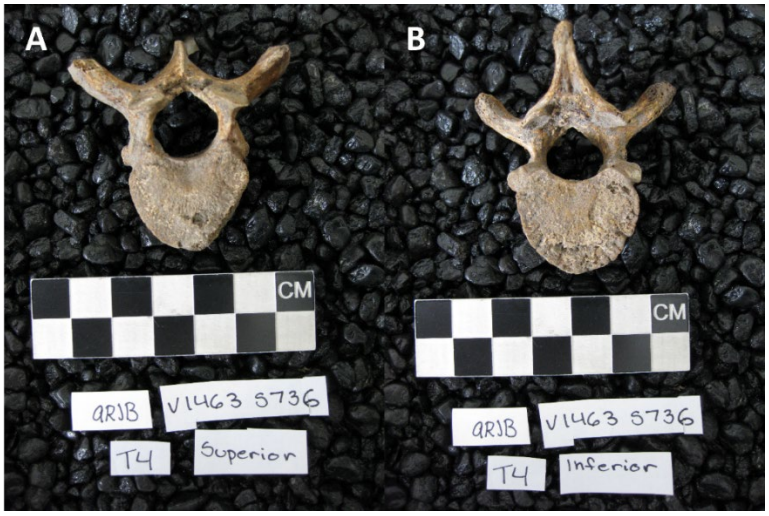

Figure D3.3 - *T4 Vertebrae – Transverse micro-CT slice of the center of the body*

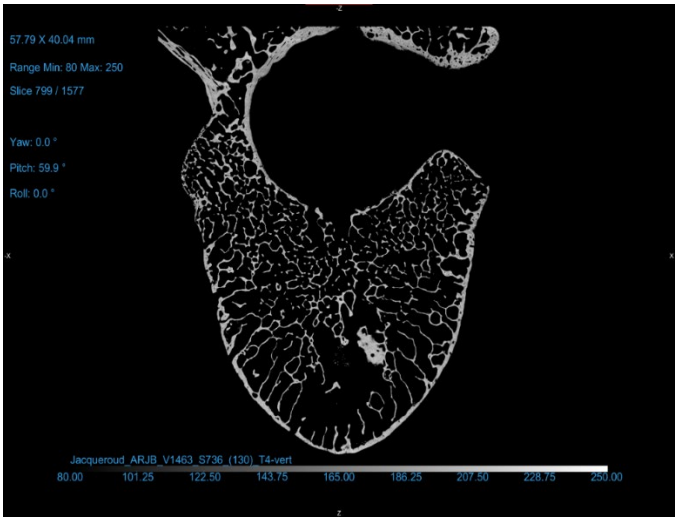

D4.0 ARJB V1556

Figure D4.1 - *L2 Vertebrae – Superior Endplate*

Figure D4.2 - *L3 vertebrae superior endplate (A), L4 superior endplate (B), L5 superior endplate (C).*

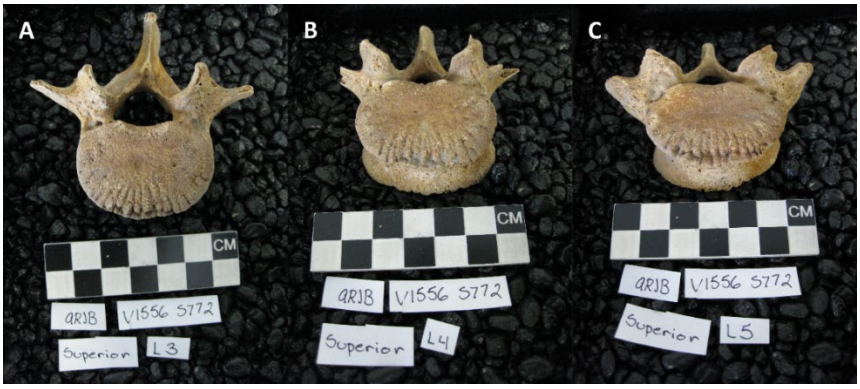

Figure D4.3 - *L5 Vertebrae – Transverse micro-CT slice.*

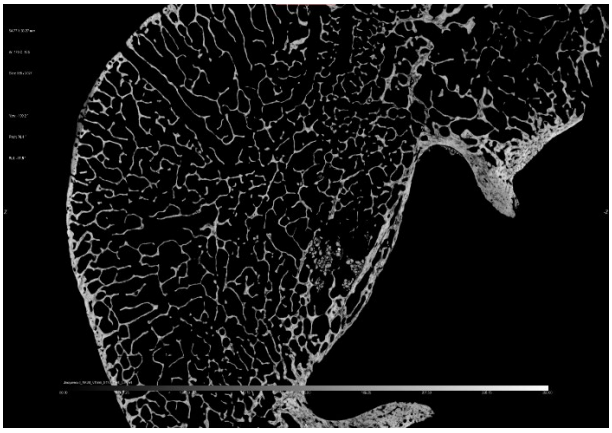

D5.0 ARJB V1583

Figure D5.1 - *T7 Vertebra – Inferior Endplate*

Figure D5.2 - *T8 vertebra superior endplate (A & B) and inferior endplate (C & D).*

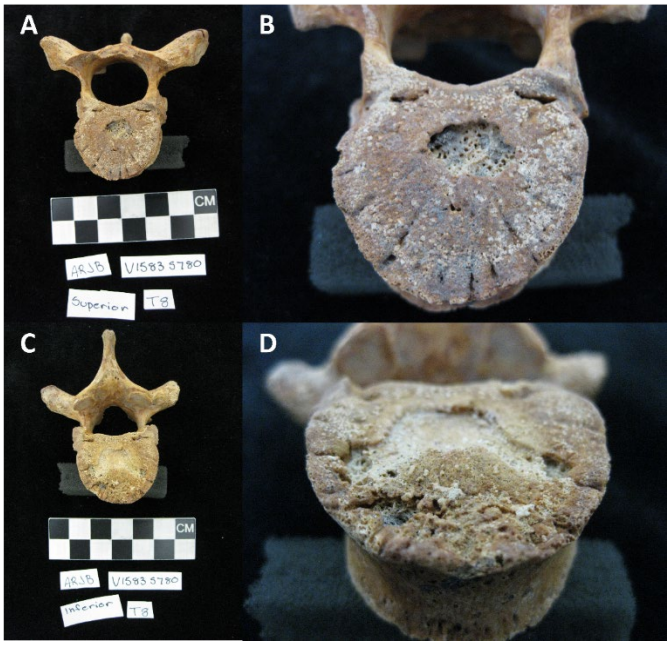

Figure D5.3 - *T9 vertebra inferior endplate.*

Figure D5.4 - *T10 vertebra superior endplate (A & B) and inferior endplate (C).*

Figure D5.5 - *T11 vertebra superior endplate (A & B) and inferior endplate (C).*

Figure D5.6 - *T12 vertebra superior endplate (A & B) and inferior endplate (C).*

D6.0 ARJB V1632

Figure D6.1 - *Left humerus with bone spicules on posterolateral aspect.*

D7.0 ARJB V1827

Figure D7.1 - *T4 vertebrae inferior endplate.*

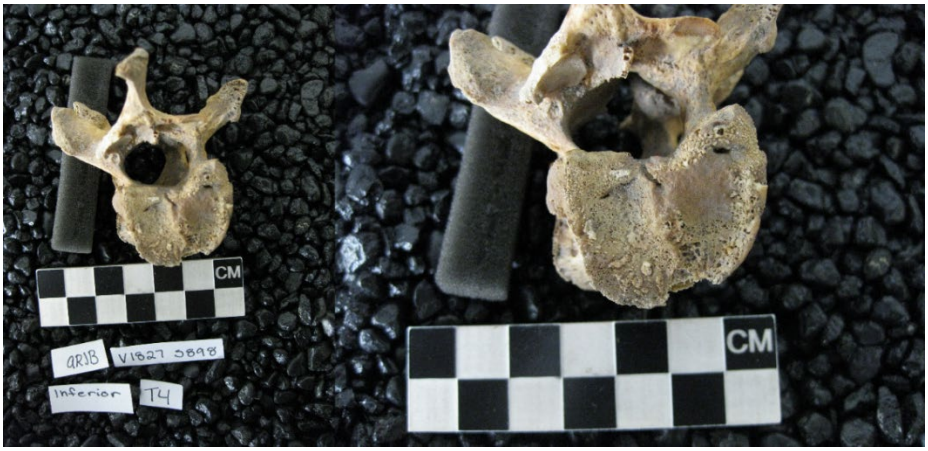

Figure D7.2 - *T5 vertebrae superior endplate.*

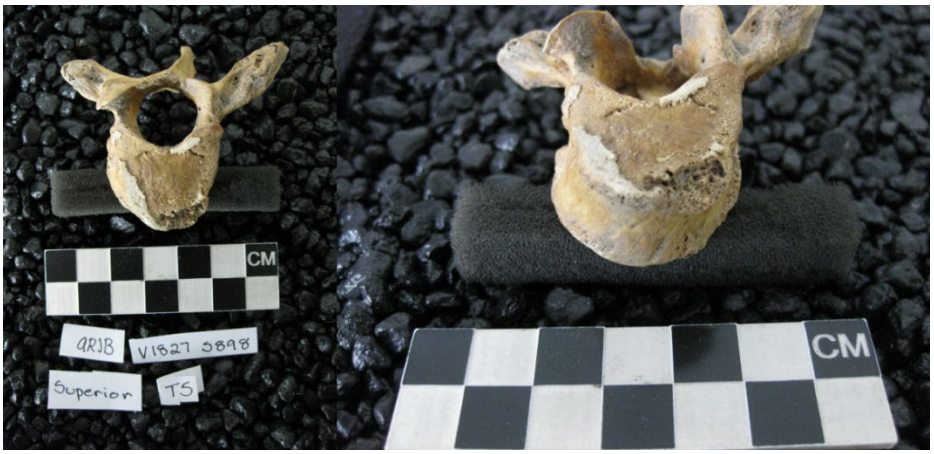

Figure D7.3 - *T6 superior endplate.*

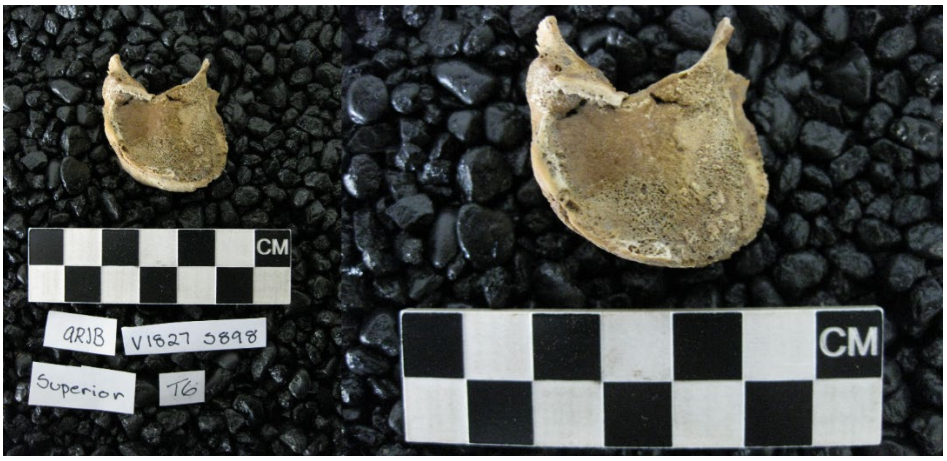

Figure D7.4 - *T7 superior endplate (A) and inferior endplate (B).*

Figure D7.5 - *T8 superior endplate (A) and inferior endplate (B).*

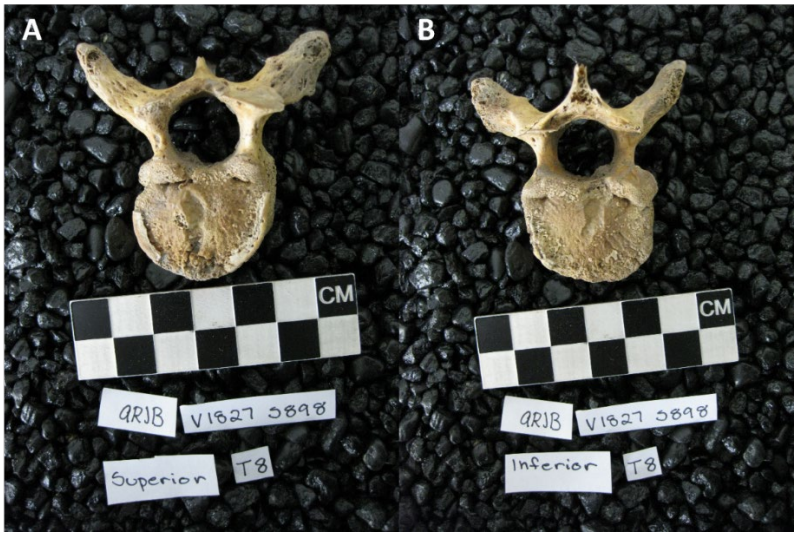

Figure D7.6 - *T9 superior endplate (A) and inferior endplate (B).*

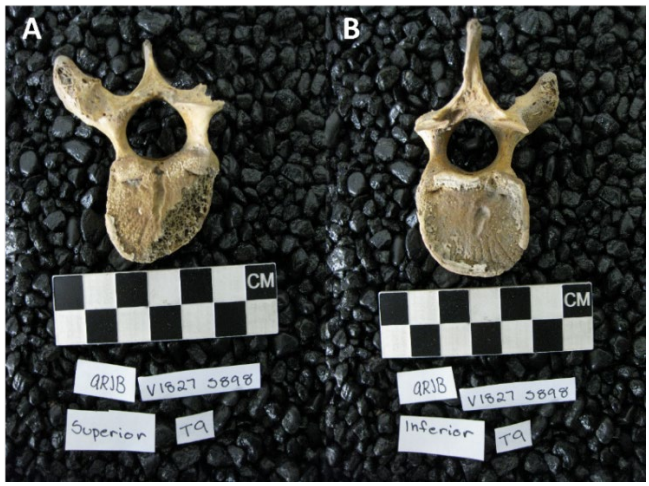

Figure D7.8 - *T10 inferior endplate.*

Figure D7.9 - *T11 superior endplate (A & B) and inferior endplate (C & D).*

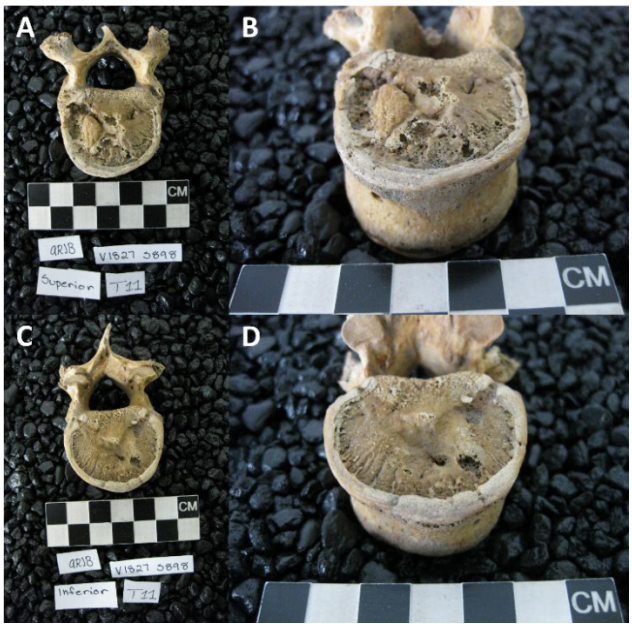

Figure D7.10 - *T12 superior endplate.*

Figure D7.11 - *Congenital fusion of T3 and T4.*

Figure D7.12 - *Coronal (A), sagittal (B), and transverse (C) slice of micro-CT reconstruction of T11 vertebra.*

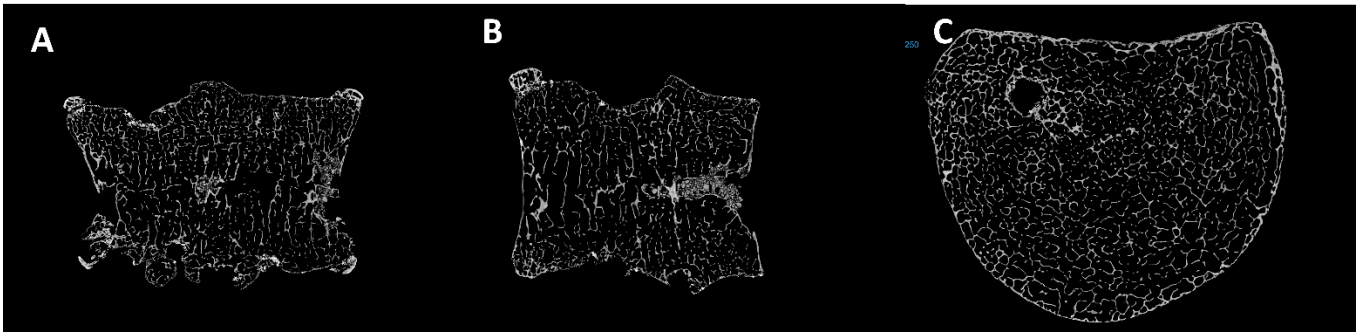

Figure D7.13 - *Microscopy image at 30x magnification of new bone formation in intrusion fracture on the superior L5 vertebra.*

D8.0 ARJB V1912

Figure D8.1 - *Superior endplates of L3 (A) and L4 (B) vertebrae.*

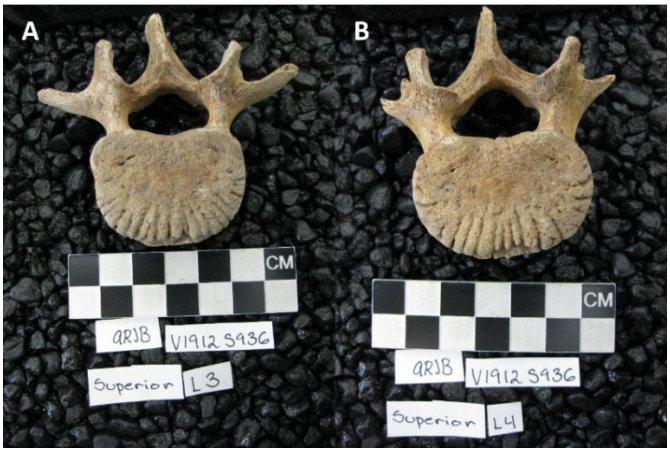

Figure D8.2 - *Superior endplate of L5 vertebra.*

Figure D8.3 - *Coronal (A) and sagittal (B) slice of micro-CT reconstruction from L4.*

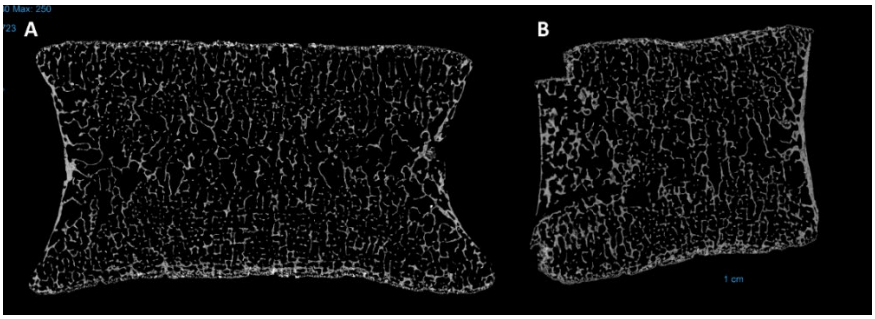

D9.0 ARJB V1945

Figure D9.1 - *L1 superior (A & B) and inferior (C) endplates.*

Figure D9.2 - *L2 superior endplate (A & B) and inferior endplate (C & D).*

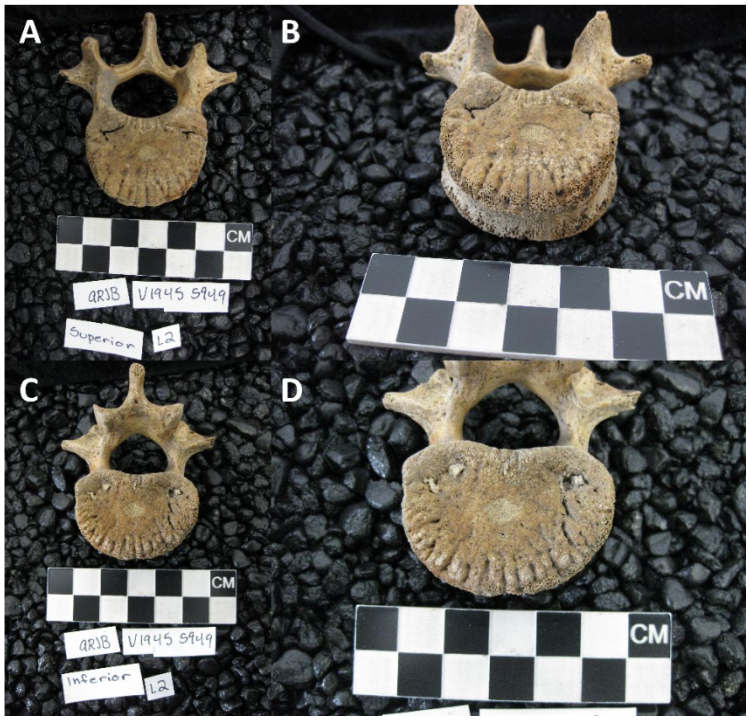

Figure D9.3 - *Superior endplate of L3.*

D10.0 EHV-CK S979

Figure D10.1 - *Left zygomatic with hairline fracture and remodeled bone.*

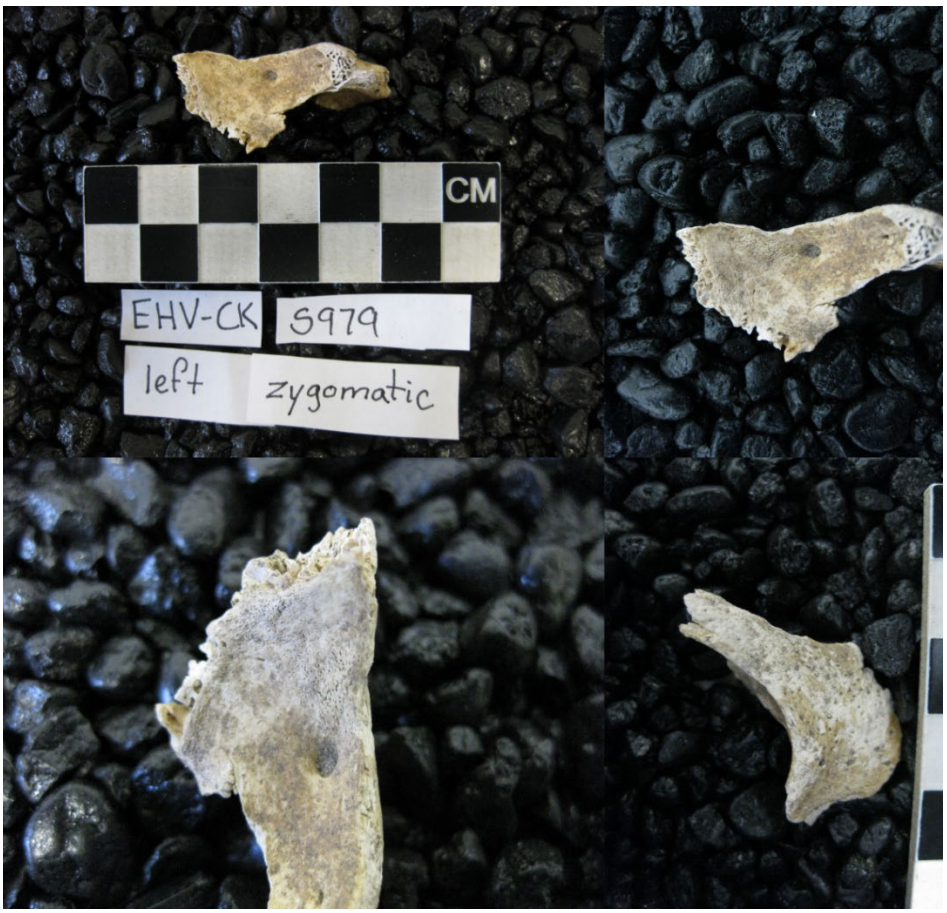

D11.0 EHV-CK S1834

Figure D11.1 - *Lower left rib with possible healed fracture, posterior surface (A & B) and visceral surface (C).*

Figure D11.2 - *Comparison between lower right rib and lower left rib.*

Figure D11.3 - *Microscopy image at 100x magnification of linear groove on visceral surface.*

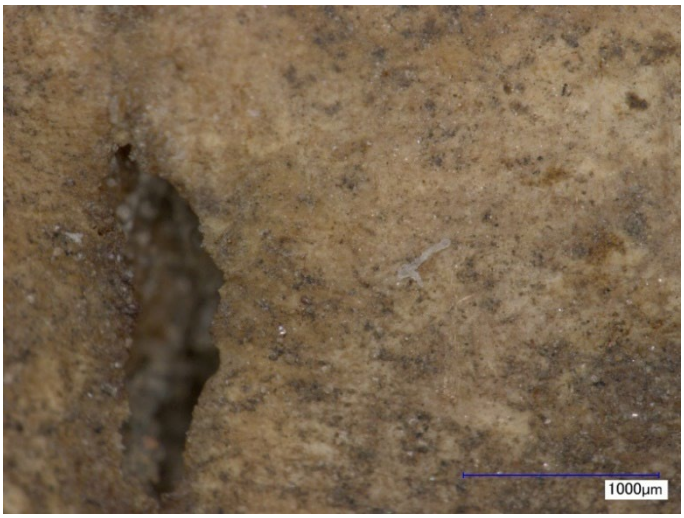

D12.0 EHV-CK S2567

Figure D12.1 - *Left humerus with porosity and new bone formation, anterior surface (A & B) and posterior surface (C & D).*

D13.0 EHV-CK S2918

Figure D13.1 - *Superior endplate of L5 vertebra.*

D14.0 EHV-CK S3507

Figure D14.1 - *Inferior endplate of T8 with small intrusion fracture.*

Figure D14.2 - *Superior endplate of T9 (A & B) and inferior (C &D) with bowl-shaped depression.*

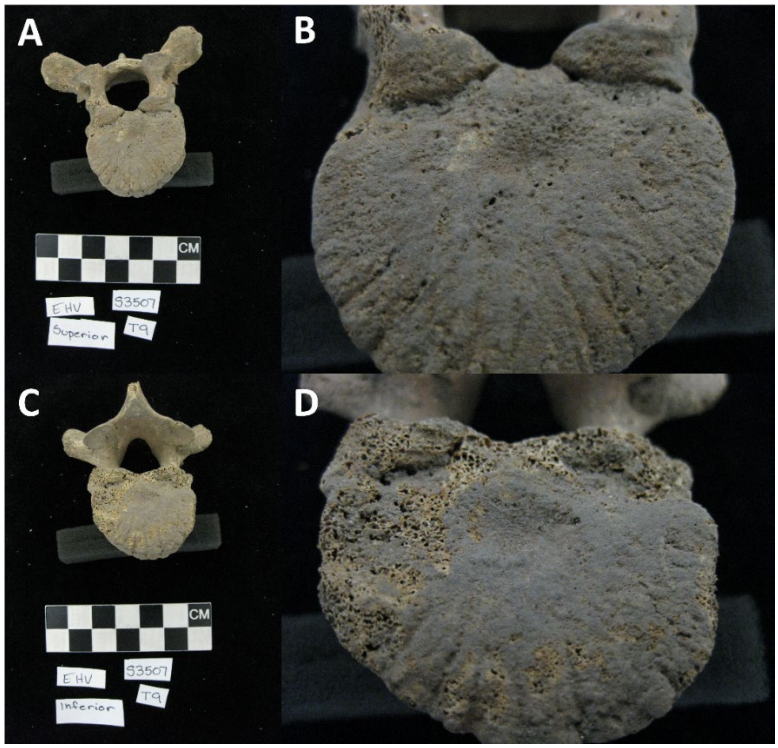

Figure D14.3 - *T10 superior endplate (A & B) and inferior (C &D) with bowl-shaped depression.*

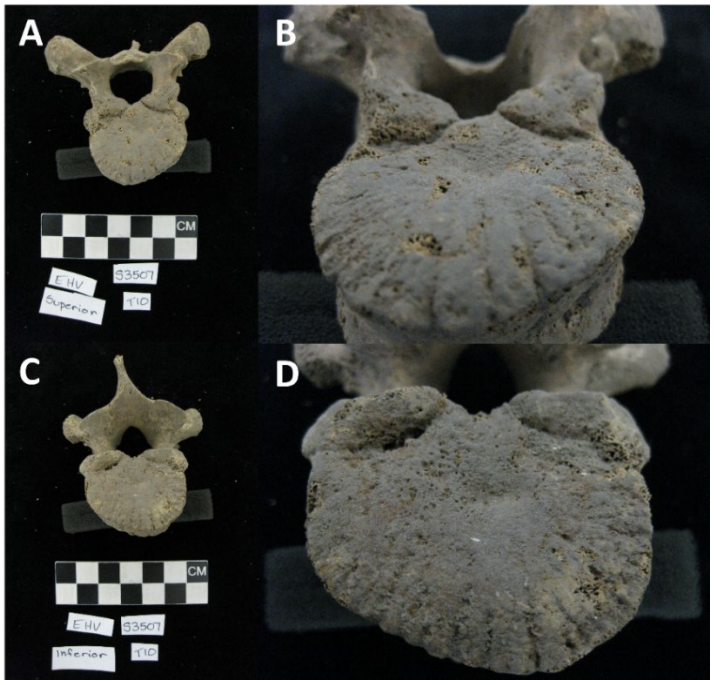

Figure D14.4 - *L1 superior endplate (A & B) and inferior endplate (C &D) with compression fracture.*

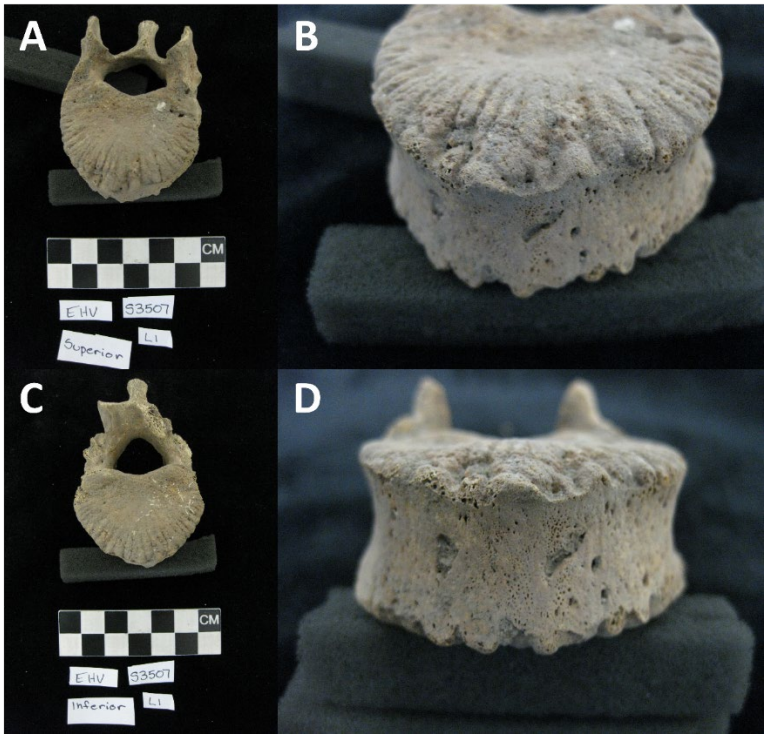

Figure D14.5 - *L3 superior endplate (A & B) and inferior endplate (C &D) with compression fracture.*

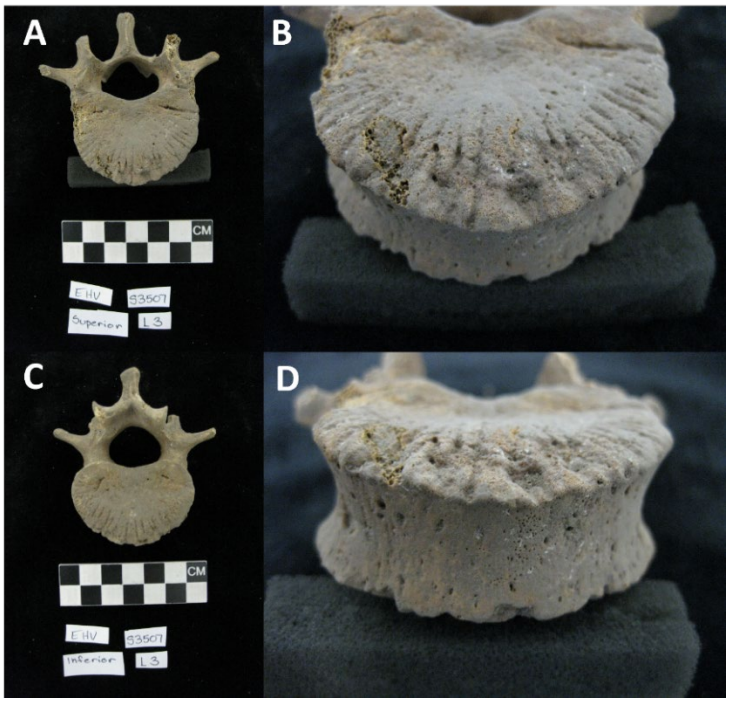

Figure D14.6 - *L4 superior endplate (A & B) and inferior endplate (C &D) with compression fracture.*

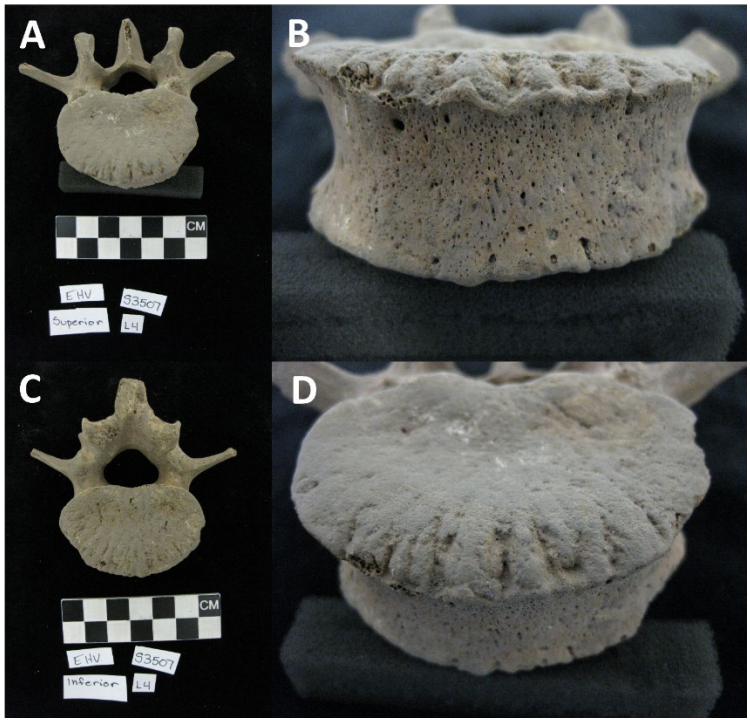

Figure D14.7 - *Coronal (A) and sagittal (B) micro-CT slices of L4 vertebra.*

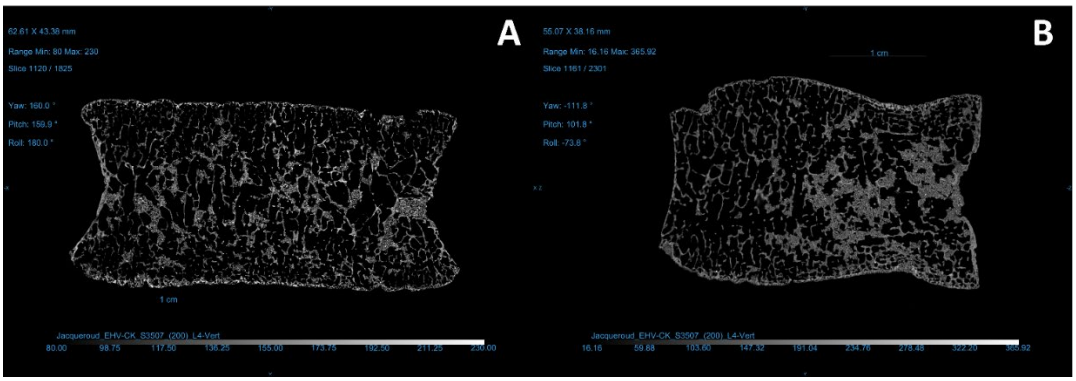

D15.0 GRK V59

Figure D15.1 - *Right fibula with mass in medullary cavity.*

Figure D15.2 - *Microscopy endoscope image of internal mass in right fibula.*

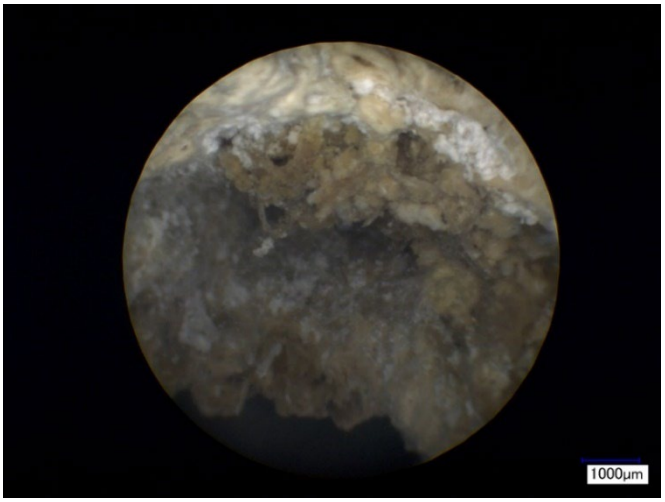

D16.0 GRK V512

Figure D16.1 - *Healed compression fracture to frontal bone.*

D17.0 ZW-87 8

Figure D17.1 - *Left rib 12 posterior shaft with fracture callus.*

Figure D17.2 - *Left rib 11 and rib 12 with interlocking fracture calluses.*

D18.0 ZW-87 67

Figure D18.1 - *Left rib A with fracture callus on visceral surface (A) and active bone on posterior surface (B).*

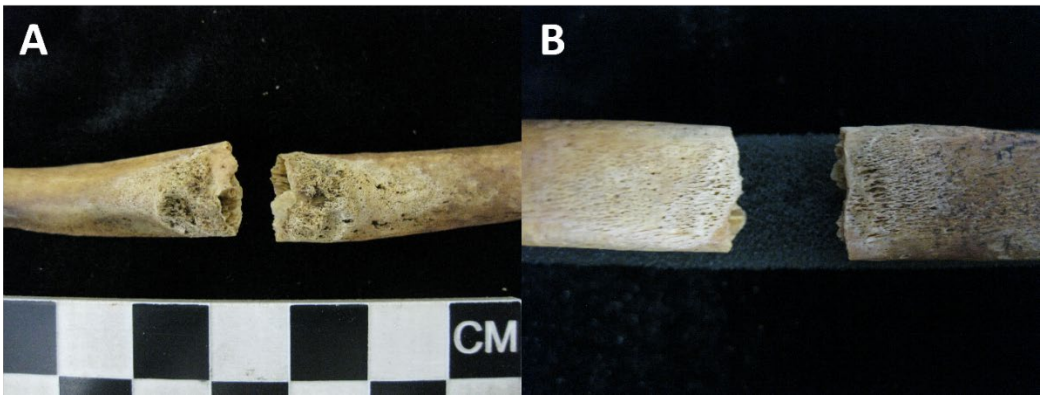

Figure D18.2 - *Left rib B with callus formation on visceral surface (A) and no active bone on posterior surface (B). Left rib C with fracture callus on visceral surface (C) and a small amount of active bone on posterior surface (D).*

D19.0 ZW-87 235

Figure D19.1 - *Inferior C3 vertebra with porous endplate.*

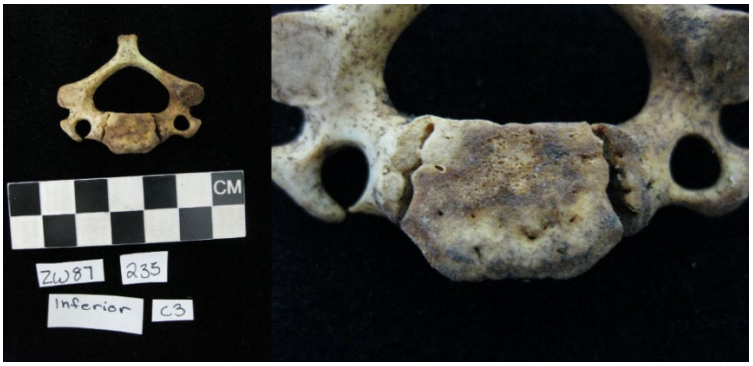

Figure D19.2 - *Inferior endplate of C4 vertebra with large compression fracture.*

Figure D19.3 - *Superior endplate (A & B) and inferior endplate (C & D) of C5 vertebra.*

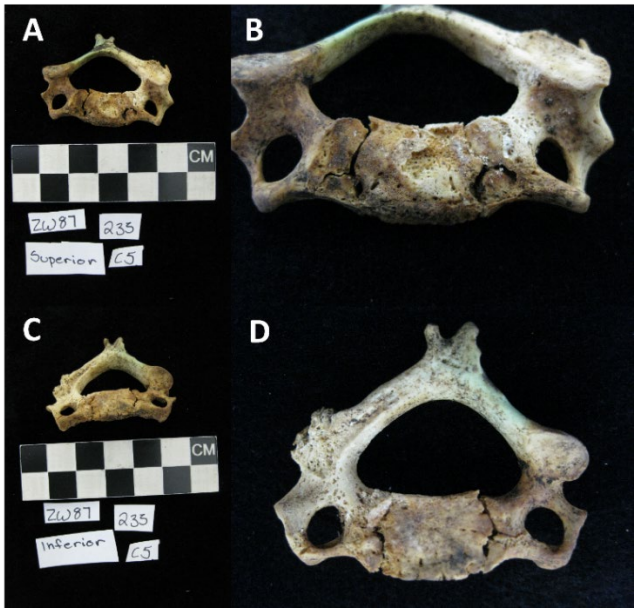

Figure D19.4 - *Superior view of C6 vertebra.*

Figure D19.5 - *Inferior view of T1 vertebra with large compression fracture to endplate.*

Figure D19.6 *Superior view of T2 vertebra with minor compression fracture on right side.*

Appendix E – Statistical Equations

E1.0 Statistical Equations

E1.1 Fischer Exact Test for Significance of Fractures and SES

	Mid- to High SES	Mid- to Low- SES	Marginal Row Totals
Fractures	5	13	18
No Fractures	11	26	37
Marginal Row Totals	16	39	55

$$\underline{p = (a+b)!\,(c+d)!\,(a+c)!\,(b+d)!}$$

$$a!\,b!\,c!\,d!\,n!$$

$$\underline{p = (5+13)!\,(11+26)!\,(5+16)!\,(13+26)!}$$

$$5!\,13!\,11!\,26!\,55!$$

$$\underline{p = 1.0000}$$

E1.2 Fischer Exact Test for Significance of Fractures in Males and Females

	Females	Males	Marginal Row Totals
Fractures	6	4	10
No Fractures	3	4	7
Marginal Row Totals	9	8	17

$$\underline{p = (a+b)!\,(c+d)!\,(a+c)!\,(b+d)!}$$

$$a!\,b!\,c!\,d!\,n!$$

$$\underline{p = (6+4)!\,(3+4)!\,(6+3)!\,(4+4)!}$$

$$6!\,4!\,3!\,4!\,17!$$

$$\underline{p = 0.6372}$$

E1.3 Fischer Exact test for Significance of Co-occurrence of CF and SN

	CF Present	CF Absent	Marginal Row Totals
SN Present	6	2	8
SN Absent	2	45	47
Marginal Row Totals	8	47	55

$$p = \frac{(a+b)!\,(c+d)!\,(a+c)!\,(b+d)!}{a!\,b!\,c!\,d!\,n!}$$

$$p = \frac{(6+2)!\,(2+45)!\,(6+2)!\,(2+25)!}{6!\,2!\,2!\,45!\,55!}$$

$$p = 0.0000$$

E1.4 Fischer Exact Test for Significance of Vertebral Fractures and SES

	Vertebral Fractures	No Vertebral Fractures	Marginal Row Totals
Mid- to High-SES	0	18	18
Low- to Mid-SES	9	28	37
Marginal Row Totals	8	44	55

$$p = \frac{(a+b)!\,(c+d)!\,(a+c)!\,(b+d)!}{a!\,b!\,c!\,d!\,n!}$$

$$p = \frac{(0+18)!\,(9+28)!\,(0+9)!\,(18+28)!}{0!\,18!\,9!\,28!\,55!}$$

$$p = 0.0232$$